LAMINAR-FLOW HEAT-TRANSFER IN NON-CIRCULAR DUCTS.

by

P. Wibulswas, B.Sc.(Eng.), A.C.G.I., D.I.C.

A thesis submitted for the degree of Doctor of Philosophy in the University of London.

Department of Mechanical Engineering,
University College London,
Gower Street, W.C.1.

May, 1966.

ABSTRACT

A numerical method is employed to obtain solutions for laminar flow heat transfer with fully developed velocity profiles and invariant fluid physical properties for rectangular ducts of various aspect ratios with the thermal boundary conditions of constant wall temperature and constant heat input per unit length of the duct. Since an analytical solution for the fully developed velocity profile in a rectangular duct is available, the varying temperature profile remains to be solved numerically from the energy equation which is transformed into a finite difference form by means of two finite difference operators in two dimensions. Numerical values of the initial and boundary temperatures are fixed by choosing a suitable dimensionless temperature depending upon the thermal boundary condition. As computation involved is very lengthy, a fast digital computer is required. Numerical results obtained from an I.C.T. Atlas computer are presented as the variation of the Nusselt number with the Graetz number.

The numerical method is extended to analyse heat transfer with simultaneously developing velocity and temperature profiles. To determine the development of the velocity profile, some simplifications of the Navier-Stokes equation

are made. Results are presented for various aspect ratios with the Prandtl number of 0.72. The effect of Prandtl number on heat transfer is also illustrated by numerical results.

The numerical method is also used to solve for heat transfer in right-angled isosceles and equilateral triangular ducts with the same hydraulic and thermal boundary conditions as in the previous cases.

The predicted results are compared with experimental data. For constant wall temperature, they agree well for Graetz numbers under 70; for constant heat input per unit length, closer agreement is shown over a much wider range of the Graetz numbers. Accuracy of the numerical method is confirmed by the facts that variations of the predicted Nusselt numbers obtained here follow the same trends as those for circular ducts and parallel plates and at the Graetz number of zero, they approach values of the limiting Nusselt numbers obtained by other methods.

ACKNOWLEDGEMENTS

The work described in this thesis was carried out in the Department of Mechanical Engineering, University College, University of London, under the supervision of Dr. S.R. Montgomery, M.A., S.M., Sc.D., A.M.I.Mech.E. I would like to express my sincere gratitude for his guidance, help, advice and criticism during the course of this work. I would also like to thank members of the workshop especially Mr. E. Farmer, for their helps in building up the test apparatus.

Finally, I am grateful to the Ministry of Education of Thailand for awarding the scholarship for research in Mechanical Engineering in the United Kingdom, which has made this work possible.

CONTENTS

Page

NOMENCLATURE

A	Area
A_c	Cross sectional area
A_s	Surface area
a	Short side of rectangular cross section
a	Short side of right-angled isosceles triangular cross section
b	Long side of rectangular cross section.
C	Constant
C_p	Specific heat at constant pressure
d_h	Hydraulic diameter ($= 4A_c/P$)
e	Ratio of finite step to hydraulic diameter ($=h/d_h$)
f	Unspecified function
h	Finite step in x and y directions
h	Coefficient of heat transfer
H	Partial Differential operator for square network
K	Partial differential operator ($= H+X$)
K'	Partial differential operator for triangular network
k	Coefficient of thermal conductivity
L	Length of duct
l	Length
N	Number of step
n	Integer
P	Perimeter of duct
p	Pressure
q	Rate of heat transfer

t Temperature

u Velocity in x direction

V Volumetric flow rate

v Velocity in y direction

w Velocity in z direction

X Partial differential operator for square network

x,y,z Cartesian coordinates

z Distance along duct

α Thermal diffusivity ($= k/C_p\rho$)

α' Aspect ratio of a rectangular duct ($= b/a$)

β Dimensionless temperature for constant heat input per unit length of duct

Δ Incremental sign

∇ Laplacian operator

θ Dimensionless temperature for constant wall temperature

μ Dynamic viscosity

ν Kinematic viscosity

Σ Summation sign

ρ Density

Dimensionless Groups

Gz Graetz number ($= Re.Pr/(z/d_h)$)

Nu Nusselt number ($= hd_h/k_b$)

Re Reynolds number ($= \rho w_b d_h/\mu$)

Pr Prandtl number ($= \mu C_p/k_b$)

w^+ Dimensionless velocity in z direction

$(= w/\frac{\text{const.}}{\mu} \cdot \frac{dp}{dz})$

Subscripts

b Bulk, average value

c Centre, correction

f Final

h Value distant h from wall

l Logarithmic

m Mean

o Initial

p Peripheral

w Wall

z Local

α Limiting value

CHAPTER 1

INTRODUCTION

Heat transfer by forced convection occurs when a fluid is induced by mechanical means such as a pump, fan etc. through a duct with wall temperature differing from fluid temperature. Since heat transfer occurs as a result of interaction between the velocity and temperature profiles of the fluid, the rate of heat transfer depends upon the shapes of the two profiles.

For a duct with a hydraulically smooth entrance such as a bell-shaped inlet for the circular duct, velocity at the entry plane is uniform. As the fluid flows along the duct, local velocities near the wall are retarded by fluid viscosity and a boundary layer grows. When the boundary layer reaches the central axis of the duct, the flow is said to be fully developed. In a circular duct, the fully developed velocity profile for a laminar flow is parabolic, but in a non-circular duct, the shape of the profile depends upon the shape of the duct.

The temperature profile also exhibits a similar boundary layer growth depending upon the thermal boundary condition. Most common ones encountered in practice are constant wall temperature, constant heat flux and constant wall temperature gradient.

Investigations of heat transfer by forced convection in circular ducts have been extensively conducted by many research workers and their analytical and experimental results may be found in various text books and journals on heat and mass transfer. In most theoretical analyses, physical properties of the fluid were assumed invariable with respect to temperature.

Recently, the need for compact heat exchangers in many fields such as air conditioning units, rocket power plants etc. has accelerated the work dealing with forced convection heat transfer in non-circular ducts, but the knowledge in this field is still incomplete. Most analytical solutions were obtained for fully developed flow and very few experimental data are available. Recommendations for further investigation have been made in an extensive literature survey up to 1961 by Montgomery and Weiss (1) for both laminar and turbulent flows.

In order to provide up-to-date informations, a brief survey of publications on laminar flow heat transfer from 1961 onwards is given below.

1.1 CIRCULAR DUCT.

Numerical solutions for laminar flow heat transfer with simultaneously developing velocity and temperature profiles were obtained by Ulrichson and Schmitz (2) for the boundary conditions of constant wall temperature and constant heat flux. The work is a refinement of an earlier work of Kays (3) to include the radial component of the velocity in the entrance region and it shows a significant decrease in the local Nusselt number from that obtained by Kays.

Hudson and Bankoff (4) solved a transient problem wherein a new wall temperature is suddenly impressed upon an initially isothermal laminar flow by double Laplace transformation. For small time or large axial distance, the solution is found to be independent of axial distance and for small distance, it becomes independent of time.

The effect of the variation of fluid physical properties with temperature was investigated theoretically by Bradley and Entwistle (5) for fully developed air flow in a circular duct. Numerical solutions are presented for a range of air temperature from 350 deg. K. to 2500 deg. K. for the conditions of constant wall temperature and constant axial temperature gradient. The solutions also show that the effect of axial conduction on the tempera-

ture profile becomes important at low Reynolds numbers and the effect of axial momentum on the velocity profile owing to different fluid densities is considerable for large temperature differences between the wall and air.

For laminar flow heat transfer with variable properties in the thermal entrance region, an analytical method was used by Koppel and Smith (6) for the thermal boundary condition of constant heat flux, the radial velocity being neglected. The method was applied to supercritical carbon dioxide whose properties vary rapidly with temperature The results show fluctuations of the heat transfer coefficien for particular values of heat flux, fluid temperatures and flow rates.

Experimental results were obtained by Kays and Nicoll (7) for large temperature differences between the wall and air for the cases of constant heat flux and constant wall temperature over a narrow range of Reynolds numbers. Data was found to agree well with analytical solutions based on constant fluid properties.

1.2 INFINITE PARALLEL PLATES

A few theoretical papers were published recently on simultaneously developing velocity and temperature profiles in the entrance region of two infinite parallel plates. Stefan (8) used an approximate series solution for the thermal condition of constant wall temperature. The case of constant heat input per unit length of the duct was solved by Han (9). He assumed Langhaar's solution (10) for the varying velocity profiles and derived an integral method to solve for the variations of the wall and fluid temperatures along the duct. Numerical solutions are given for Prandl numbers of 3.2, 1.6, 0.8 and 0.4.

A more rigorous analysis of the simultaneously developing flow was done by Hwang and Fan (11). They applied the finite difference analysis to the Navier-Stokes equation and the continuity equation to solve the developing velocity profiles which are then substituted in the energy equation to dertermine temperature profiles. Nusselt numbers are given for Prandtl numbers in the range of 0.01 to 50. For the constant wall temperature case, their solutions agree very well with those of Stefan (8); as for the constant heat flux, their results differ appreciably from Han's results (9), but agree closely with an earlier work by Siegel and Sparrow (12) who used Langhaar's velocity profiles.

Solutions of heat transfer in the thermal entrance region with an interesting thermal boundary condition of unequal wall temperatures were obtained by Hatton and Turton (13). They show that the Nusselt numbers for the two walls do not reach the limiting value until the fluid temperature gradient becomes linear after a very long entry length. The entry length also depends on the magnitude of the fluid entry temperature in comparison to the wall temperature.

A transient problem on heat transfer for an incompressible laminar flow was theoretically analysed by Perlmutter and Siegel (14). The transient is caused by sudden changes of the fluid driving pressure and the wall temperature. Solutions are given for both zero and finite wall thermal resistances.

1.3 RECTANGULAR DUCTS.

Since laminar flow heat transfer in a rectangular duct is strongly affected by the aspect ratio of the duct, theoretical analysis is more complex than those for the circular duct and parallel plates. Solutions for flows with fully developed velocity and temperature profiles were obtained by various authors and their works were fully compiled by Montgomery and Weiss (1).

Variations of wall temperature for fully developed laminar flow in channels with the aspect ratios from 1 to ∞ were investigated by Savino and Siegel (15). Solutions are available for various ratios of heat fluxes between the short sides and the broad sides from 0 to 1, while the total heat flux per unit length of the channels is kept constant. Results show that the peak temperatures occur at the corners owing to low fluid velocities. When only the broad sides are heated, the peak temperatures are lowest and decrease rapidly as the aspect ratio increases.

1.4 OTHER CROSS SECTIONS.

Fully developed Nusselt numbers for isosceles triangular, right triangular and circular sector ducts were computed by Sparrow and Haji-Sheik (16) and results are presented over a wide range of opening angle of the cross sections for the boundary condition of constant heat flux. For small opening angles, results for the sector and the isosceles triangular ducts are very close to each other. Among the triangular cross sections, the equilateral triangular duct gives the highest Nusselt number. Nusselt number for the circular sectors reaches a maximum value when the opening angle approaches 180 deg., i.e. it represents an infinite plate.

Analytical solution of heat transfer in a cone with a small opening angle was obtained by Cobble (17). Variations of the Nusselt numbers with the Graetz numbers for a finite cone angle of 0.1 radian are plotted with various cone lengths as a parameter.

1.5 SCOPE OF THE PRESENT WORK.

As already mentioned in (1.3) and (1.4), analytical solutions are available only for fully developed flows in a few types of non-circular ducts, but in practice, heat transfer usually begins simultaneously with the development of velocity profile, and in some applications, though the velocity profile is fully developed when the heat transfer process begins, the whole region where heat transfer occurs must be taken into consideration. Since no theoretical and very few experimental data exist for the stated conditions, the present work attempts to provide them.

Theoretical analyses here are concerned with laminar flow heat transfer in rectangular ducts with different aspect ratios and in triangular ducts of various cross sections under the following boundary conditions :

(1) Fully developed velocity profile and developing temperature profile. This is also known as the ' thermal entrance region.' At the entrance of the duct, the fluid temperature is uniform. The exact solutions for the fully developed velocity profiles in rectangular and triangular ducts can be found in a text book by Rouse (18).

(2) Simultaneouly developing velocity and temperature profiles. Both of them are assumed uniform at the entrance.

Thermal boundary conditions of constant heat input per unit length of the duct and of constant wall temperature are considered. In all cases, fluid properties are assumed invariable with respect to temperature.

Experimental results were obtained for a rectangular duct of aspect ratio of 2.0 with constant heat input per unit length and with constant wall temperature, and for an equilateral triangular duct with constant heat input per unit length.

CHAPTER 2

APPARATUS

2.1 GENERAL DESCRIPTION.

A general flow diagram of the apparatus is given in fig.1, p.22. Before entering the test section, atmospheric air was sucked through an unheated duct to produce a fully developed velocity profile. Various test sections were employed for the thermal boundary conditions of constant heat input per unit length and constant wall temperature, and their details will be described later on. On leaving the test section, the heated air entered an insulated mixing chamber, fig.2, p.23, which was a box containing a wire mesh to even out the final temperature of the air. A rotameter was provided for measuring the flow rate of the air which could be controlled by varying the opening of a by-pass chamber, fig.3, p.23. Circulation of the air was maintained by a high speed centrifugal fan (21), the fluctuation of which was damped by inserting a piece of wire wool in the duct between the rotameter and the by-pass chamber.

Air in

Fig. 1 General Flow Diagram of Apparatus.

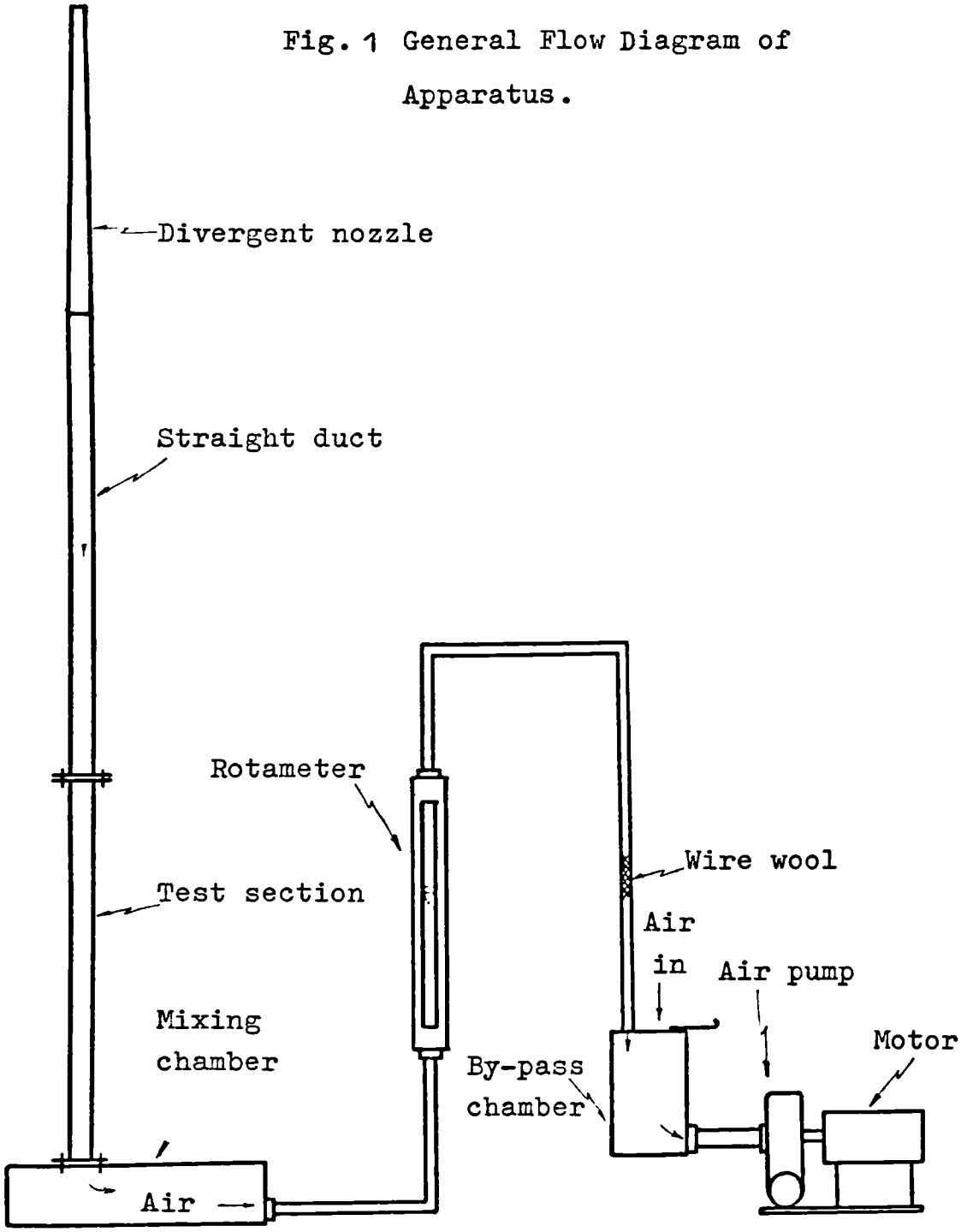

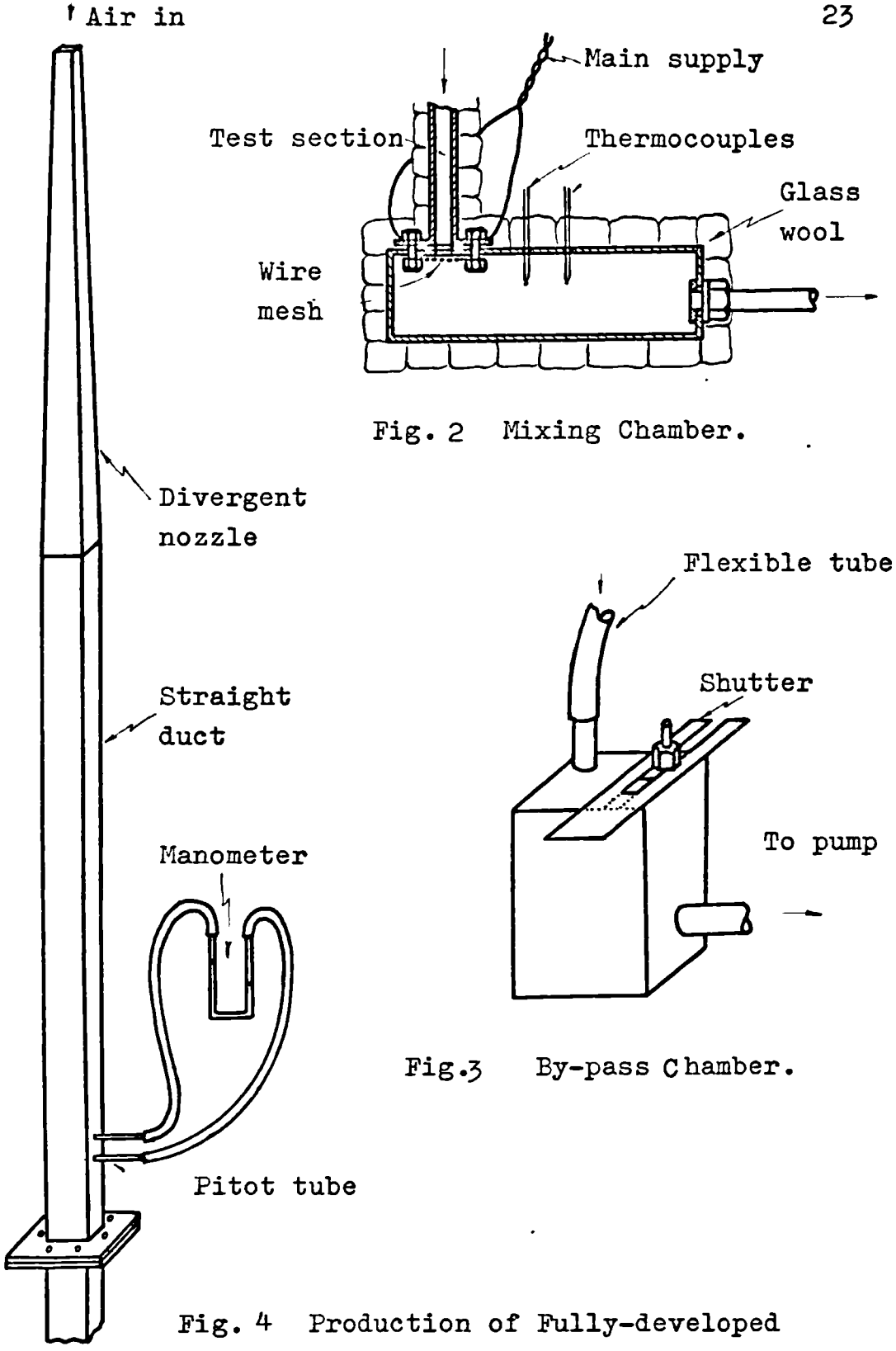

Fig. 2 Mixing Chamber.

Fig.3 By-pass Chamber.

Fig. 4 Production of Fully-developed Velocity Profile.

2.2 PRODUCTION OF A FULLY DEVELOPED VELOCITY PROFILE.

In order to produce a fully developed velocity profile for laminar flow in a non-circular duct, a length of about 100 hydraulic diameters was required. However, if air is allowed to flow through a divergent nozzle first and then through a straight duct, the production of the fully developed velocity profile can be greatly accelerated (22). In the case of the rectangular duct used in the present experiments, the cross sectional area of the nozzle varied from 0.5 x 1.0 in^2 to 1.0 x 2.0 in^2 with a length of 30 in. The air then entered a straight rectangular duct of 1.0 x 2.0 in^2 in cross sectional area and 3.0 ft. in length, fig.4, p.23. The velocity profile of the air at the end of the straight duct was determined by means of a pitot tube and a micromanometer which gave an accuracy of about 14 % for the worst measurement.

Fig.5 shows a comparison of the central line velocities between the flow in the straight duct and the flow in the same duct with an additional divergent nozzle over a range of Reynolds numbers from 840 to 2480 . The central line velocity was appreciably increased by the divergent nozzle.

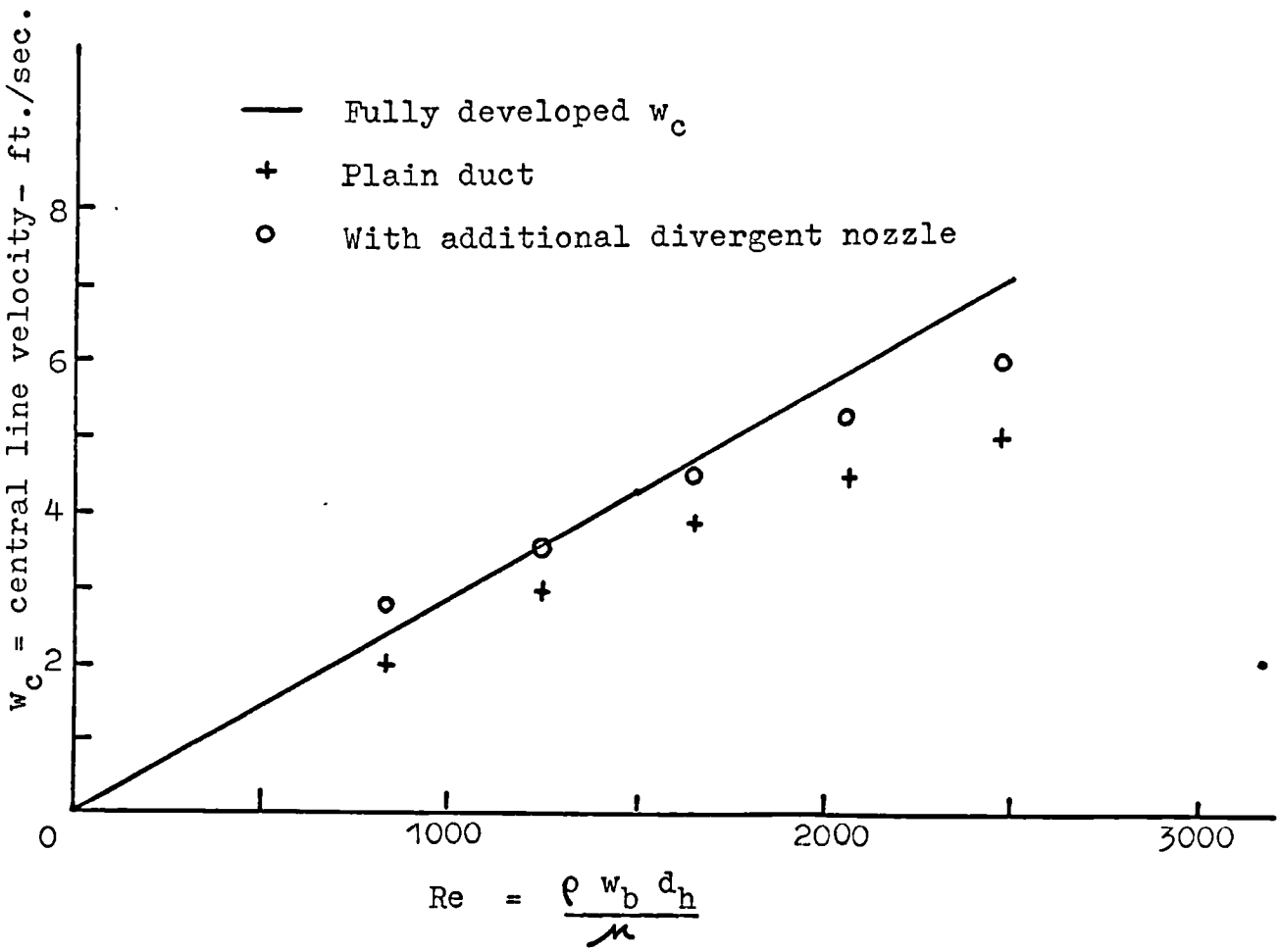

Fig. 5 Effect of the additional divergent nozzle on the velocity profile in a rectangular duct.

2.3 RECTANGULAR TEST SECTION FOR CONSTANT HEAT INPUT.

To obtain a constant heat input per unit length of the duct, alternating current was fed through a metal duct made of an electrical resistance material called Ferry Metal (23) of 0.006 in. thick. A vertical mounting of the duct was chosen because, in a horizontal position, the temperature profile of the heated air is distorted owing to natural convection.

The Ferry Metal was supplied in the form of a strip of 1.0 in. wide. To construct a rectangular duct of 1 x 2 in^2. in cross sectional area, a wooden former of the required cross section was employed as a guide. Six metal strips were placed around the wooden form and joined together with thermosetting plastic tapes. To make sure that the cross section of the duct would remain rectangular after the withdrawal of the form, the outer surface of the duct was covered with a double bond resin called Hermetal (24) which set hard afterwards. A brass flange was soldered to each end of the duct to form an electrical terminal, fig.6, p.28. The whole duct was heavily insulated with glass wool to reduce heat lost to the atmosphere to a minimum.

The heating circuit is shown in fig.9, p.29. The main voltage was stepped down by a transformer from 240 V. to a voltage under 2.5 V. The input power was controlled by

a variable transformer and measured by an ammeter, (0-50A), and a voltmeter, (0-2.5V). By comparing the input power to the total change of enthalpy of the heated air, heat lost to surroundings could be estimated.

2.4 RECTANGULAR TEST SECTION FOR CONSTANT WALL TEMPERATURE

To obtain a condition as close to a constant wall temperature as possible, the test section was made of copper which is a good heat conductor. Its dimensions were originally 2 ft. in length and 2 x 1 in^2 in cross section. For rigidity, a wall of 1/8 in. in thickness was chosen. The copper duct was placed inside a jacket which was filled with heating water at constant temperature, fig.7, p.28. A pump heater was employed to circulate heating water the temperature of which was kept constant by a thermostat.

To cover a wide range of Graetz numbers, the test section was later on shortened to 7½ and 13 in. and the same test procedure was repeated. The reason is explained in (3.7.2).

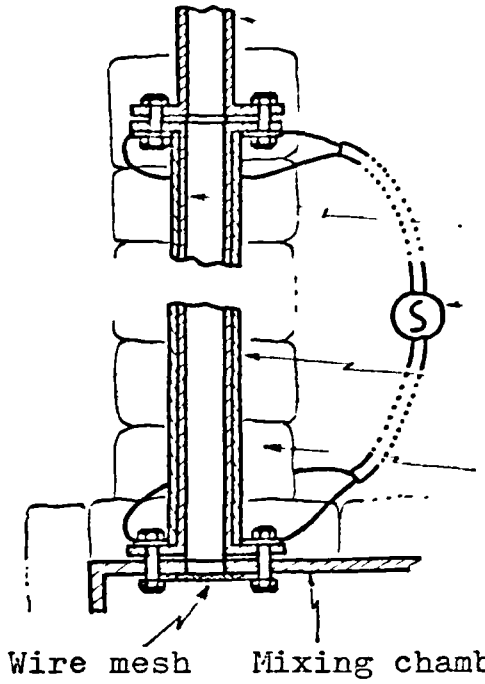

FIG. TEST SECTION FOR CONST. HEAT FLUX.

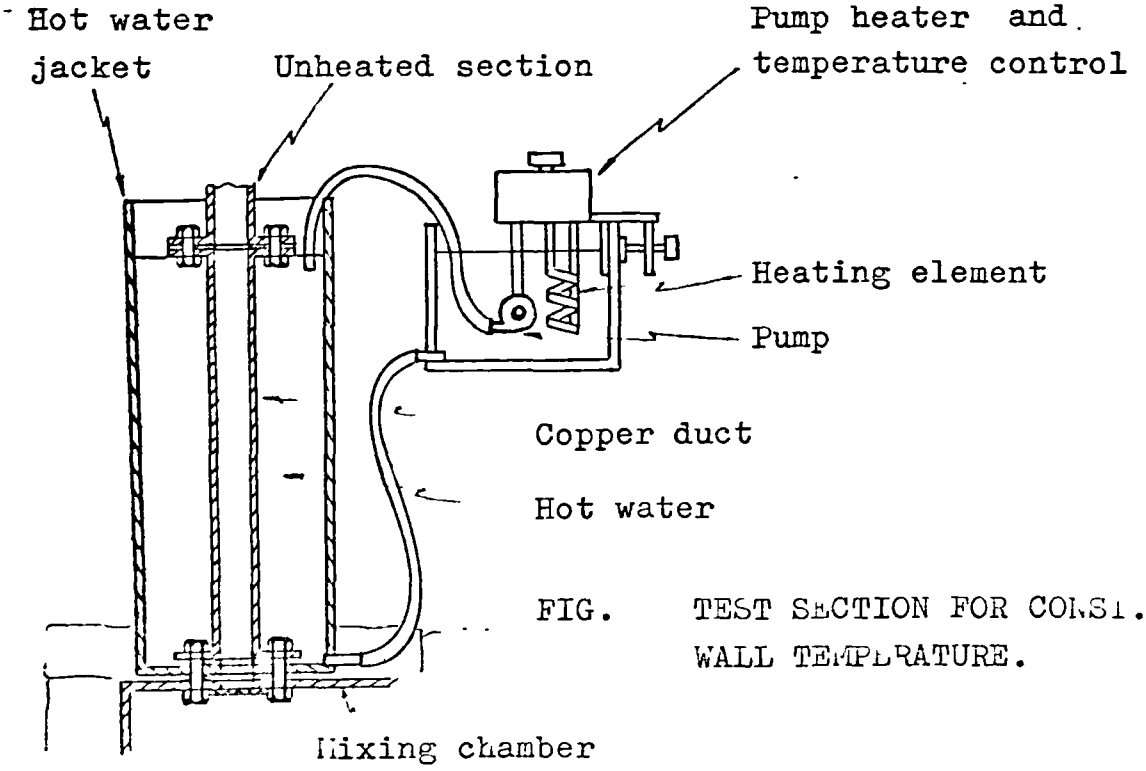

FIG. TEST SECTION FOR CONST. WALL TEMPERATURE.

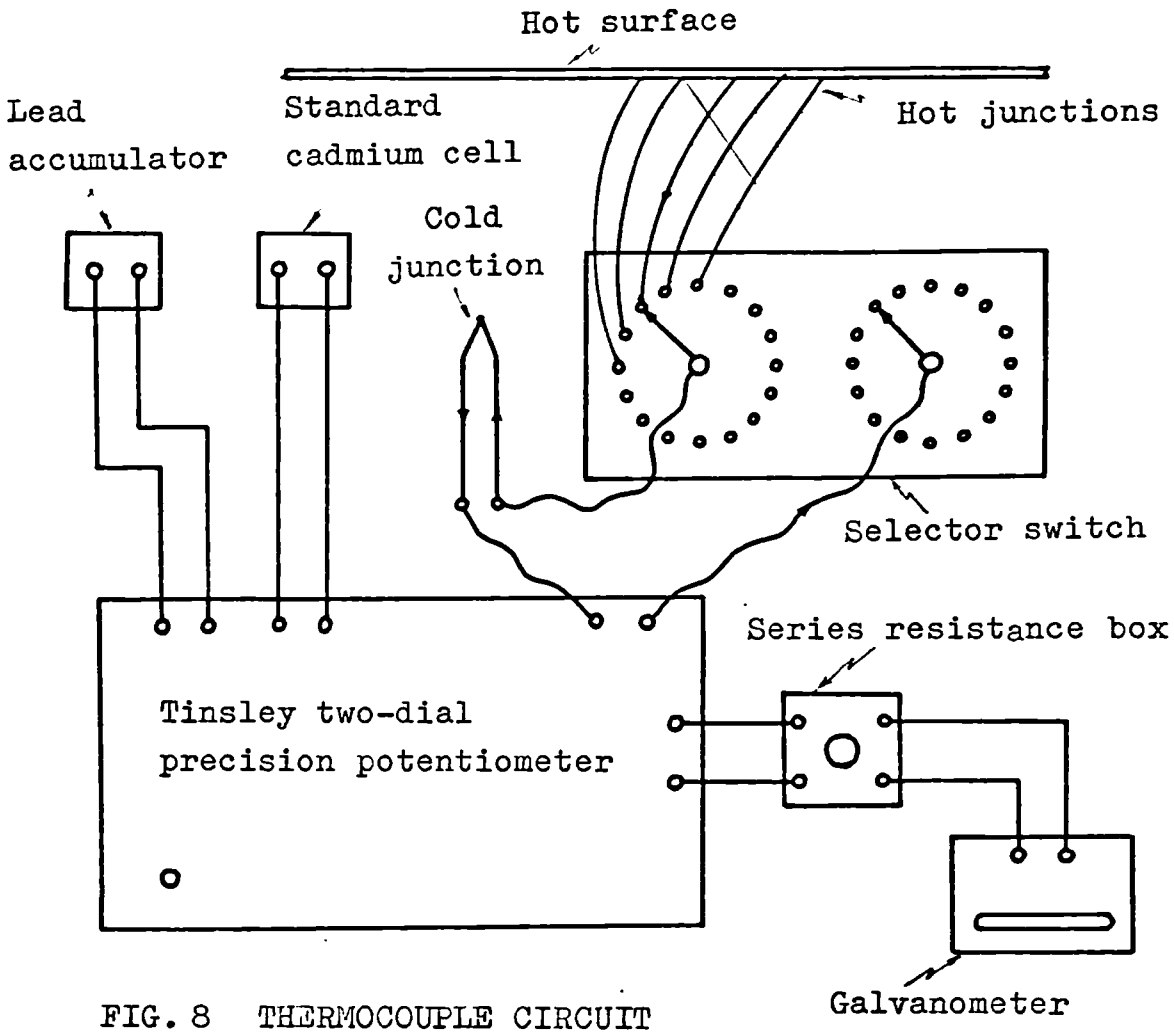

FIG. 8 THERMOCOUPLE CIRCUIT

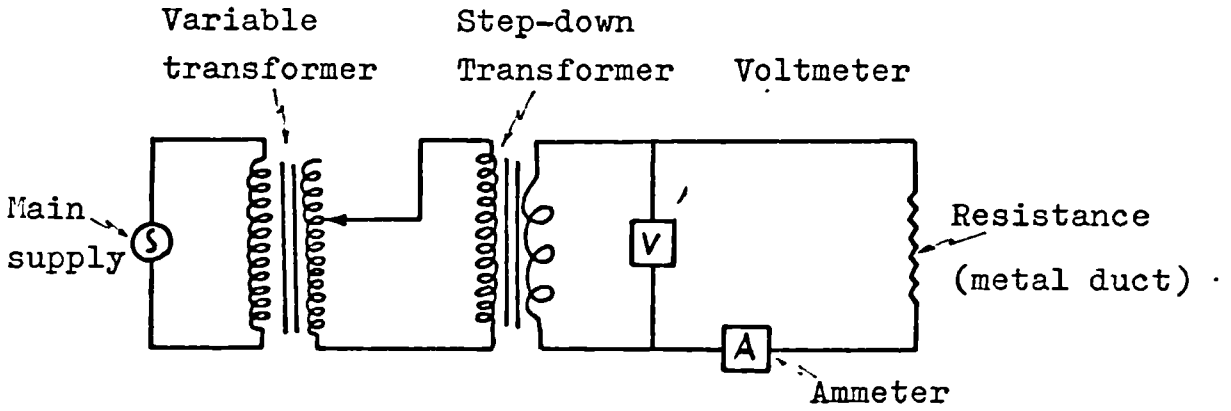

FIG. 9 HEATING CIRCUIT.

2.5 MEASUREMENT OF TEMPERATURE

Chromel-constantan thermocouples of 0.01 in. dia. were used for measuring initial and final temperatures of the air and wall temperatures. As a large number of thermocouples were used, they were connected to a common reference junction via a selector switch the terminals of which were gold-plated to ensure good electrical contact. The ice point was used as the reference temperature and its construction is described in (25).

Fig.8, p.29, shows a null-typed thermocouple circuit which consisted of a Tinsley two-dial precision potentiometer (26), a moving mirror galvanometer, a Weston standard cadmium cell and a series resistance box for controlling the sensitivity of the galvanometer. Accuracy of the measuring circuit was 1 μV and consequently, with chromel-constantan thermocouples, could measure temperature within about 0.05 deg. F.

For the thermal boundary of constant heat input per unit length, measurement of wall temperature presented some difficulties. Thermocouples could not be attached directly to the outside surface of the duct because it carried an electric current. To form an electrical insulator, a thin film of Hermetal was painted on the surface of the metal where the measurement of temperature was required

and then the thermocouple junction was attached on the Hermetal film. As the film was very thin and Hermetal is a moderate heat conductor, the error in measurement of the wall temperature owing to the presence of another medium was very small and the measured temperature was assumed equal to that of the wall.

For the constant heat input per unit length, the wall temperature varies around as well as along the duct. Though the variation around the duct is rather small when the duct is made of a good heat conductor, at each distance along the duct, five thermocouples were placed around the perimeter in order to obtain a good average of the wall temperature at that distance.

The final temperature of the heated air was measured by four thermocouples at different points in the mixing chamber and an average value was determined.

2.6 EQUILATERAL TRIANGULAR TEST SECTION FOR CONSTANT HEAT INPUT PER UNIT LENGTH OF THE DUCT

The unheated section for producing the fully developed velocity profile consisted of a divergent nozzle and a straight duct similar to the combination employed in (2.2). The heated section was made of three strips of Ferry metal, each being 1 in. wide and $15\frac{1}{4}$ in. long. Along the section, chromel-constantan thermocouples were placed at 3, $4\frac{1}{4}$, 6 and 12 in. from the entry plane of the duct. At each distance along the duct, four thermocouples were placed around the perimeter in order that a small variation of the wall temperature could be measured. An aluminium equilateral triangular form was provided as a guide in construction of the duct. Constructional details were similar to those of the rectangular test section, (2.3).

CHAPTER 3

HEAT TRANSFER IN THE THERMAL ENTRANCE REGIONS OF RECTANGULAR DUCTS

3.1 BASIC DIFFERENTIAL EQUATIONS

The Navier-Stoke's' equation for a laminar flow of a fluid in the z direction is

$$\frac{\mu}{\rho}\left(\frac{\partial^2 w}{\partial x^2}+\frac{\partial^2 w}{\partial y^2}+\frac{\partial^2 w}{\partial z^2}\right) = \frac{1}{\rho}\frac{\partial p}{\partial z}+u\frac{\partial w}{\partial x}+v\frac{\partial w}{\partial y}+w\frac{\partial w}{\partial z} \qquad (1)$$

where u, v, w = velocities in the x, y, z directions,

p = pressure.

If the flow in a duct is hydraulically fully developed, the velocity profile does not vary with the axial distance, z.

$$\therefore \quad \partial w/\partial z = 0, \quad u, v = 0,$$

$$\partial^2 w/\partial z^2 = 0, \quad \partial p/\partial z = \text{constant}.$$

Equation (1) is then reduced to

$$\frac{\partial^2 w}{\partial x^2}+\frac{\partial^2 w}{\partial y^2} = \frac{1}{\mu}\frac{\partial p}{\partial z} \qquad (1a)$$

The energy equation for an incompressible fluid with invariable physical properties is

$$\alpha\left(\frac{\partial^2 t}{\partial x^2}+\frac{\partial^2 t}{\partial y^2}+\frac{\partial^2 t}{\partial z^2}\right) = u\frac{\partial t}{\partial x}+v\frac{\partial t}{\partial y}+w\frac{\partial t}{\partial z} \qquad (2)$$

where t = local temperature,

α = thermal diffusivity, $k/C_p\rho$

Since the conduction term in the axial direction, $\partial^2 t/\partial z^2$ is negligible in comparison to those in the x and y directions, and for a fully developed flow, the velocity components u and v are zero, the energy equation is therefore reduced to

$$\frac{\partial^2 t}{\partial x^2} + \frac{\partial^2 t}{\partial y^2} = \frac{w}{\alpha}\frac{\partial t}{\partial z} \qquad (2a)$$

3.2 ANALYSIS OF PARABOLIC EQUATION

Equations (1a) and (2a) are parabolic partial differential equations. Their solution can be conveniently obtained by numerical methods. The left hand sides of both equations contain second derivatives in two dimensions and these can be replaced by finite difference approximations. For a duct of rectangular cross section, a square network is most convenient for computations.

First, the following partial differential operators are defined :-

$$Hf(x,y) = f(x+h,y) + f(x-h,y) + f(x,y+h) + f(x,y-h) - 4f(x,y)$$

$$Xf(x,y) = \tfrac{1}{2}\left(f(x+h,y+h) + f(x-h,y+h) + f(x-h,y-h) + f(x+h,y-h) - 4f(x,y) \right)$$

The two operators can be represented diagrammatically by :

H = 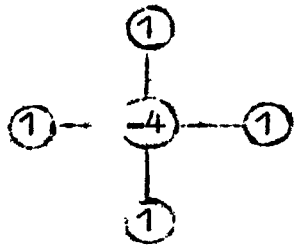 ; X = 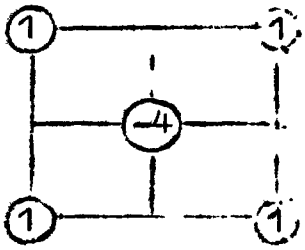

A relationship between $\frac{\partial^2 f}{\partial x^2} + \frac{\partial^2 f}{\partial y^2}$ and the two operators, H and X, can be found (19), as follows :-

Let $\alpha \equiv h.\frac{\partial}{\partial x}$ and $\beta \equiv h.\frac{\partial}{\partial y}$

The operators, H and X, can be written in terms of α and β as :

$$H = 2\cosh\alpha + 2\cosh\beta - 4$$

$$X = 2\cosh\alpha \,.\, \cosh\beta - 2$$

Solving for $\cosh\alpha$ and $\cosh\beta$ and then substituting for these in terms of $\sinh^2\alpha/2$ and $\sinh^2\beta/2$ gives

$$2\sinh\alpha/2 = \left(\tfrac{1}{2}(H + \sqrt{H^2 + 8H - 8X})\right)^{\frac{1}{2}} = A$$

$$2\sinh\beta/2 = \left(\tfrac{1}{2}(H + \sqrt{H^2 + 8H - 8X})\right)^{\frac{1}{2}} = B$$

But $\alpha = 2\sinh^{-1} A/2$

Hence $\alpha^2 = A^2 - \frac{2A^4}{4!} + \frac{2.2^2.A^6}{6!} - \frac{2.2^2.3^2.A^8}{8!} + \ldots\ldots$

and similarly,

$$\beta^2 = B^2 - \frac{2B^4}{4!} + \frac{2.2^2.B^6}{6!} - \frac{2.2^2.3^2.B^8}{8!} + \ldots\ldots$$

But $$h^2 \left(\frac{\partial^2}{\partial x^2} + \frac{\partial^2}{\partial y^2} \right) = \alpha^2 + \beta^2$$

$$= (A^2 + B^2) - \frac{1}{12}(A^4 + B^4) + \frac{1}{90}(A^6 + B^6) + \ldots\ldots$$

Replacing A and B in the above equation by their values in terms of H and X

$$h^2 \left(\frac{\partial^2}{\partial x^2} + \frac{\partial^2}{\partial y^2} \right) = H - \frac{1}{12}(H^2 + 4H - 4X) + \frac{1}{90}(H^3 + 6H^2 - 6HX) - \ldots.$$

$$= \frac{2H}{3} + \frac{X}{3} + \frac{H^2}{60} + \frac{HX}{15} + \ldots.$$

In the present work, the first order terms will give sufficient accuracy so that

$$\frac{\partial^2 f}{\partial x^2} + \frac{\partial^2 f}{\partial y^2} = \frac{1}{6h^2}(4H + 2X)\, f(x,y)$$

It is convenient to define a new operator, K,

where $$K \equiv (4H + 2X)$$

The operator K can be represented diagrammatically as :

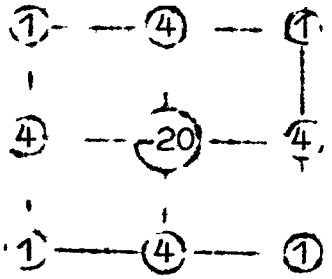

$$\frac{\partial^2 f}{\partial x^2} + \frac{\partial^2 f}{\partial y^2} = \frac{1}{6h^2} K\, f(x,y) \qquad (3)$$

Finite difference applied to Simpson's Rule in two dimensions.

The average value of a quantity over an area such as velocity or temperature, can be computed numerically by means of Simpson's Rule in two dimensions. For a function f(x,y), the average value can be written in finite difference form (20) as :

$$\frac{1}{A}\int_{o}^{A} f(x,y)dA = \frac{h^2}{9N}\sum\big(\,4f(x+h,y) + 4f(x-h,y) + 4f(x,\,y+h) + 4f(x,y-h) + f(x+h,y+h) + f(x+h,y-h) + f(x-h,y+h) + f(x-h,y-h) + 16f(x,y)\,\big) \qquad (4)$$

where N is the number of squares of side, h, into which the area A is divided.

Diagrammatically,

$$\int_{A} f(x,y)dA = \frac{h^2}{9}$$

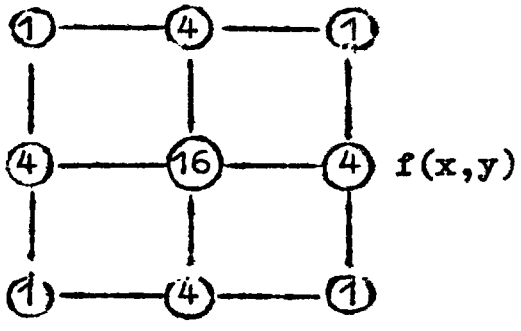

3.3 EXACT SOLUTION TO THE NAVIER-STOKE'S EQUATION

For fully developed laminar flow in a rectangular duct, equation (1a) can be solved exactly (18).

In a duct having dimensions a and b in the x- and y-directions respectively, the velocity, w, at any point (x,y) on the cross section is given by :

$$w = C(x^2-bx) + \sum_{m=1}^{\infty}\left[\sin \frac{m\pi x}{b} \left(A_m \cosh \frac{m\pi y}{b} + B_m \sinh \frac{m\pi y}{b} \right)\right]$$

where $C = \frac{1}{\mu}\frac{dp}{dz}$

$$A_m = 2b^2C \left(\cos m\pi - 1 \right) / m^3\pi^3$$

$$B_m = -A_m \left(\cosh \frac{m\pi a}{b} - 1 \right) / \sinh \frac{m\pi a}{b}$$

It is convenient to define a number of dimensionless parameters as follows :

aspect ratio, $\alpha^+ = b/a$,

velocity, $w^+ = -w/\frac{a^2}{\mu}\frac{dp}{dz}$,

co-ordinates $x^+ = x/a$, and $y^+ = y/a$.

Hence,

$$w^+ = \tfrac{1}{2}(\alpha^+ x^+ - x^{+2}) + \sum_{m=1}^{\infty} \left\{(\cos m\pi - 1) \sin \frac{m\pi x^+}{\alpha^+} \cdot \frac{2\alpha^{+2}}{m^3\pi^3}\right.$$

$$\left. X \left(\cosh \frac{m\pi y^+}{\alpha^+} - \frac{\cosh \frac{m\pi}{\alpha^+} - 1}{\sinh \frac{m\pi}{\alpha^+}} \sinh \frac{m\pi y^+}{\alpha^+}\right)\right\} \qquad (5)$$

To determine the average dimensionless velocity, w_b^+, the cross sectional area of the duct is divided into a square network and velocities at nodal points are calculated from the above equation.

The average velocity is defined as

$$w_b^+ = \frac{\iint w^+ \, dx \, dy}{A_c}$$

By applying the Simpson's rule in two dimensions, equation (4), to the velocity distribution, the average velocity can be computed.

3.4 NUMERICAL SOLUTION TO THE ENERGY EQUATION

By combining equations (2a) and (3), the energy equation can be put into finite difference form as :

$$\frac{K\, t(x,y,z)}{6h^2} = \frac{w}{\alpha} \frac{t(x,y,z+\Delta z) - t(x,y,z)}{\Delta z}$$

Rearranging this, the energy equation becomes

$$t(x,y,z+\Delta z) - t(x,y,z) = \frac{w_b}{w} \frac{\alpha \Delta z}{w_b d_h^2} \frac{1}{e^2} \frac{K\, t(x,y,z)}{6} \qquad (6)$$

where e = ratio of the side of the square grid, h, to the hydraulic diameter of the duct, d_h.

Using this equation, the temperature distribution at any cross section of the duct can be computed from the

temperature distribution at the preceding finite step in the z-direction, i.e. along the axis of the duct. The computing procedure is as follows :

First, the cross sectional area is divided into a square grid of side h.

From equation (6), $\frac{\alpha \Delta z}{w_b d_h^2}$ can be written as $\frac{z/d_h}{Re.Pr}$ where Re is the Reynolds number $\frac{\rho w_b d_h}{\mu}$, Pr is the Prandtl number $C_p \mu/k$ and $Re.Pr/(z/d_h)$ is the Graetz number, Gz. Hence, $\alpha \Delta z/w_b d_h^2$ is a small increment of the reciprocal of the Graetz number, and it must be chosen so that $\frac{w_b^+}{w} \frac{\alpha \Delta z}{w_b d_h^2} \frac{1}{e^2}$ is smaller than $\frac{1}{2}$ in order that the solution to the equation (6) is in a steady state.

The ratio w_b/w in the equation (6) at any nodal point in the cross section of the rectangular duct can be calculated from equation (5) since $w_b/w = w_b^+/w^+$.

To solve equation (6) numerically, initial and wall values of temperature are also required, and they can be obtained by using a suitable dimensionless temperature, the form of which depends upon the thermal boundary condition.

3.5 SOLUTION FOR CONSTANT WALL TEMPERATURE

For a duct with constant wall temperature, a dimensionless temperature, θ, is defined as

$$\theta = \frac{t_w - t}{t_w - t_o}$$

where t = local fluid temperature,

t_w = wall temperature = constant,

t_o = fluid initial temperature = constant.

$\therefore \quad \theta_{b,o} = 1 \quad \text{and} \quad \theta_{w,o} = \theta_w = 0.$

The energy equation (2a) can be written as

$$\frac{\partial^2\theta}{\partial x^2} + \frac{\partial^2\theta}{\partial y^2} = \frac{w}{\alpha}\frac{\partial\theta}{\partial z}$$

and consequently, equation (6) becomes

$$\theta(x,y,z+\Delta z) - \theta(x,y,z) = \frac{w_b}{w}\frac{\alpha\,\Delta z}{w_b d_h^2}\frac{1}{e^2}\frac{K\theta(x,y,z)}{6} \qquad (7)$$

Temperature distributions along the duct can be computed step by step by means of the above equation and hence, the Nusselt numbers along the duct are deduced. However, because the computation involved is very lengthy, a fast digital computer is required.

Nusselt Numbers, Nu.

By definition, the coefficient of convective heat transfer, $h = \dot{q} / A_s(t_w - t_b)$

where $\dot{q}$ = heat transfer rate,

A_s = surface area from which heat is transferred.

Consider an elementary length, dz, of the duct.

Heat transfer by convection, $d\dot{q} = h\, dA_s(t_w - t_b)$

$= h\, P\, (t_w - t_b)\, dz$

where P is the perimeter of the duct.

Rate of change of enthalpy, $d\dot{H} = \rho w_b A_c C_p \frac{dt_b}{dz} dz$

where A_c is the cross sectional area of the duct.

By the first law of thermodynamics, $d\dot{q} = d\dot{H}$, since no shaft work is done.

Hence $h\, P\, (t_w - t_b) = \rho w_b A_c C_p \frac{dt_b}{dz}$

and $h = \frac{k}{\alpha} w_b \frac{d_h}{4} \frac{dt_b}{dz} / (t_w - t_b)$

or in dimensionless form,

$$h = \frac{k}{\alpha} w_b \frac{d_h}{4} \frac{\Delta\theta_b}{\Delta z} / \theta_b$$

By definition, the peripheral Nusselt number,

$$Nu_p = h.d_h / k_b$$

Hence, $$Nu_p = \frac{1}{4} \frac{w_b d_h^2}{\alpha \Delta z} \frac{\Delta\theta_b}{\theta_b} \qquad (8)$$

In the above equation, $\frac{w_b d_h^2}{\alpha \Delta z}$ has already been chosen in order to solve the energy equation as described in (3.4). The bulk dimensionless temperature, θ_b, at any position along the duct can be determine by applying the Simpson's rule in two dimension, equation (4), to the temperature distribution at that position which has already been computed numerically from equation (7).

For design purposes, a mean value of the Nusselt number is more suitable than the local one. The mean Nusselt number, Nu_m, is defined as :

$$Nu_m = \frac{\int_0^z Nu_p \, dz}{z}$$

The mean Nusselt number can be computed numerically from the peripheral Nusselt numbers, Nu_p, determined at small equal intervals along the duct.

$$Nu_m = \sum_0^N Nu_p/N \qquad (9)$$

where N = number of intervals considered = $z/\Delta z$.

Experimentally, it is inconvenient to determine the mean Nusselt number defined above, and the logarithmic mean Nusselt number, which is based upon the logarithmic mean temperature difference, is employed instead. This can be calculated as follows:

Consider a length z of the duct.

$$h\,P\,z\,\Delta t_l = w_b \rho\, C_p (t_b - t_o)\, A_c$$

where Δt_l = logarithmic temperature difference,

$$= \frac{(t_w - t_o) - (t_w - t_b)}{\ln \dfrac{(t_w - t_o)}{(t_w - t_b)}}$$

$$= (t_b - t_o) / \ln \frac{t_w - t_o}{t_w - t_b}$$

$$Nu_l = \frac{h.d_h}{k_b} = \frac{\rho C_p}{k_b} \frac{w_b A_c}{P\,z} d_h \ln \frac{t_w - t_o}{t_w - t_b}$$

$$= \frac{w_b d_h^2}{4\alpha \Lambda z} \frac{1}{N} \ln 1/\theta_b \qquad (10)$$

It has been found from the results that the mean Nusselt numbers predicted by equations (9) and (10) agree within 0.5 %.

Example of Computation

For the aspect ratio, α^+, of 2.0.

Let the dimensions of the duct be a x 2a.

Hydraulic diameter, $d_h = \frac{4 \times 2a \times a}{6a} = 4a/3$.

Choose the finite step, $h = a/10 = 3d_h/40$.

Equation (7) becomes

$$\Delta\theta = \frac{1}{6}\,\frac{w_b}{w}\cdot\frac{\alpha\Delta z}{w_b d_h^2}\cdot\frac{1600}{9}\cdot K\theta(x,y,z)$$

Choose $$\frac{\alpha\Delta z}{w_b d_h^2} = \frac{9}{32000}$$

$$\Delta\theta = \frac{w_b}{w}\,\frac{K\theta(x,y,z)}{120}$$

From equation (8), $$Nu_p = \frac{8000}{9}\,\frac{\Delta\theta_b}{\theta_b}$$

and from equation (10), $$Nu_1 = \frac{8000}{9}\,\frac{\ln 1/\theta_b}{N}$$

With all the necessary variables obtained numerically above, a computer program can be written to solve for the temperature distributions and the local and mean Nusselt numbers along the rectangular duct. The flow diagram of a computer program can be seen on p. 46 and 47. Computer programs were written for aspect ratios from 1 to 6 and some of the results obtained by using an I.C.T. Atlas computer are shown in figs. 11 & 12. Because of similarity, only a quarter of the rectangular cross sectional area had to be considered during the computation.

FIG. 10 FLOW DIAGRAM OF COMPUTER PROGRAM FOR HEAT TRANSFER IN THE THERMAL ENTRANCE REGIONS OF RECTANGULAR DUCTS.

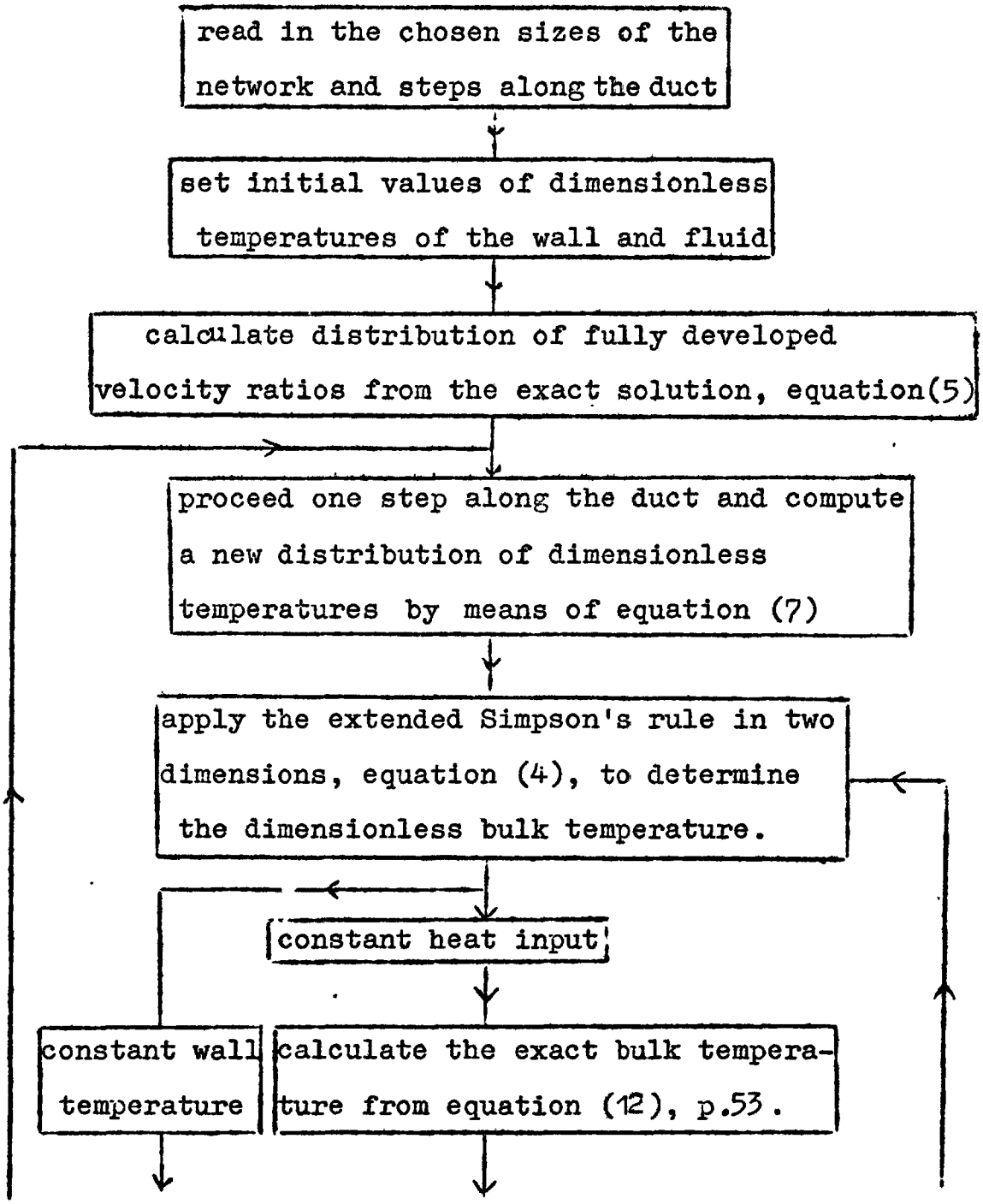

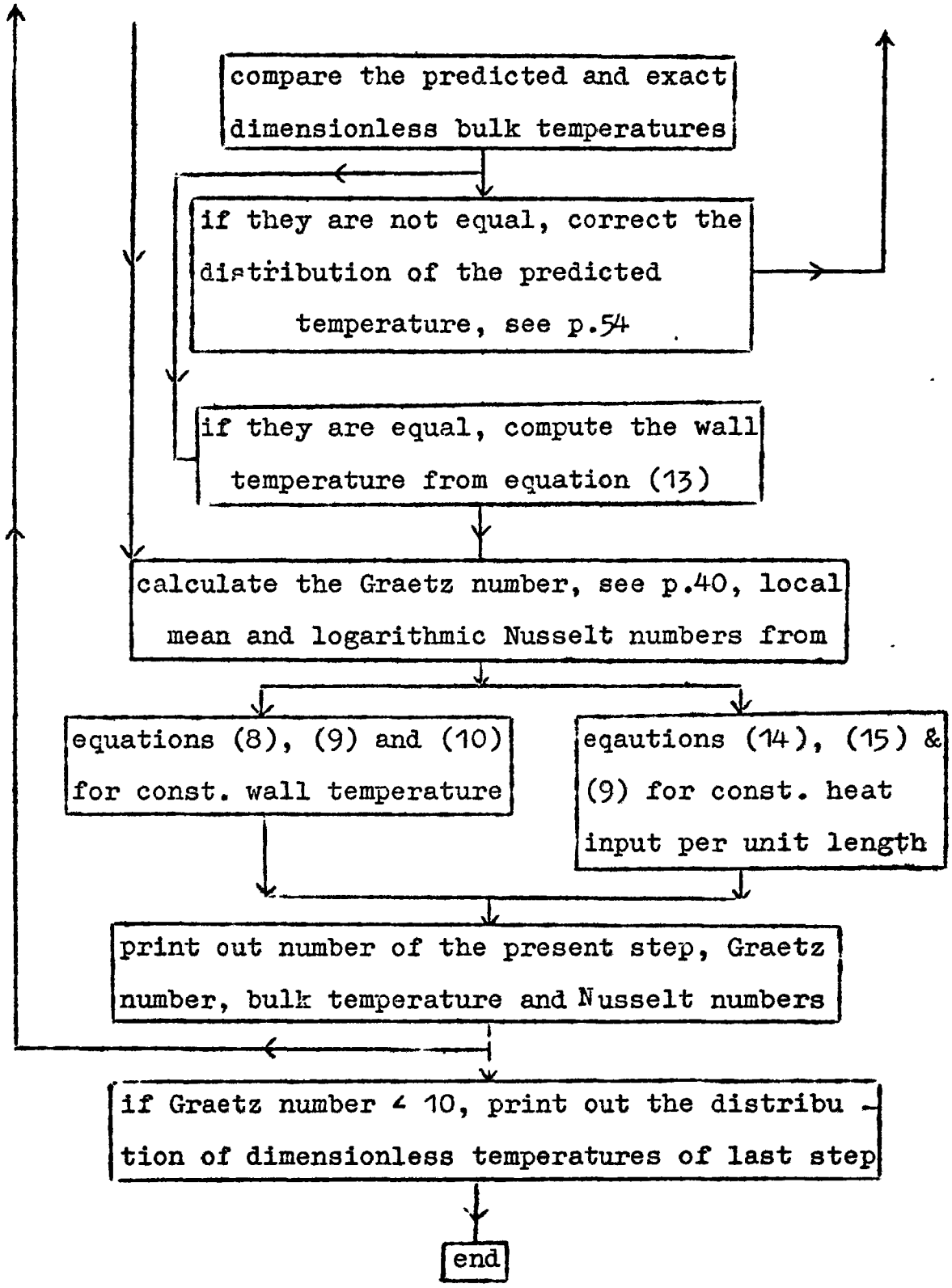
compare the predicted and exact dimensionless bulk temperatures
if they are not equal, correct the distribution of the predicted temperature, see p.54
if they are equal, compute the wall temperature from equation (13)
calculate the Graetz number, see p.40, local mean and logarithmic Nusselt numbers from
equations (8), (9) and (10) for const. wall temperature
eqautions (14), (15) & (9) for const. heat input per unit length
print out number of the present step, Graetz number, bulk temperature and Nusselt numbers
if Graetz number < 10, print out the distribution of dimensionless temperatures of last step
end

Variations of the dimensionless bulk temperature of the fluid with the reciprocal of the Graetz number, $(z/d_h)/Re.Pr.$

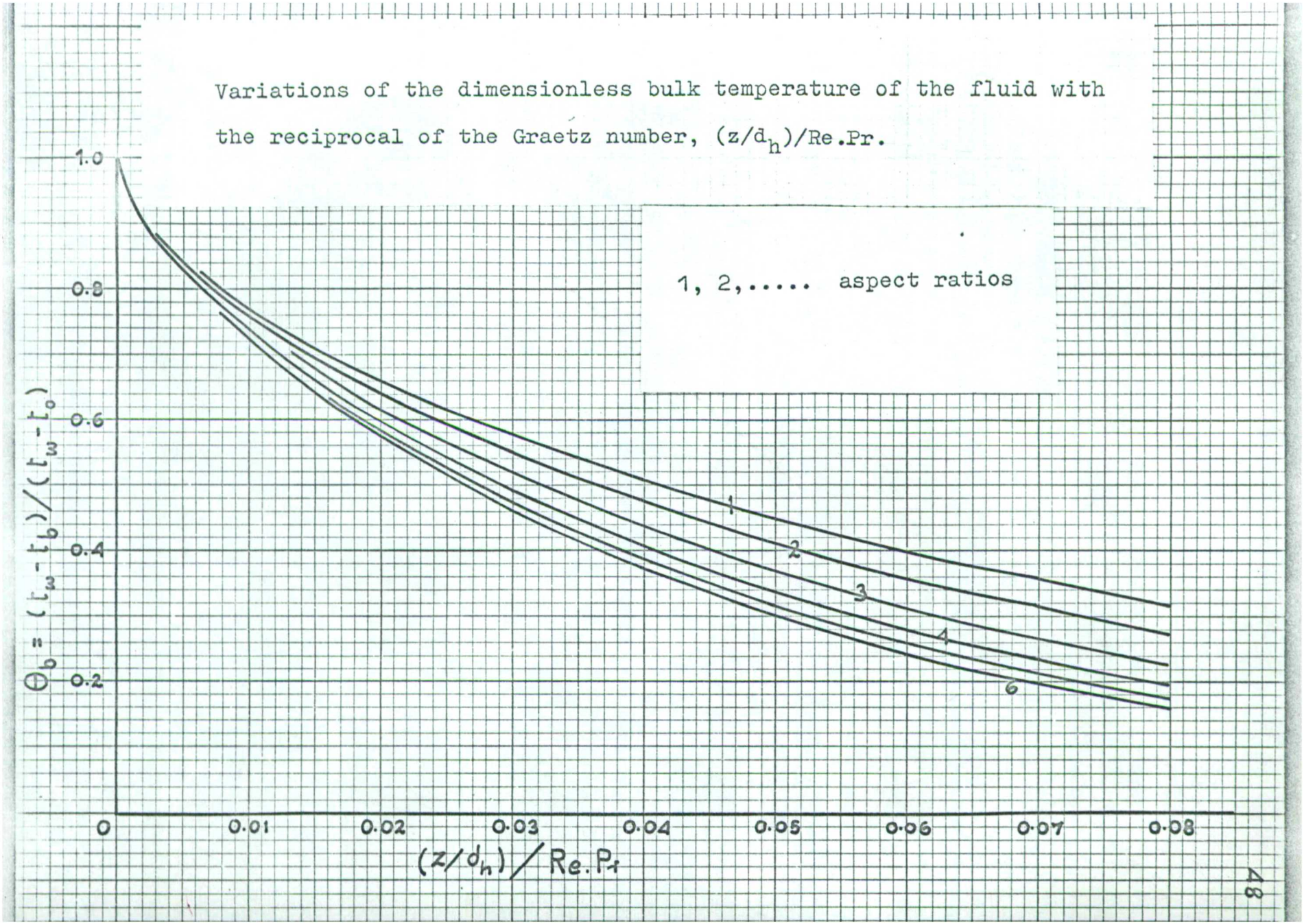

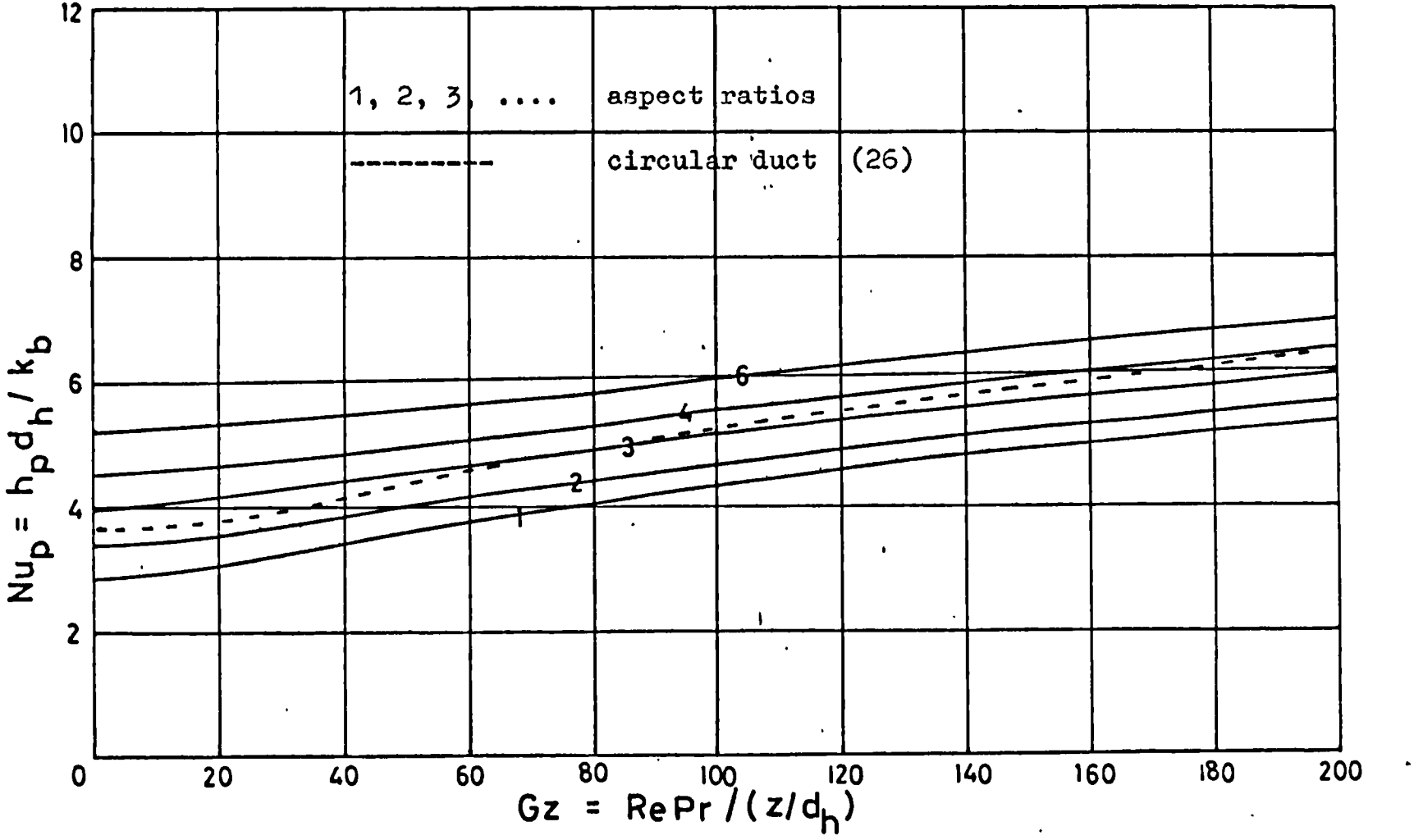

Fig. 11 Predicted peripheral Nusselt numbers versus Graetz numbers for fully developed velocity profiles in rectangular ducts with constant wall temperature.

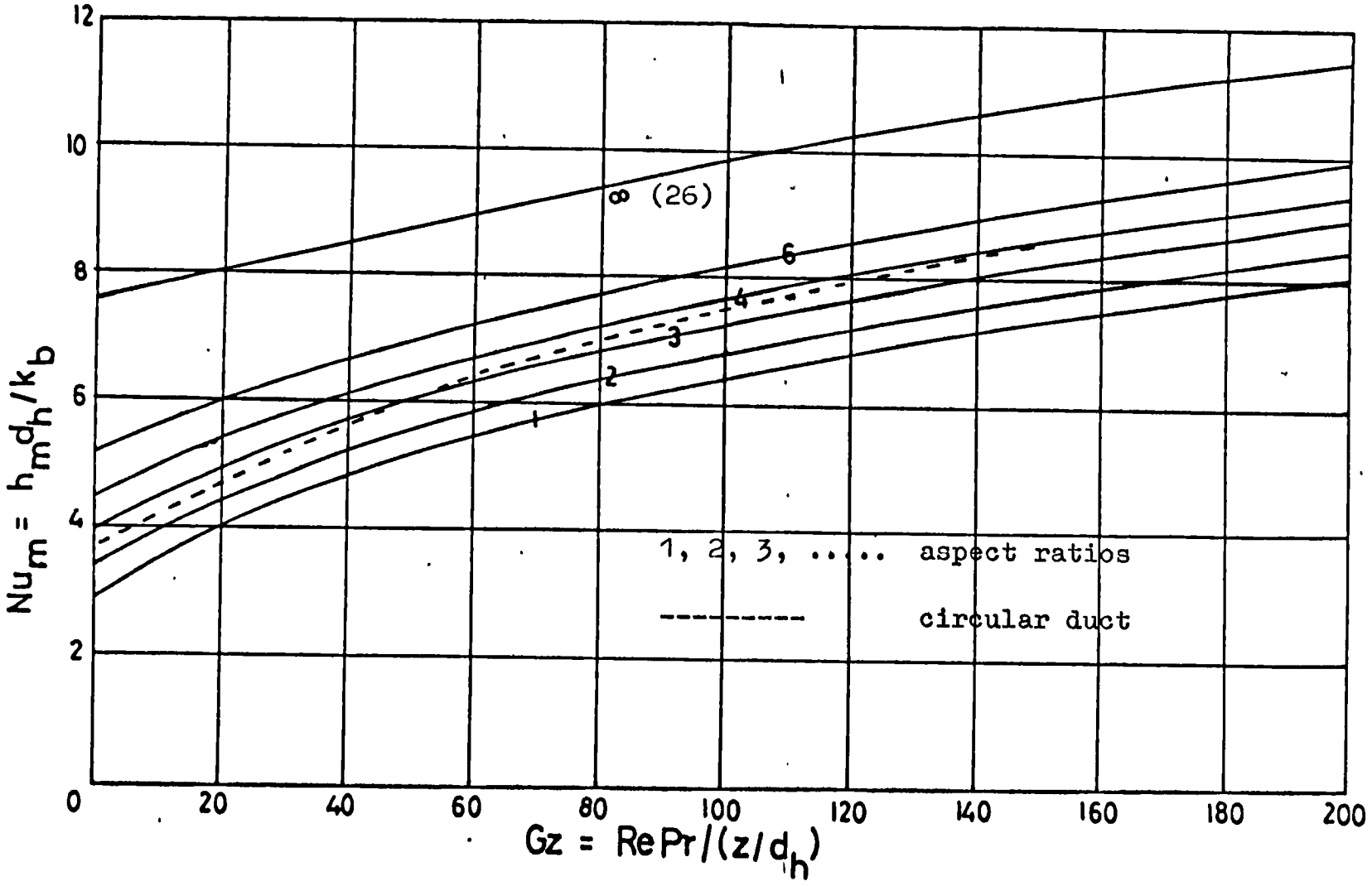

Fig. 12 Predicted mean Nusselt numbers v.s. Graetz numbers for fully developed velocity profiles in rectangular ducts with constant wall temperature.

3.5 SOLUTION FOR CONSTANT HEAT INPUT PER UNIT LENGTH

For this thermal boundary condition, it can be shown that the bulk temperature of the fluid rises linearly along the duct as follows :

From the first law of thermodynamics, heat input per unit length of the duct = rate of change of enthalpy.

$$q' = w_b \rho C_p A_c \frac{dt_b}{dz} = \text{constant.}$$

For a given flow rate of the fluid assumed incompressible, w_b, ρ, C_p and A_c are constant.

$$\therefore \quad \frac{dt_b}{dz} = \text{constant.}$$

When the heat input per unit length of the duct is constant, the wall temperature varies along and around the duct. However, if the duct is made of a good heat conductor, the wall temperature can be assumed constant around the parameter at any cross section and to vary only with distance along the duct. At each step of computation, a new value of wall temperature has to be computed from the boundary condition of constant heat input.

3.6.1 Determination of Fluid Temperatures

For constant heat input per unit length of the duct, it is convenient to define a dimensionless temperature

$$\beta = \frac{t - t_o}{\frac{dt_b}{dz}\frac{d_h^2 w_b}{\alpha}}$$

where t_o = initial temperature of the fluid assumed uniform.

At any cross section, the distribution of fluid temperatures can be predicted numerically from the fluid temperatures at the previous section by combining equations (2a) and (3) and substituting for t in terms of β.

$$\beta(x,y,z+\Delta z) - \beta(x,y,z) = \frac{w_b^+}{w^+}\frac{\alpha \Delta z}{w_b d_h^2}\frac{1}{e^2}\frac{K\beta(x,y,z)}{6} \qquad (11)$$

An approximate bulk temperature β_b' at the new position can be evaluated from the distribution of temperatures by means of equation (4).

However, by definition, the true bulk temperature is :

$$\beta_b = \frac{t_b - t_o}{\frac{dt_b}{dz}\frac{w_b d_h^2}{\alpha}}$$

$$= \frac{t_b - t_o}{z}\frac{z}{\frac{dt_b}{dz}\frac{w_b d_h^2}{\alpha}}$$

As already shown, $\frac{dt_b}{dz}$ = constant for constant heat input per unit length, hence

$$\frac{dt_b}{dz} = \frac{t_b - t_o}{z}$$

$$\therefore \quad \beta_b = \frac{\alpha z}{w_b d_h^2} = \frac{\alpha \Delta z N}{w_b d_h^2} \qquad (12)$$

where N = the number of step being considered.

Since $(w_b d_h^2)/\alpha \Delta z$ has been chosen to have a definite value when equation (11) is solved numerically, the bulk temperature at any position can readily be calculated from equation (12).

If the prediction of fluid temperatures by means of equation (11) were accurate, the predicted bulk temperature, β_b', would be the same as β_b calculated from equation (12). In computation, it will be found that β_b' differs from β_b and a correction is needed for the predicted fluid temperatures, β, such that $\beta_b' = \beta_b$.

Because of non-linearity of the temperature and velocity profiles, the correction will have to be varied from point to point on the mesh with the maximum correction at the centre. The following expression would be most suitable.

$$\text{Corrected temperature} = \beta + \frac{(\beta_w - \beta)}{(\beta_w - \beta_b)}(\beta_b - \beta_b')$$

But the factor, $\frac{(\beta_w - \beta)}{(\beta_w - \beta_b)}$, cannot yet be determined since the wall temperature, β_w, is still not known. A good approximation can, however, be obtained by using the velocity ratio, w/w_b, for fully developed velocity profile instead of $(\beta_w - \beta)/(\beta_w - \beta_b)$. This is justifiable because the two terms differ only slightly, and moreover, $(\beta_b - \beta_b')$ is quite small in comparison to β_b during any step.

$$\therefore \text{ corrected temperature } \simeq \beta + \frac{w}{w_b}(\beta_b - \beta_b')$$

A new value of the approximate bulk temperature, β_b', is then computed from the new distribution of fluid temperatures, and if it is still not equal to β_b, the same procedure is repeated.

3.6.2 Determination of Wall Temperature

To predict the temperature at the wall from the values at other points inside the duct, it is necessary to satisfy the energy equation. It is convenient to consider a surface B at a constant distance h/2 inside the wall of the duct and of axial length dz, fig. 13, p.55.

By the first law of thermodynamics, the heat transferred across B must equal the change of enthalpy of the fluid flowing inside B. The latter can be evaluated as the

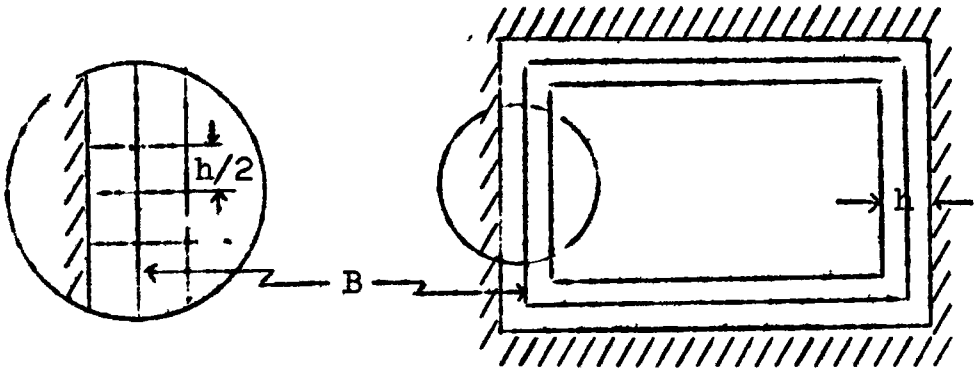

Fig.13

difference between the change of enthalpy for the entire duct less that for the gap between the surface B and the wall of the duct.

These quantities can be expressed in the finite difference form. Across any section of B of area h.dz, the temperature gradient is $(t_w - t_h)/h$, where t_h refers to the fluid temperature at a distance h from the wall of the duct and the corresponding heat transfer rate is

$$k.h.dz(t_w - t_h)/h$$

Similarly the rate of change of enthalpy through an element of area $h.\frac{h}{2}$ between the wall and surface B can be expressed as

$$\frac{h^2}{2} \rho w C_p \frac{dt}{dz} dz$$

Summing up round the perimeter, one can equate the total heat transfer through B to the net change of enthalpy inside B as

$$\sum k(t_w - t_h)dz = \rho\, w_b\, C_p\, A_c \frac{dt}{dz}b\, dz - \sum \frac{h^2}{2} \rho\, w\, C_p \frac{dt}{dz}\, dz$$

Certain assumptions must be made to solve this equation. For a metal duct, the temperature variation around the periphery is small and it is assumed that t_w is constant. From experimental results, this is justifiable.

If the gap between the surface B and the duct wall is small compared to the duct dimension d_h, the mean velocity in any element can be taken as $w_h/4$ and the axial temperature gradient as dt_h/dz.

$$\therefore \quad knt_w - \sum t_h = \rho\, w_b\, C_p\, A_c \frac{dt}{dz}b - \sum \frac{h^2 \rho\, w_h C_p}{8} \frac{dt}{dz}h$$

where n is the grid points on the duct wall.

This can be written in terms of the dimensionless temperature β and solved for the wall temperature.

$$\therefore \quad \beta_w = \frac{e}{4} + \frac{1}{n}\sum \beta_h - \frac{e^2}{8n} \sum \frac{w_b d_h^2}{\alpha \Delta z} \frac{w_h}{w_b} \Delta \beta_h \qquad (13)$$

In the first summation for β_h, the values at the four corners have to be included twice so that there are n terms in the summation. In the second summation, each value is included only once.

In this equation, the values of e, n and $\frac{w_b\, d_h}{\alpha \Delta z}$ can be calculated as soon as h is fixed; the velocity w_h/w_b has been obtained above, while $\Delta\beta_h$ and $\sum \beta_h$ can be

determined from the figures found in (3.6.1) . Hence β_w can be determined at any point in the duct.

3.6.3 Nusselt numbers

By the same approach as that for the condition of constant wall temperature, the peripheral heat transfer coefficient, h_p, for constant heat input per unit length is

$$\frac{k}{\alpha} w_b \frac{d_h}{4} \frac{dt_b}{dz} / (t_w - t_b)$$

or in terms of dimensionless temperature, β

$$h_p = \frac{k}{4d_h} \frac{1}{(\beta_w - \beta_b)}$$

$\therefore$ peripheral Nusselt number, $Nu_p \equiv \frac{h_p d_h}{k}$

$$= \frac{1}{4(\beta_w - \beta_b)} \qquad (14)$$

The logarithmic mean temperature difference, Δt_l

$$\equiv \frac{(t_w - t_b) - (t_{w,o} - t_o)}{\ln \frac{t_w - t_b}{t_{w,o}}}$$

$$\equiv \frac{\beta_w - \beta_b - \beta_{w,o}}{\ln \frac{\beta_w - \beta_b}{\beta_{w,o}}} \quad \frac{w_b d_h^2}{\alpha} \frac{dt_b}{dz}$$

$$\therefore \quad h_1 = \frac{k}{4d_h} \frac{\ln \frac{\beta_w - \beta_b}{\beta_{w,o}}}{\beta_w - \beta_b - \beta_{w,o}}$$

$$\text{and} \quad Nu_1 = \frac{1}{4} \frac{\ln \frac{\beta_w - \beta_b}{\beta_{w,o}}}{\beta_w - \beta_b - \beta_{w,o}} \qquad (15)$$

The mean Nusselt number, Nu_m, can be computed by means of equation (9) like that for constant wall temperature.

Example of Computation.

For the aspect ratio, α^+, of 2.0.

Let the dimensions of the cross section be a x 2a

Hydraulic diameter, d_h = 4a/3

Choose the finite step, h = a/16

$\therefore$ Ratio, $e = h/d_h$ = 3/64

Energy equation (11) becomes

$$\beta(x,y,z+\Delta z) - \beta(x,y,z) = \frac{w_b}{w} \frac{\alpha \Delta z}{w_b d_h^2} \left(\frac{64}{3}\right)^2 \frac{K\beta(x,y,z)}{6}$$

Choose the step $\frac{\alpha \Delta z}{w_b d_h^2} = \left(\frac{3}{64}\right)^2 \frac{1}{20} = \frac{9}{81920}$

$$\therefore \quad \beta(x,y,z+\Delta z) = \frac{w_b}{w} \frac{K\beta(x,y,z)}{120} + \beta(x,y,z)$$

Equation(13) for the wall temperature becomes

$$\beta_w = \frac{3}{256} - \frac{20}{8n} \sum \frac{w_h}{w_b} \Delta\beta_h + \frac{\sum^n \beta_h}{n}$$

At the first step, $\beta_o = 0$, and $\beta_{w,o} = \frac{3}{256}$.

As the initial temperatures and finite steps now have numerical values, a computer program can be written for solving the temperature distributions and the Nusselt numbers along the duct. Computer programs were written for aspect ratios from 1 to 4 and results obtained from the I.C.T. Atlas computer are plotted on p. 60 to 62, and tabulated in Appendix(7.4). The flow diagram of such a program can be seen on p.46 & 47. A comparison of the Nusselt numbers between the thermal conditions of constant heat input per unit length and of constant wall temperature is shown in fig.17, p.63.

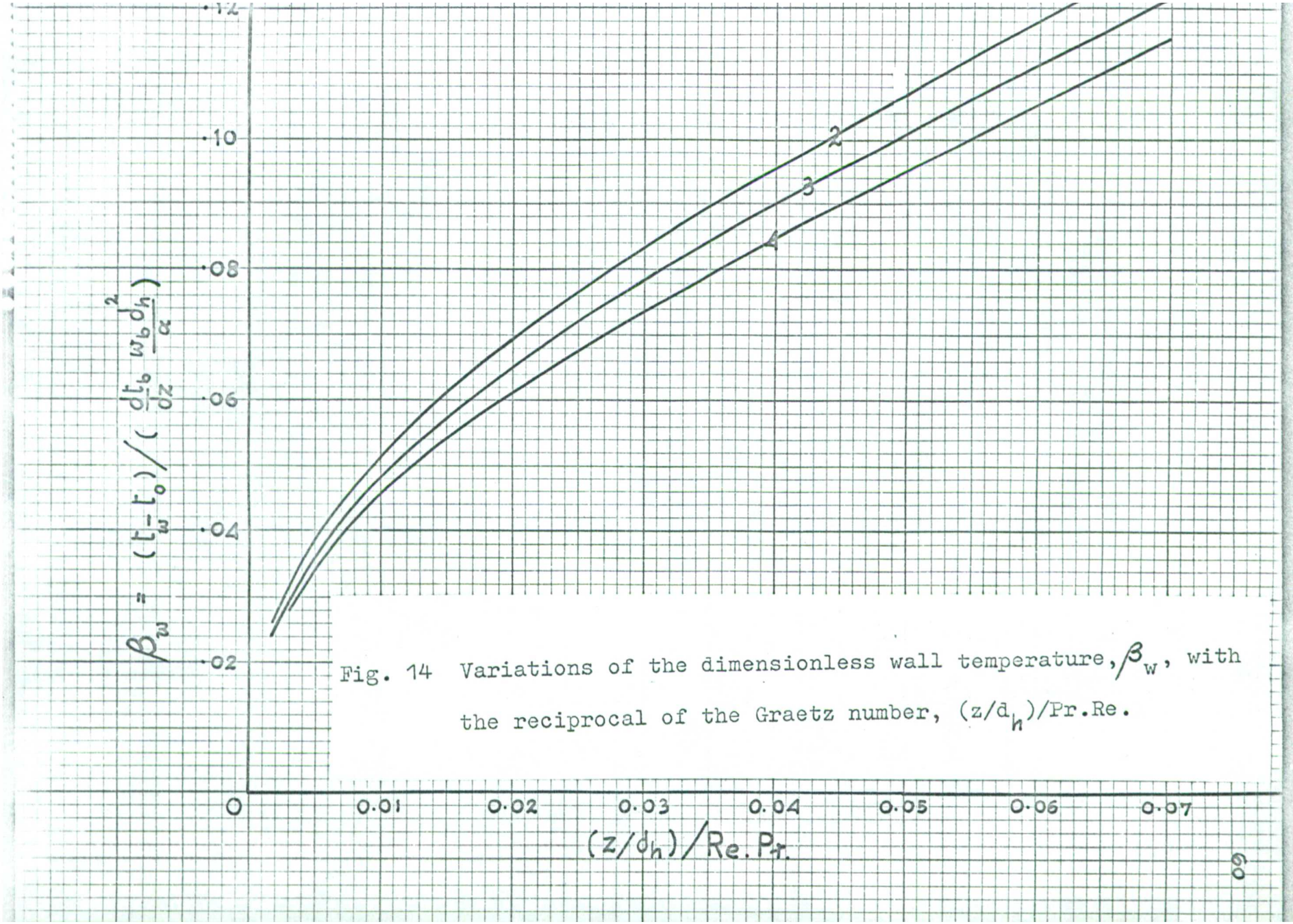

Fig. 14 Variations of the dimensionless wall temperature, β_w, with the reciprocal of the Graetz number, $(z/d_h)/Pr.Re.$

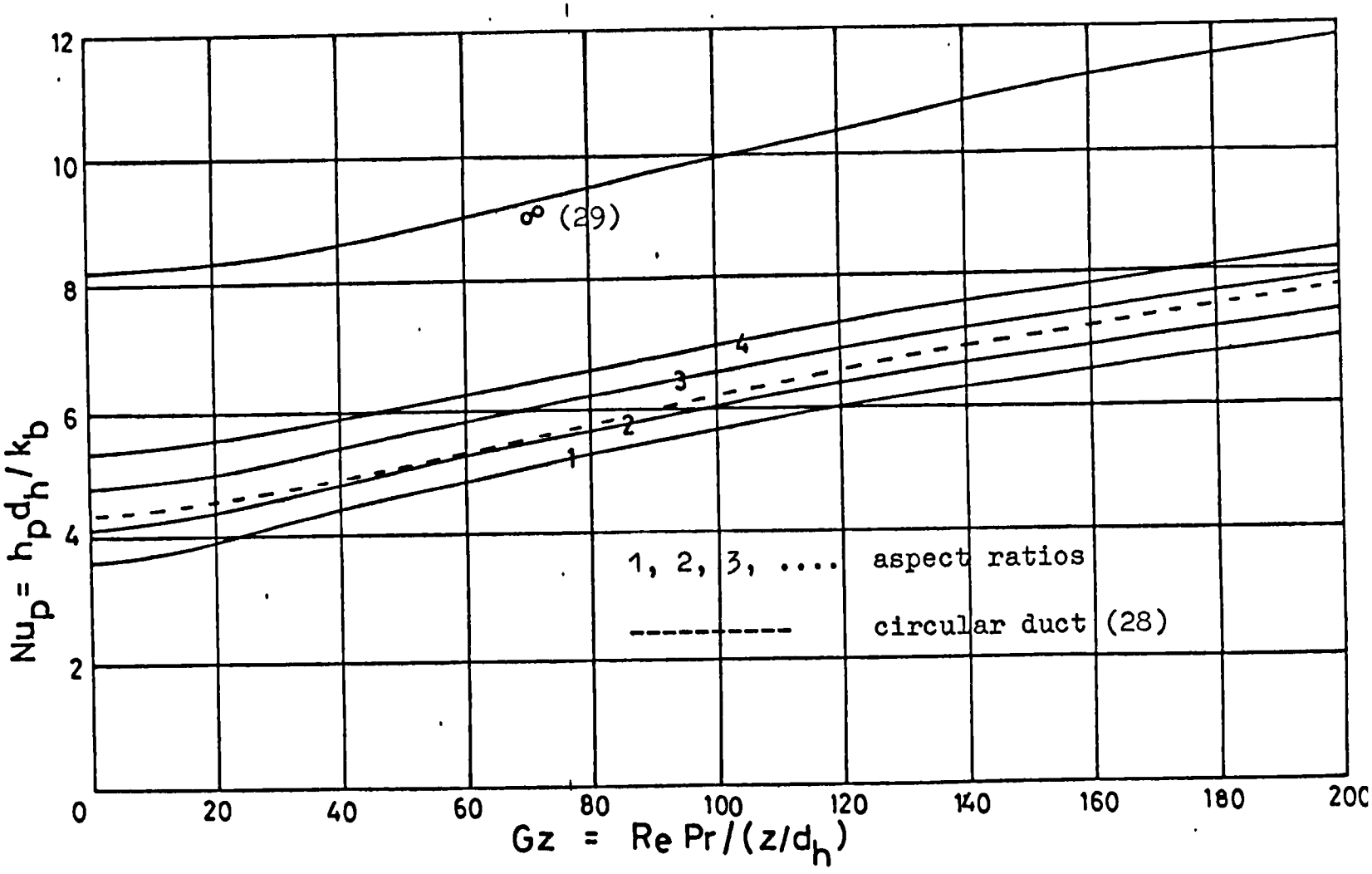

Fig. 15 Predicted peripheral Nusselt numbers v.s. Graetz numbers for fully developed velocity profiles in rectangular ducts with constant heat input per unit length of the ducts.

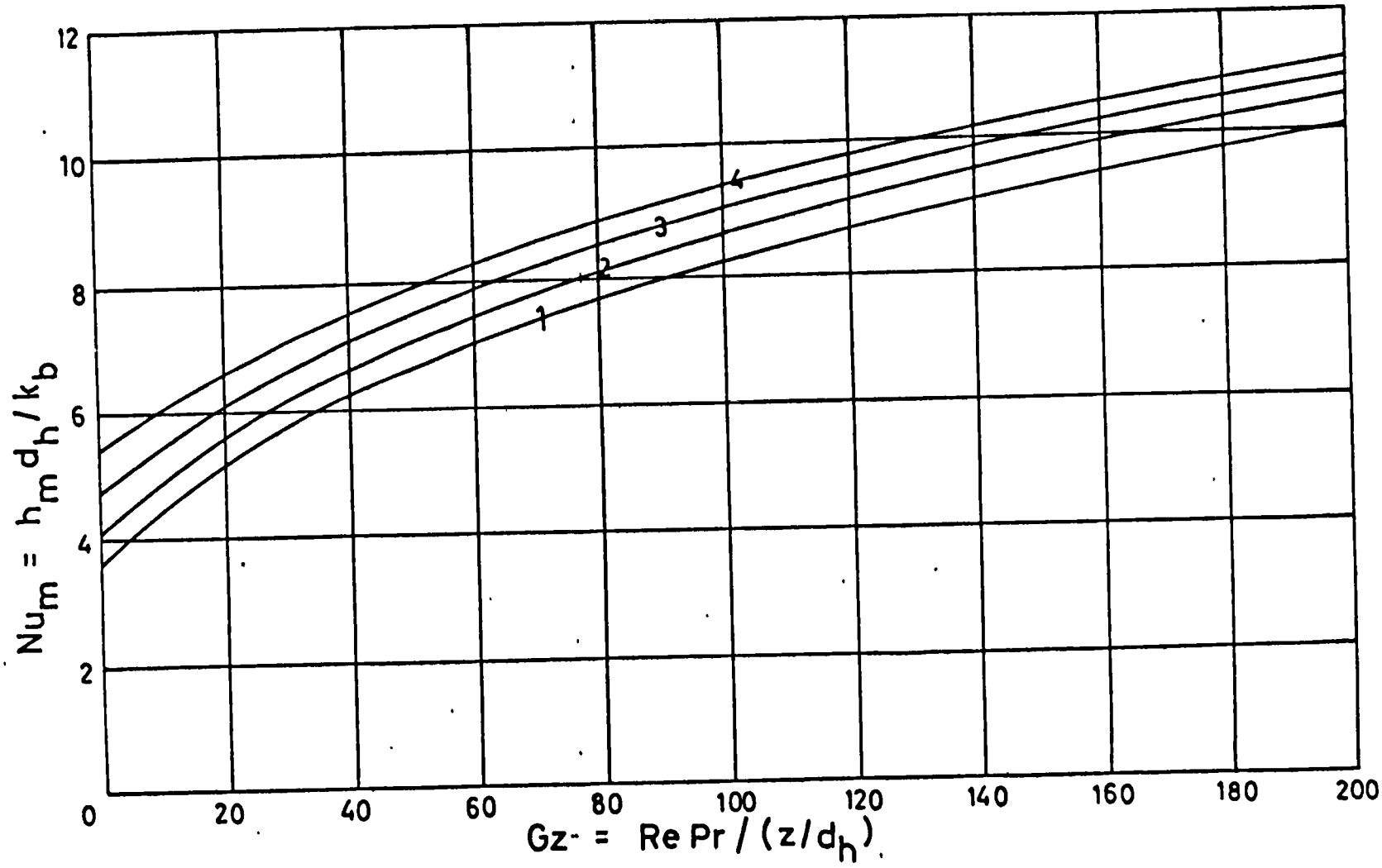

Fig. 16 Predicted mean Nusselt numbers v.s. Graetz numbers for fully developed velocity profiles in rectangular ducts with constant heat input per unit length of the ducts.

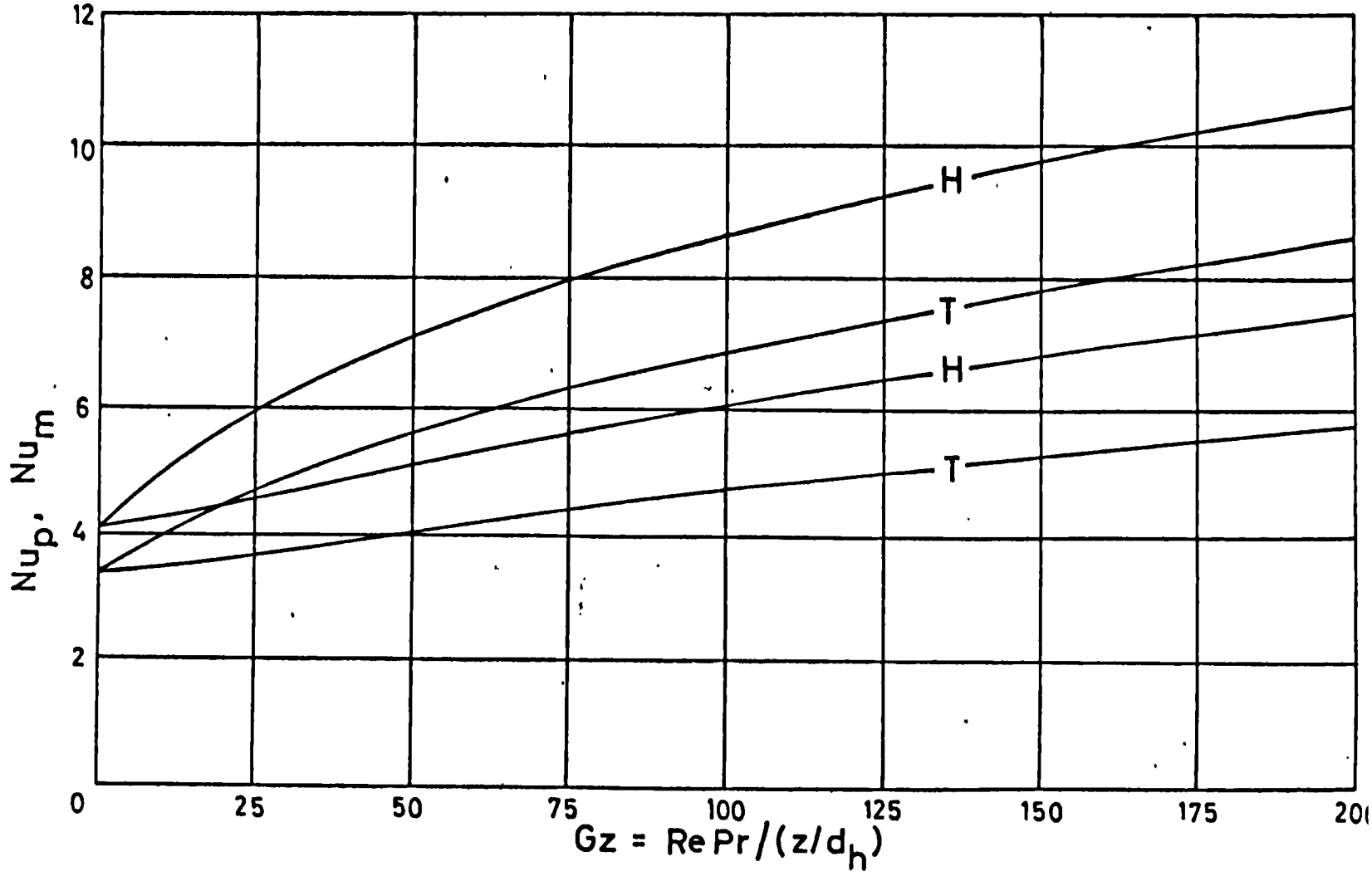

Fig. 17 Comparison of predicted Nusselt numbers between the thermal conditions of constant wall temperature and constant heat input per unit length for a rectangular duct of aspect ratio of 2.0.

3.7 EXPERIMENTAL RESULTS

3.7.1 Constant Heat Input Per Unit Length

Tests were carried out over a range of Reynolds numbers from 735 to 1960, which is well in the transition regime for non-circular ducts. The wall temperatures were measured at 7.5, 12.0 and 23.5 inches from the entry plane of the duct. The initial and final temperatures of the air were also recorded.

To determine the Nusselt number at a position along the duct, the bulk temperature of the fluid at that position must be known. In experiments, though intermediate values of the bulk temperature could not be measured conveniently and accurately, they could still be deduced from the measured values of the initial and final temperatures of the air.

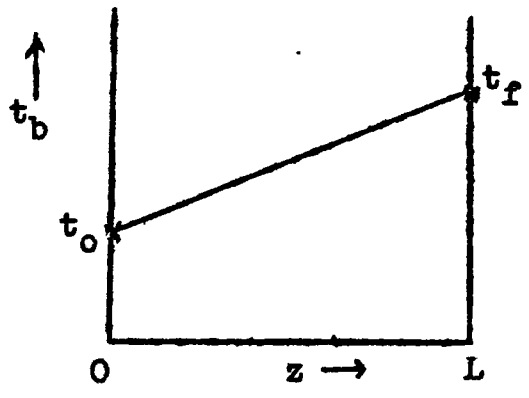

Fig. 18

For constant heat input per unit length of the duct, it has been shown in (3.6) that the bulk temperature of the fluid rises linearly along the duct.

$$\therefore \quad \frac{dt_b}{dz} = \text{constant} = \frac{t_f - t_o}{L}$$

Hence the bulk temperature of the fluid at any position along the duct can be obtained directly from a linear relationship between the initial and final bulk temperatures of the fluid and the total length of the duct, see fig. 18, p.64.

Specimen of Calculation

Data

Aspect ratio, α^+	= 2.0	
Cross sectional area, A_c	= 1.0 x 2.0	$in.^2$
Total length, L	= 29.5	in.
Volumetric flow rate of air, V	= 1.7	c.f.m.
Initial bulk temperature, t_o	= 71.6	deg.F.
Final bulk temperature, t_f	= 94.0	deg.F.
Initial wall temperature, $t_{w,o}$	= 84.0	deg.F.

Position along the duct	Local wall temperature	Average wall temperature	Fluid bulk temperature
inch.	deg.F.	deg.F.	deg.F.
7.5	115.0 113.8 114.0 115.2	114.5	76.6
12.0	124.3 125.1 125.6 127.3	125.6	80.0
23.5	136.4 136.3 138.5 139.8	137.2	89.3

Hydraulic diameter, $d_h = 4A_c/P = \frac{4x2x1}{3} = 1.333$ in.

Mean velocity of the air, $w_b = 60V/A_c = \frac{60x1.7}{27144}$

$= 7.33x10^3$ ft/h

Rate of heat transfer by convection per unit length of the duct $= h_p P (t_w - t_b)$ B.Th.U/h.ft.

Rate of change of enthalpy per unit length of the duct

$= C_p \rho w_b A_c \frac{dt_b}{dz}$ .Th.U/h.ft.

∴ by the first law of thermodynamics,

$$h_p = \frac{C_p \rho w_b A_c (t_f - t_o)}{P L (t_w - t_b)} \quad \text{B.Th.U/h.ft}^2$$

$$Nu_p = \frac{h_p d_h}{k_b} = \frac{0.24 \times 0.075 \times 60 \times 1.7 (94.0 - 71.6)4}{\frac{6}{12} \times \frac{29.5}{12} (t_w - t_b) k_b \times 12}$$

$$= 3.73/k \ (t_w - t_b)$$

Logarithmic mean temperature difference, $(t_w - t_b)_l$

$$= \frac{\Delta t_{max.} - \Delta t_{min.}}{\ln (\Delta t_{max.}/\Delta t_{min.})}$$

$$= \frac{t_w - t_b - 84.0 + 71.6}{\ln \{(t_w - t_b) / 12.4\}}$$

$$Nu_l = \frac{h_l d_h}{k_b} = \frac{3.73 \ln \{(t_w - t_b)/12.4\}}{k_b (t_w - t_b - 12.4)}$$

$$\text{Reynolds number, } Re = \frac{\rho\, w_b\, d_h}{\mu} = \frac{0.075 \times 7.33 \times 10^3 \times 1.333}{0.0442 \times 12}$$

$$= 1385$$

$$\text{Graetz number, } Gz = \frac{Re.Pr}{z/d_h} = \frac{1385 \times 0.72 \times 1.333}{z\ (\text{in.})}$$

$$= 1330/z$$

$$\text{Dimensionless wall temperature, } \beta_w = \frac{t_w - t_o}{t_f - t_o} L \frac{\alpha}{w_b\, d_h^2}$$

$$= \frac{t_w - 71.6}{94.0 - 71.6}\, 2.46\, \frac{0.82 \times 12^2}{7.33 \times 10^3 \times 1.333^2}$$

$$= 0.997 \times 10^{-4}\ (t_w - 71.6)$$

z	Gz	t_w	t_b	Δt_l	Nu_p	Nu_l	β_w
in.		deg.F	deg.F	deg.F			x 10^3
7.5	177.0	114.5	76.6	22.7	6.7	11.2	3.78
12.0	111.0	125.5	80.0	25.5	5.5	9.8	4.54
23.5	56.5	137.2	89.3	26.4	5.2	9.3	4.78

Fig.20, p.70 shows a rise of the measured dimensionless wall temperature, β_w, with the reciprocal of the Graetz number, $(z/d_h)/Re.Pr$. Variation of the measured Nusselt numbers with the Graetz numbers

is plotted in fig. 19, p.69 and tabulated in Appendix (7.5).

3.7.2 Constant Wall Temperature

Details of the test section were described in Section(2.4). Tests were conducted over the same range of Reynolds numbers as for constant heat input. Since the rise of the bulk temperature along the duct was not linear as in the previous case and it could not be measured conveniently and accurately, the local heat input could not be estimated. The initial and final bulk temperatures of the air were, however, measured and recorded, hence the total heat input and the logarithmic mean Nusselt number were deduced.

Because of the same reasons as above, ducts of different lengths were employed in order to cover a wide range of the Graetz numbers.

Results were computed by a similar procedure as that in the preceding section(3.7.1). Variation of the logarithmic mean Nusselt number with the Graetz number is shown in fig.21, p.71 and tabulated results are available in Appendix(7.6).

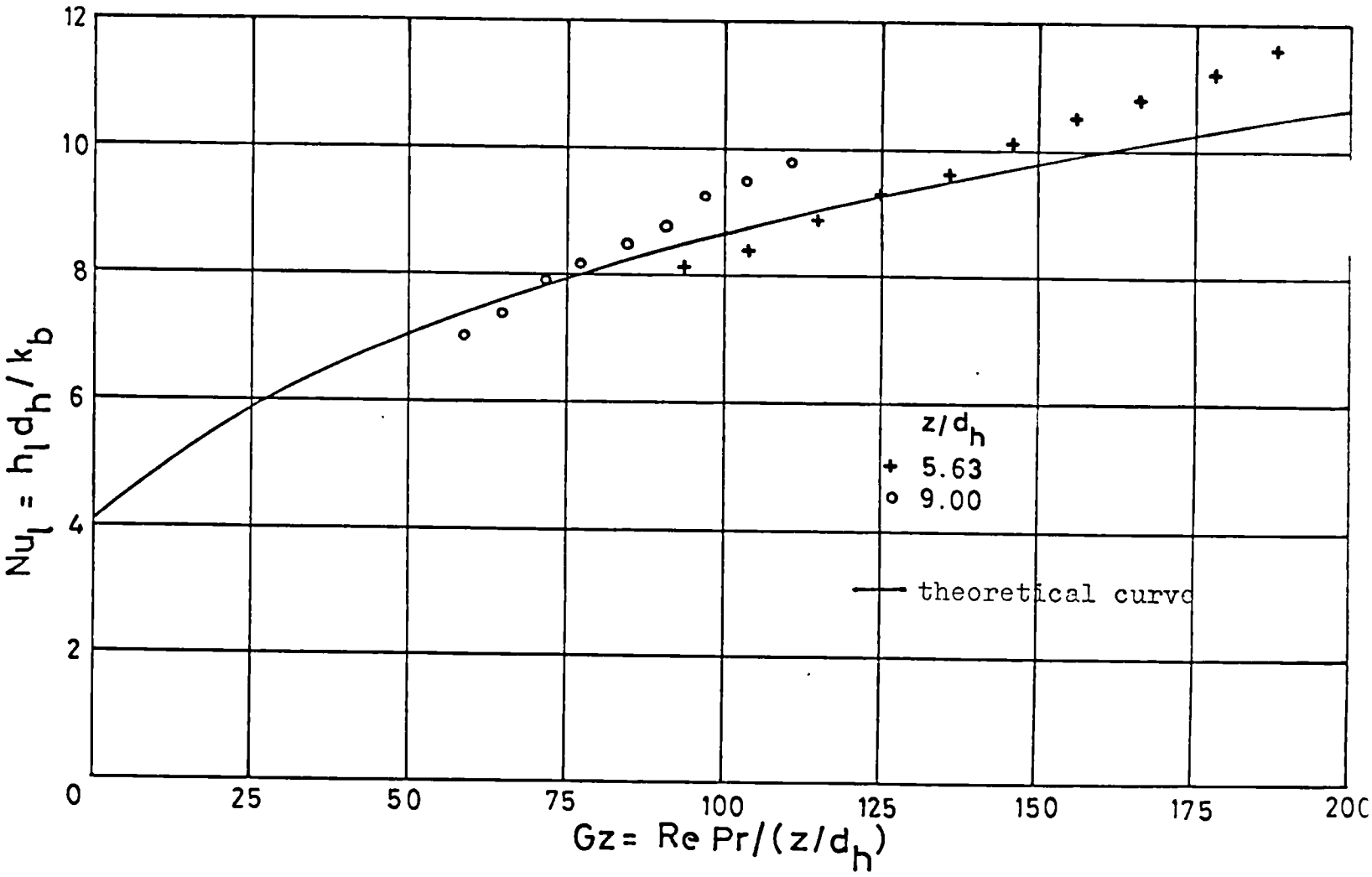

Fig.19 Measured logarithmic mean Nusselt numbers, Nu_l, plotted a ainst Graetz numbers for fully developed velocity profile in a rectangular duct with constant heat input per unit length; aspect ratio = 2.0.

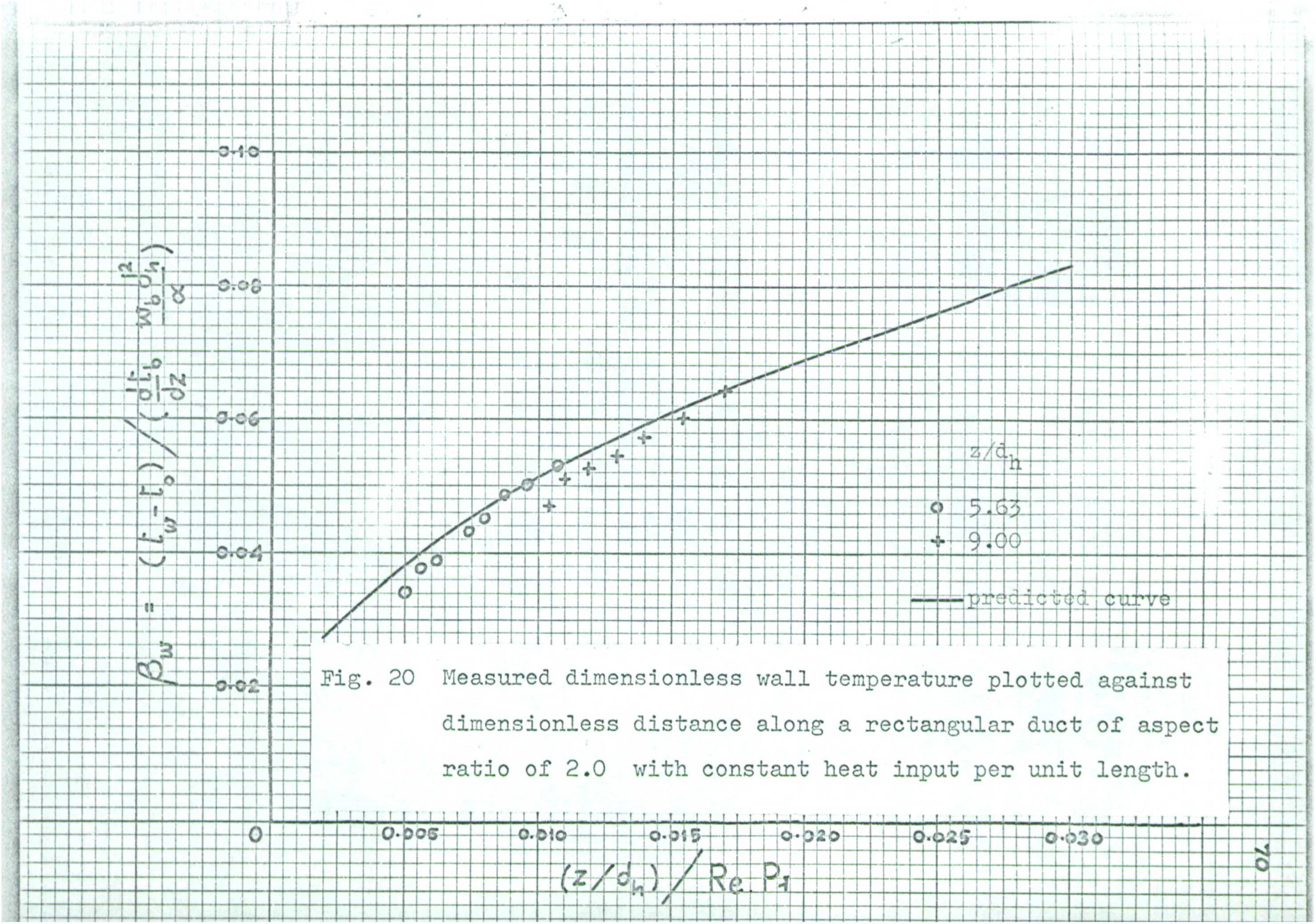

Fig. 20 Measured dimensionless wall temperature plotted against dimensionless distance along a rectangular duct of aspect ratio of 2.0 with constant heat input per unit length.

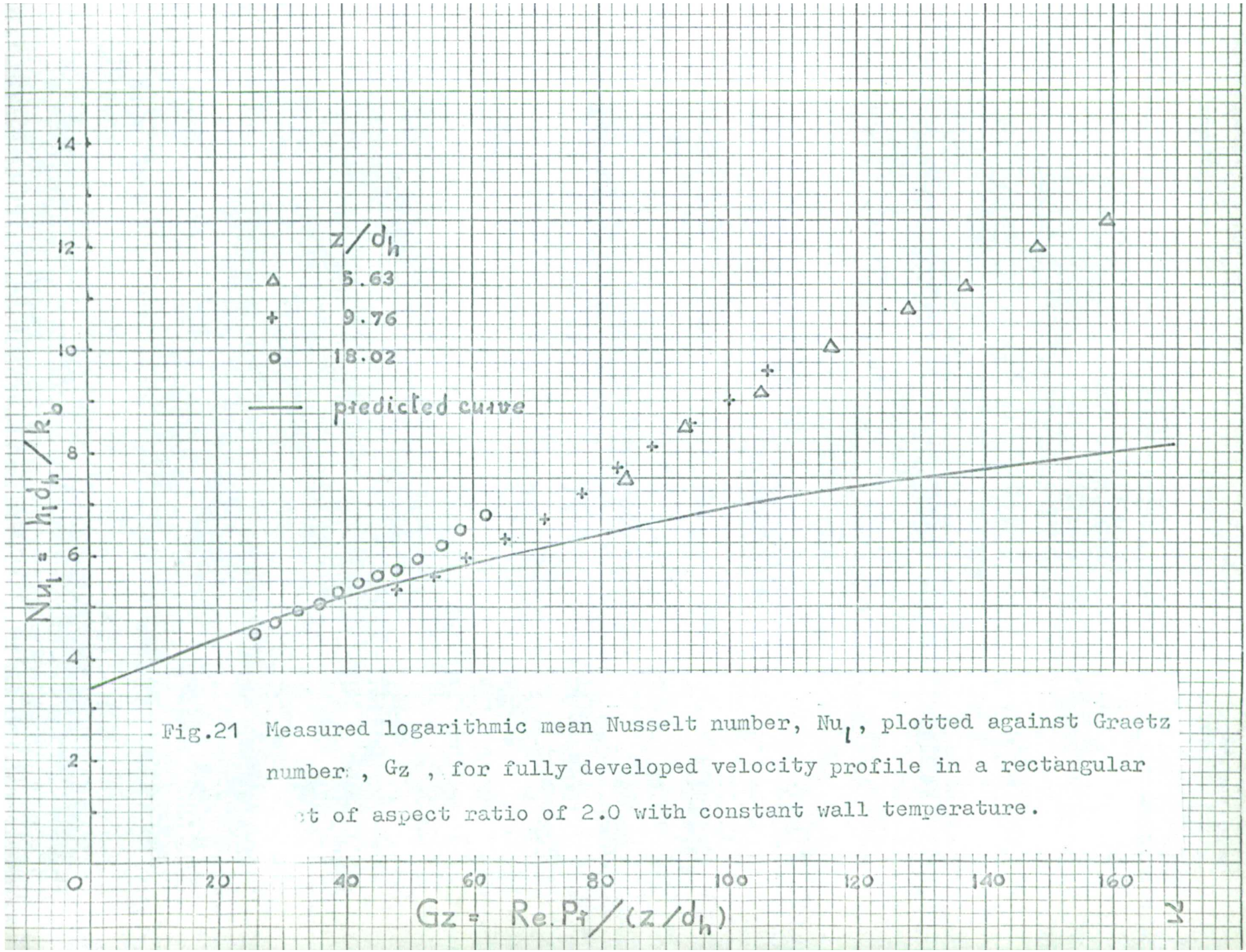

Fig.21 Measured logarithmic mean Nusselt number, Nu_l, plotted against Graetz number, Gz, for fully developed velocity profile in a rectangular duct of aspect ratio of 2.0 with constant wall temperature.

CHAPTER 4

HEAT TRANSFER FOR SIMULTANEOUSLY DEVELOPING VELOCITY AND TEMPERATURE PROFILES IN RECTANGULAR DUCTS.

4.1 THEORETICAL ANALYSIS.

In the previous chapter, fully developed velocity profiles have been assumed and this condition exists in practice only when a long duct is allowed for the flow to become fully established before the heat transfer process begins. In many cases, heat transfer takes place as soon as the fluid enters the duct, so that both temperature and velocity profiles are developing simultaneously.

The Navier-Stokes' equation (1) for the velocity w, in the z-direction is :

$$\frac{\mu}{\rho}\left\{\frac{\partial^2 w}{\partial x^2}+\frac{\partial^2 w}{\partial y^2}+\frac{\partial^2 w}{\partial z^2}\right\} = \frac{1}{\rho}\frac{\partial p}{\partial z}+u\frac{\partial w}{\partial x}+v\frac{\partial w}{\partial y}+w\frac{\partial w}{\partial z}$$

Langhaar (10) obtained an approximate solution for a flow between two parallel plates by using the following assumptions :

(i) The term $\partial^2 w/\partial z^2$, which represents the rate of change of the viscous force in the z-direction with respect to z may be neglected in comparison to those with respect to x and y.

(ii) The velocity components u and v are negligible in comparison to the main stream velocity, w.

(iii) The pressure gradient, dp/dz, is a function of z alone.

$$\therefore \quad \frac{\mu}{\rho}\left\{\frac{\partial^2 w}{\partial x^2}+\frac{\partial^2 w}{\partial y^2}\right\} = \frac{1}{\rho}\frac{dp}{dz} + w\frac{\partial w}{\partial z} \qquad (16)$$

The above assumptions will also be used for solving the developments of velocity profiles in rectangular ducts.

The pressure term in equation (16) may be eliminated by considering the flow at the central axis of the duct.

$$\frac{\mu}{\rho}\left\{\frac{\partial^2 w}{\partial x^2}_c+\frac{\partial^2 w}{\partial y^2}_c\right\} = \frac{1}{\rho}\frac{dp}{dz} + w_c\frac{\partial w}{\partial z}_c$$

where the suffix 'c' refers to the central axis. Hence

$$\frac{\mu}{\rho}\left\{\frac{\partial^2 w}{\partial x^2}+\frac{\partial^2 w}{\partial y^2}\right\} - \frac{\mu}{\rho}\left\{\frac{\partial^2 w}{\partial x^2}_c+\frac{\partial^2 w}{\partial y^2}_c\right\} + w_c\frac{\partial w}{\partial z}_c = w\frac{\partial w}{\partial z}$$

The above equation can be put in a finite difference form by means of the operator 'K' defined on p.36 .

$$\frac{\mu}{6\rho h^2}\left\{K\,w(x,y,z) - K\,w(x,y,z)_c\right\} + w_c\frac{\Delta w}{\Delta z}_c = w\frac{\Delta w}{\Delta z}$$

$$\Delta w \equiv w(x,y,z+\Delta z) - w(x,y,z)$$

$$= \frac{1}{6}\frac{w_b}{w}\left(\frac{d_h}{h}\right)^2\left(\frac{\mu \Delta z}{\rho w_b d_h^2}\right)\left\{ K\, w(x,y,z) - K\, w(x,y,z)_c \right\}$$

$$+ \frac{w_c}{w}\left\{ w(x,y,z+\Delta z)_c - w(x,y,z)_c \right\} \qquad (17)$$

Equation (17) will be solved simultaneously with the energy equation (2a) which can be written in the finite difference form as :

$$t(x,y,z+\Delta z) - t(x,y,z) = \frac{1}{6}\left(\frac{d_h}{h}\right)^2\frac{w_b}{w}\left(\frac{\alpha \Delta z}{w_b d_h^2}\right) K\, t(x,y,z)$$

As already mentioned in the previous analysis, the term $(\alpha \Delta z / w_b d_h^2)$, which represents the dimensionless finite step in the z-direction will be given a suitable value when the energy equation is solved numerically, (see p.40). The same value can be applied to the term $(\mu \Delta z / \rho w_b d_h^2)$ in equation (17) as follows :

$$\frac{\mu \Delta z}{\rho w_b d_h^2} = \frac{\Delta z}{w_b d_h^2}\frac{k}{\rho c_p}\frac{c_p \mu}{k} = \left(\frac{\alpha \Delta z}{w_b d_h^2}\right) Pr$$

Define the velocity ratio, $w^* \equiv w/w_b$

Equation (17) can be written in terms of w^* as :

$$w^*(x,y,z+\Delta z) = \frac{1}{6}\frac{Pr}{w^*_e{}^2}\left(\frac{\alpha\Delta z}{w_b d_h^2}\right)\left\{ K\, w^*(x,y,z) - K w^*(x,y,z)_c \right\}$$

$$+ \frac{w_c}{w}\left\{ w^*(x,y,z+\Delta z)_c - w^*(x,y,z)_c \right\}$$

$$+ w^*(x,y,z) \qquad (18)$$

Boundary conditions :

(i) With a bell-shaped inlet, the velocity of the fluid at the entry plane is constant everywhere and equal to the bulk velocity, w_b, hence at $z = 0$, $w^*_o = w^*_b = 1$.

(ii) The fluid at the wall is stationary,

$$\therefore \quad w^*_w = 0.$$

In the above equation, the value of 'e' is fixed from the size of the network chosen; $(\alpha\Delta z/w_b d_h^2)$ has been given a value when the energy equation is solved in the previous section; the Prandtl number, Pr, has to be given a numerical value depending upon the type of fluid under consideration, for example 0.72 for atmospheric air; lastly the term $w^*(x,y,z+\Delta z)$ can be approximated by the following steps :

(i) Solve equation (18) numerically for all nodal points in the network assuming that

$$w^*(x,y,z+\Delta z)_c - w^*(x,y,z)_c = 0.$$

Hence, the first approximation of the velocity distribution at $(z+\Delta z)$.

(ii) Compute the dimensionless bulk velocity, w_b^*, from the first approximation. As the correct $w_b^* = 1$, the error of the velocity at each nodal point is $(1 - w_b^*)$.

(iii) Add $(1 - w_b^*)$ to the term $\{ w^*(x,y,z+\Delta z)_c - w^*(x,y,z)_c \}$ in (i) and resolve equation (18).

(iv) Repeat the same procedure until $w_b^* = 1.$

When the velocity distribution at $(z+\Delta z)$ is known the energy equation can now be solved by the same procedure as in the previous analysis (3.4).

Computer programs were written for rectangular ducts with aspect ratios from 1 to 4, for the thermal boundary conditions of constant wall temperature and constant heat input per unit length of the duct. An example of a computer program is shown in Appendix (7.7). Results obtained from the computer are plotted in fig. 22-25, p.78-81. A comparison of the predicted Nusselt numbers between the hydraulic boundary conditions of fully developed velocity profiles and simultaneously developing profiles for rectangular ducts of aspect ratio of 2.0 with the two usual thermal boundary conditions is shown in fig. 26.

From equation (18), it can be seen that the effect of the Prandtl number on the development of the velocity

profiles is quite significant. As a result, solutions of the heat transfer for simultaneously developing profiles contain the Prandtl number as a parameter. Fig.27 & 28, p.83 & 84, show variations of the predicted peripheral and mean Nusselt numbers with the Graetz numbers and the Prandtl numbers of 0.72, 0.10, and 10 for rectangular ducts of aspect ratio of 2.0 with constant heat input per unit length of the duct.

4.2 EXPERIMENTAL RESULTS.

Test equipments were the same as those in section (3.7) but without the unheated inlet section so that the velocity and temperature profiles could develop simultaneously. Tests were performed for the thermal boundary condition of constant heat input per unit length over the same range of Reynolds numbers as in section (3.7). Results are shown in fig.29, p.85.

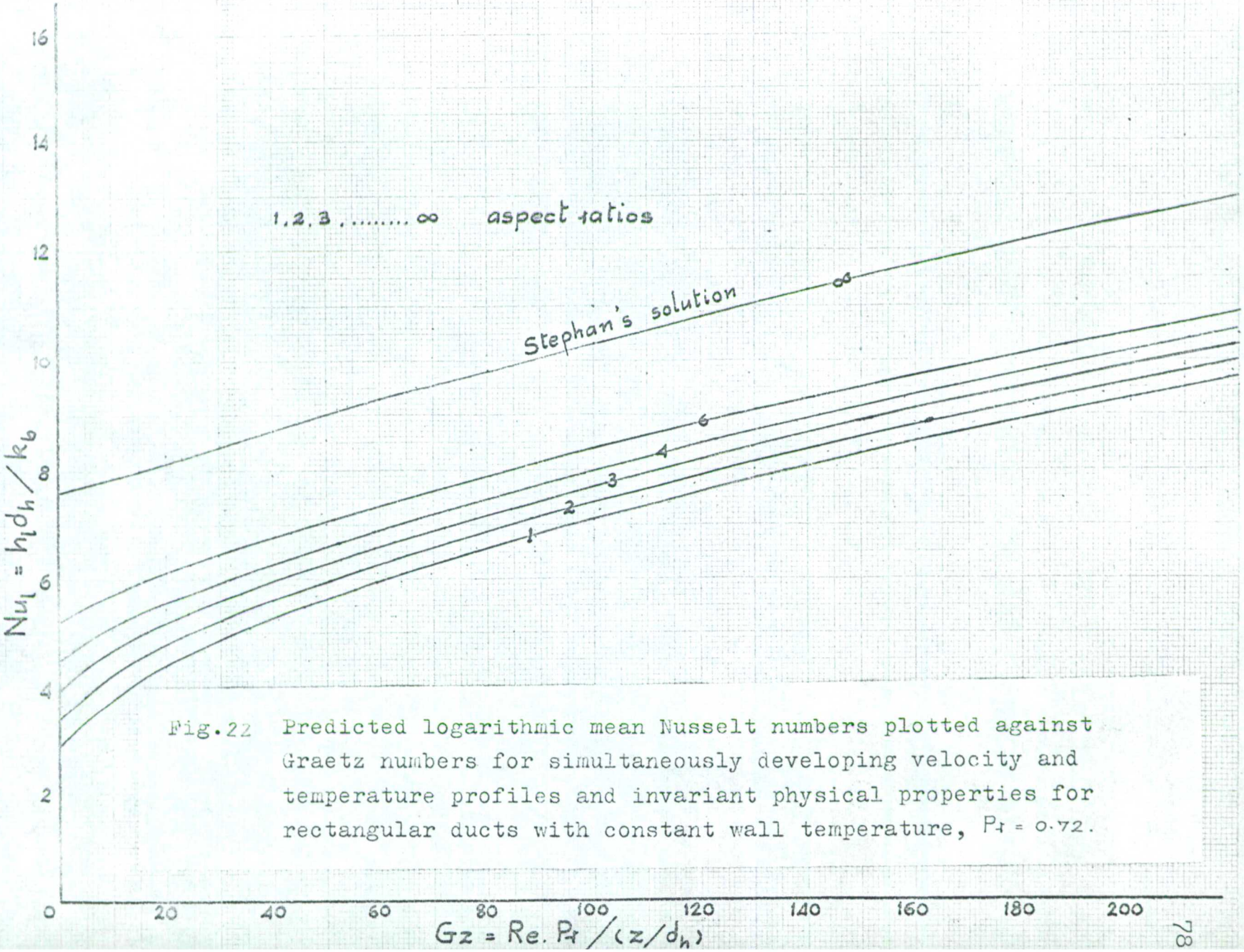

Fig.22 Predicted logarithmic mean Nusselt numbers plotted against Graetz numbers for simultaneously developing velocity and temperature profiles and invariant physical properties for rectangular ducts with constant wall temperature, $P_r = 0.72$.

Fig.23 Variations of dimensionless bulk temperature with dimensionless distance along the duct, $(z/d_h)/Re.Pr$, for constant wall temperature, Pr = 0.72.

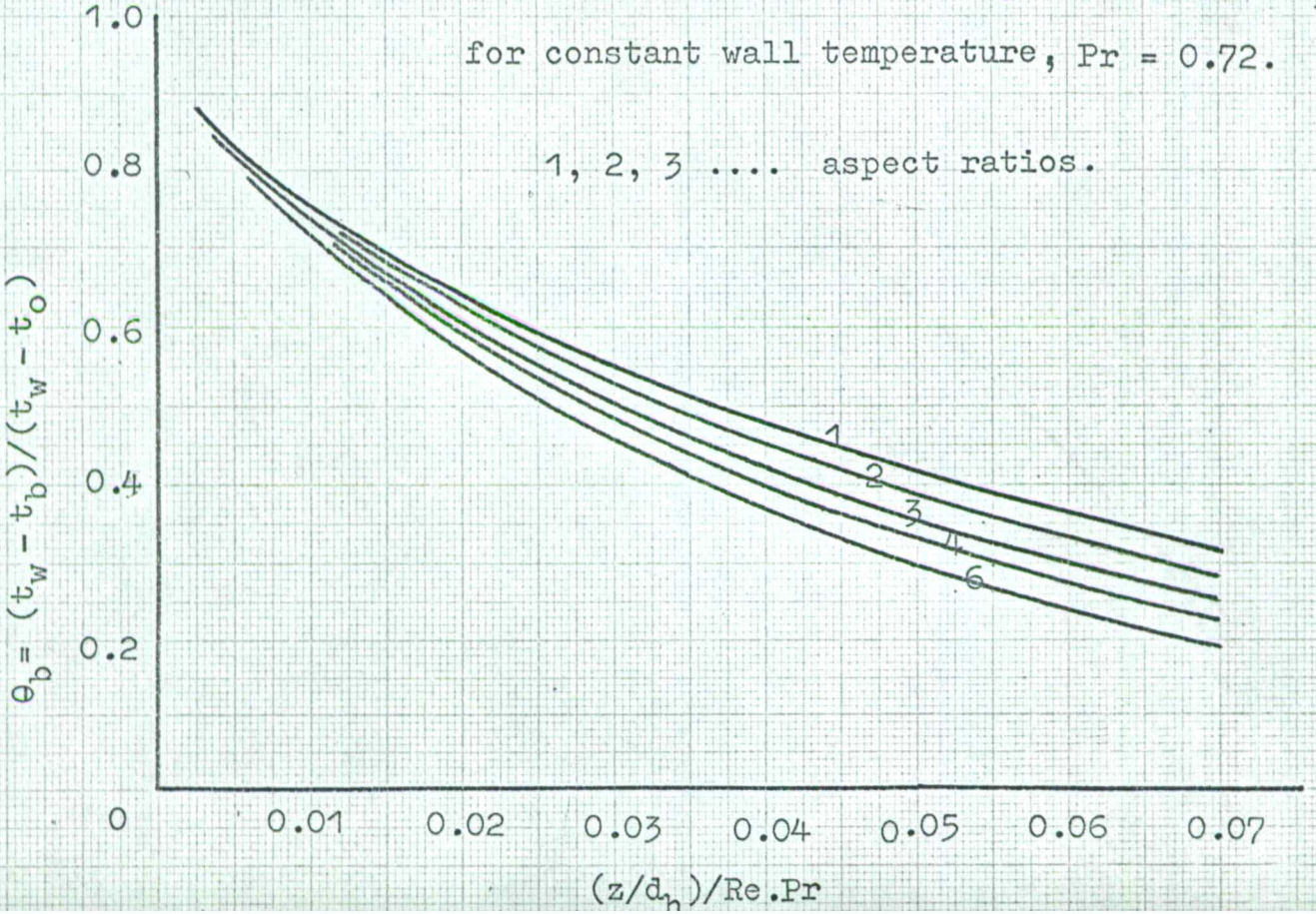

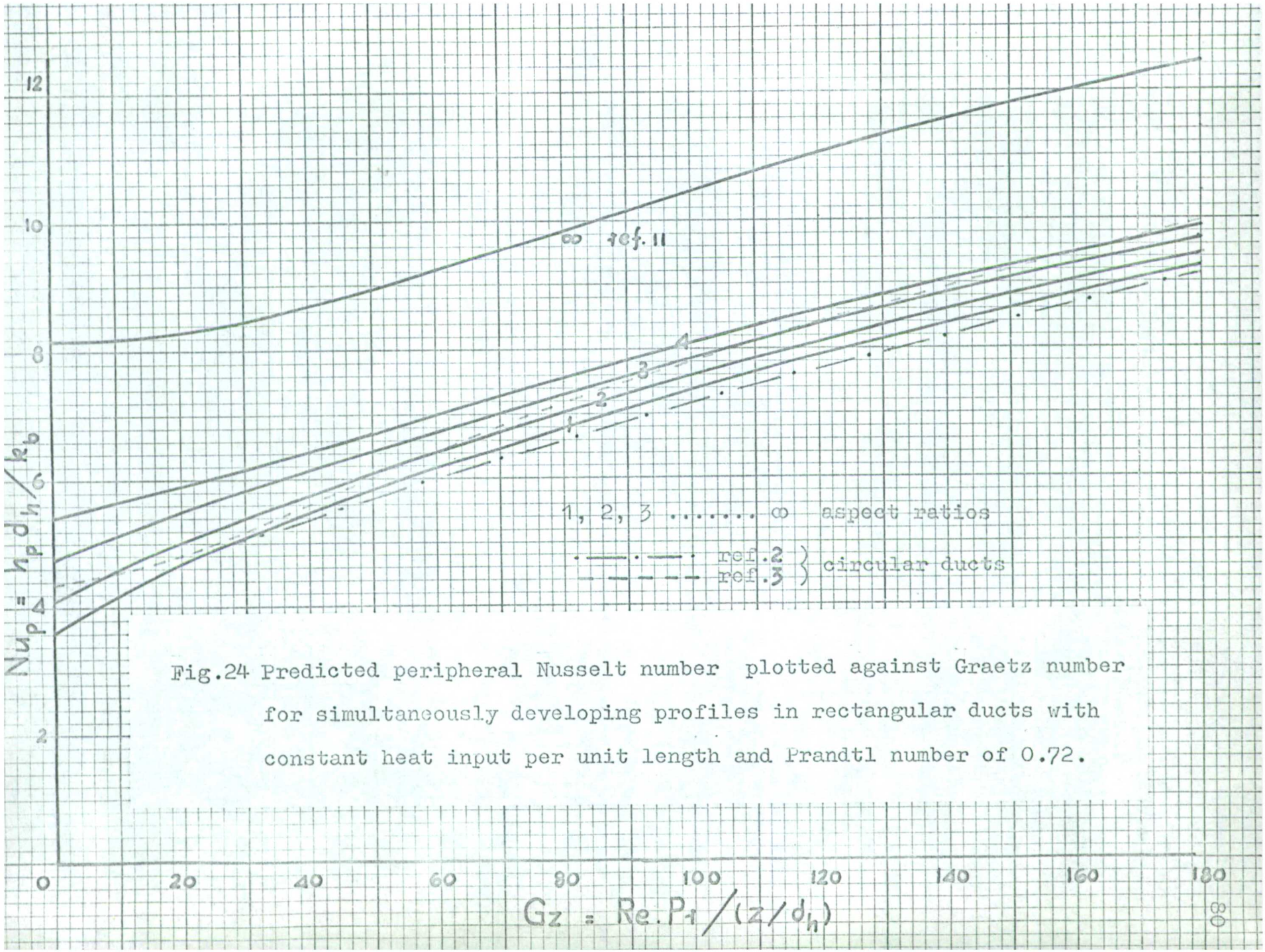

Fig.24 Predicted peripheral Nusselt number plotted against Graetz number for simultaneously developing profiles in rectangular ducts with constant heat input per unit length and Prandtl number of 0.72.

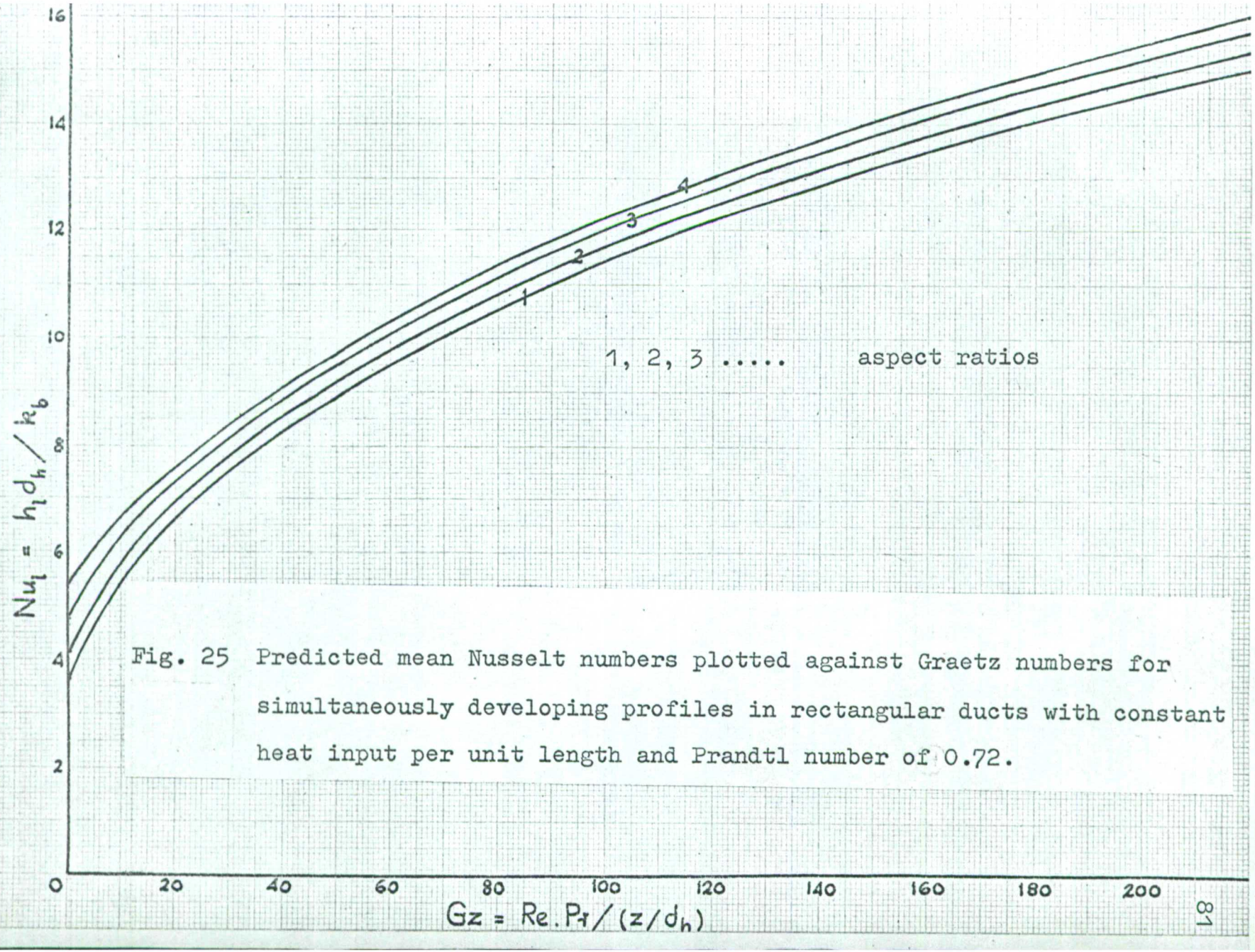

Fig. 25 Predicted mean Nusselt numbers plotted against Graetz numbers for simultaneously developing profiles in rectangular ducts with constant heat input per unit length and Prandtl number of 0.72.

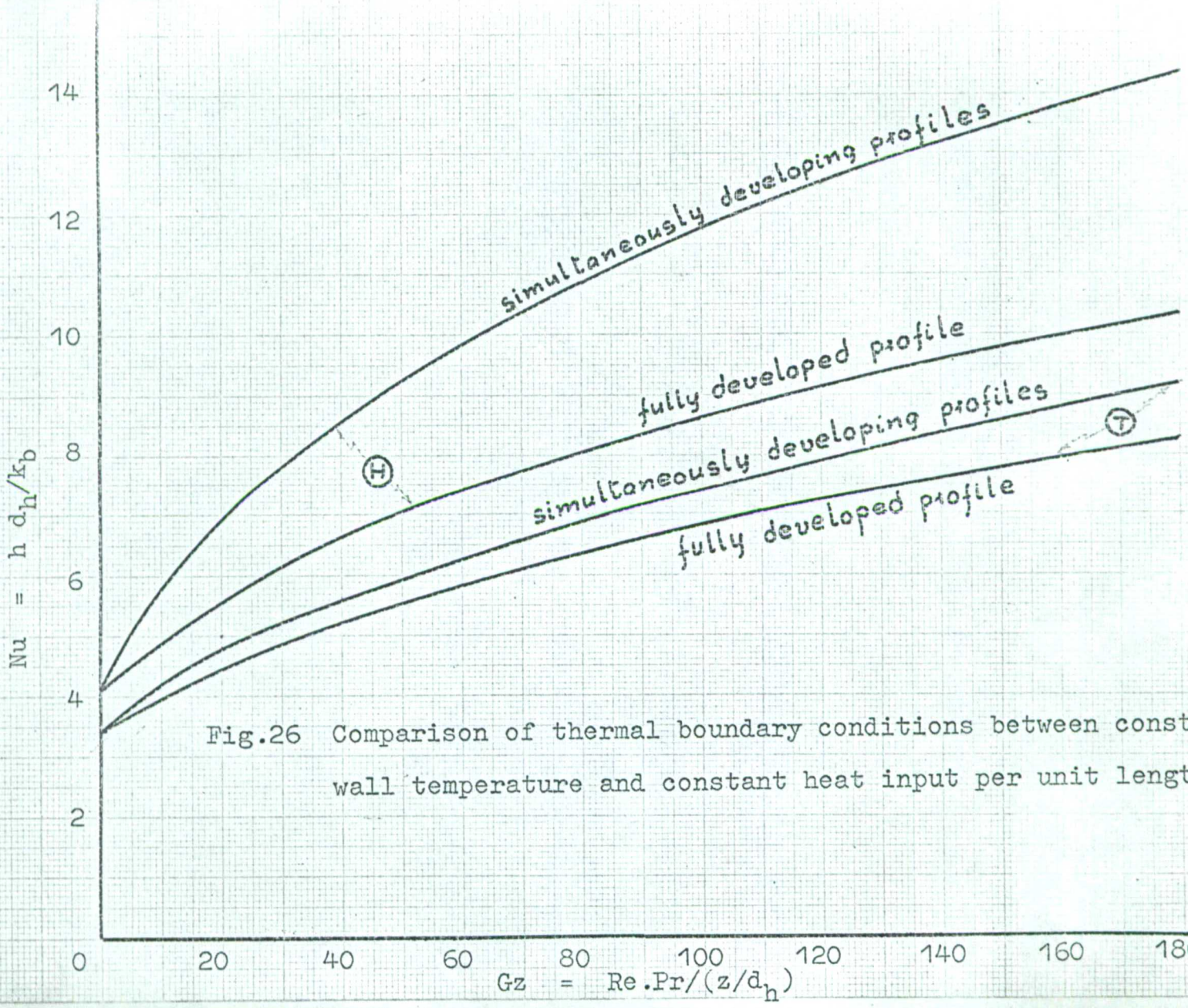

Fig.26 Comparison of thermal boundary conditions between constant wall temperature and constant heat input per unit length.

Fig.27 Effect of the Prandtl numbers on the predicted mean Nusselt numbers for simultaneously developing profiles in a rectangular duct of aspect ratio of 2.0 with constant heat input per unit length of the duct.

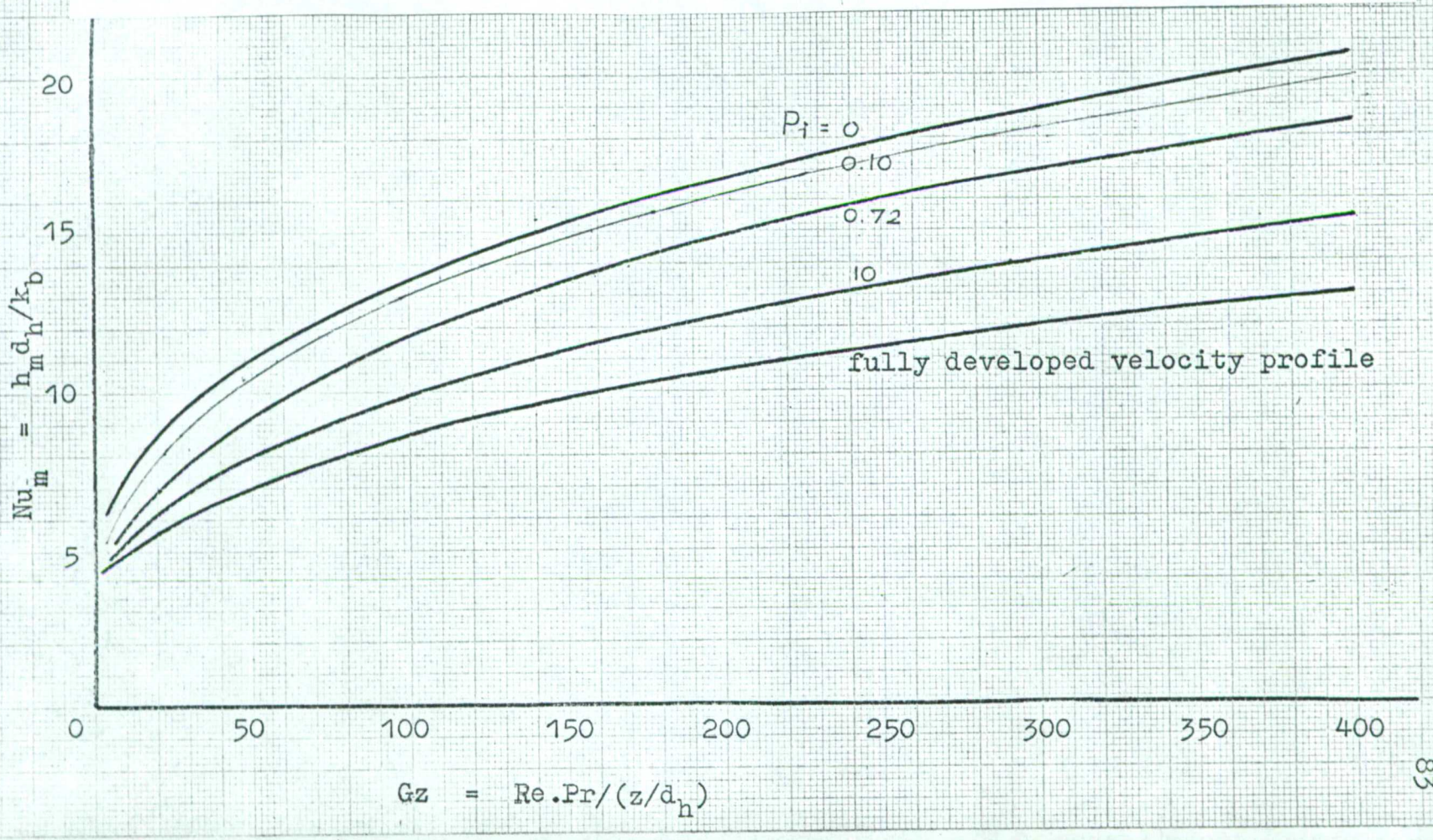

Fig.28 Effect of the Prandtl numbers on the predicted peripheral Nusselt numbers for simultaneously developing profiles in a rectangular duct of aspect ratio of 2.0 with constant heat input per unit length.

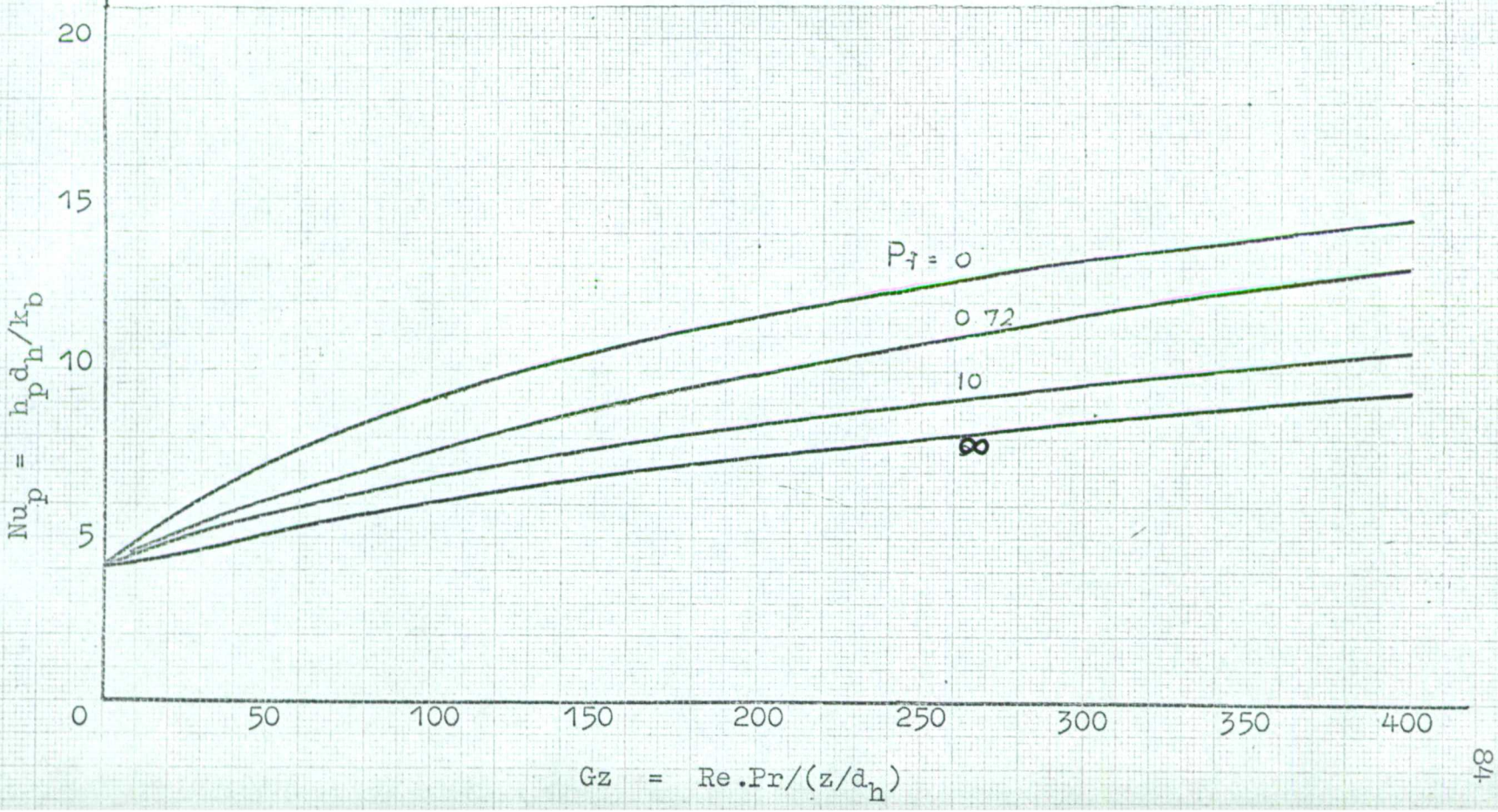

Fig.29 Measured logarithmic mean Nusselt numbers plotted against Graetz numbers for simultaneously developing profiles in a rectangular duct of aspect ratio of 2.0 with constant heat input per unit length and Pr = 0.72.

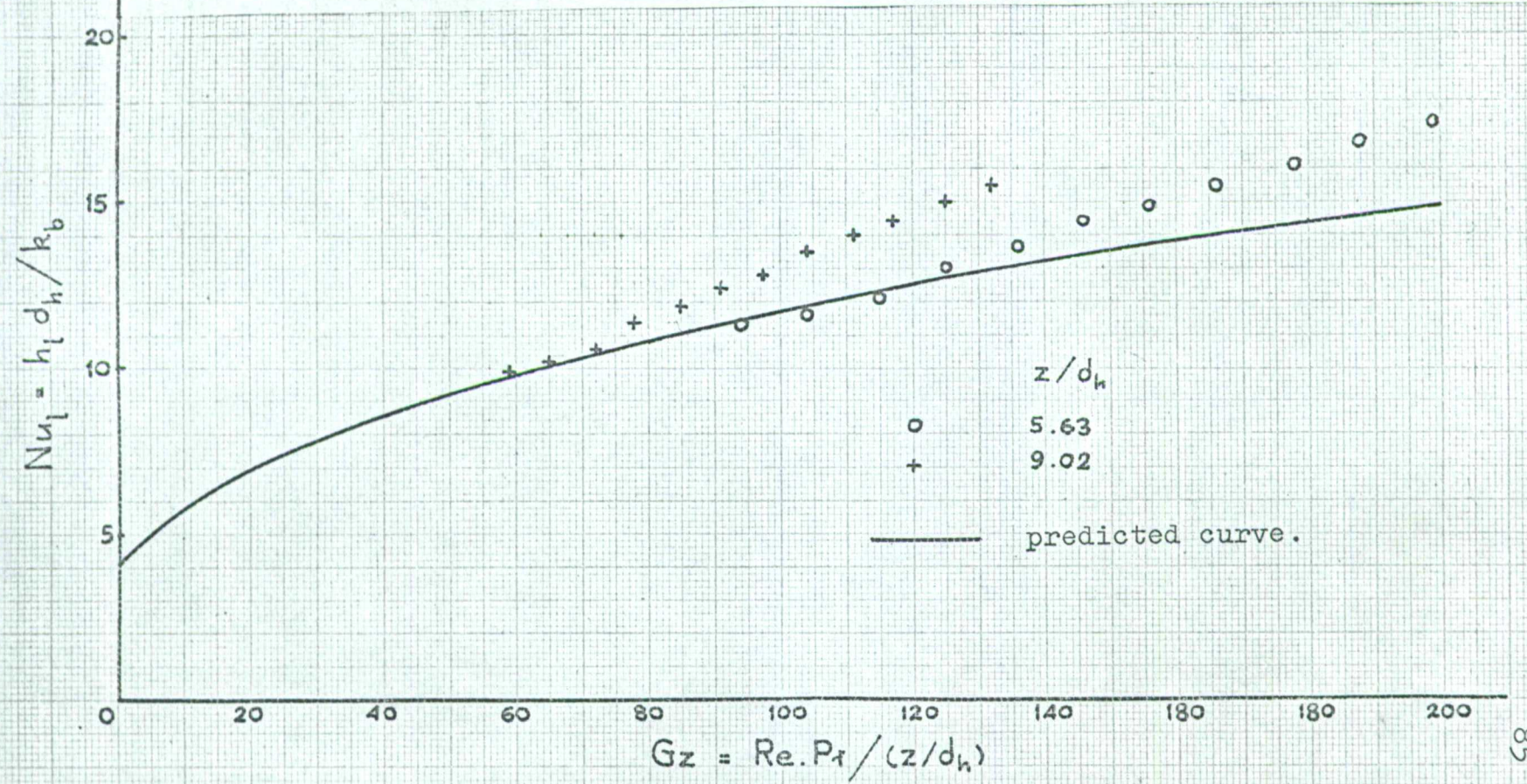

CHAPTER 5

HEAT TRANSFER IN TRIANGULAR DUCTS.

5.1 RIGHT ANGLED ISOSCELES TRIANGULAR DUCT.

The exact solution of the Navier-Stokes equation (2a) for a fully developed laminar flow in a right angled isosceles triangular duct of sides $x+y = 0$, $x = a$ and $y = a$, is given in ref.(30) as :

$$w = \tfrac{1}{2} K \left[a(x+y) - \tfrac{1}{2}(x+y)^2 - \left(\frac{2}{a}\right) \sum_{n=0}^{\infty} (-1)^n N^{-3} \operatorname{cosech}(Na) \right.$$

$$\left. \{ \sinh(Nx)\cos(Ny) + \sinh(Ny)\cos(Nx) \} \right]$$

where $2aN = (2n+1)\pi$

Put $w^+ \equiv 2w/Ka^2$, $x^+ \equiv x/a$ and $y^+ \equiv y/a$.

$$w^+ = (x^+ + y^+) - \tfrac{1}{2}(x^+ + y^+)^2 - 16 \sum_{n=0}^{\infty} (-1)^n \frac{\operatorname{cosech}(2n+1)\pi/2}{(2n+1)^3\pi^3}$$

$$\left\{ \sinh\frac{(2n+1)\pi}{2} x^+ \cos\frac{(2n+1)\pi}{2} y^+ + \sinh\frac{(2n+1)\pi}{2} y^+ \cos\frac{(2n+1)\pi}{2} x^+ \right\} \quad (19)$$

The network used in computations is shown in fig.30, p.87 . Velocity ratios at nodal points in the

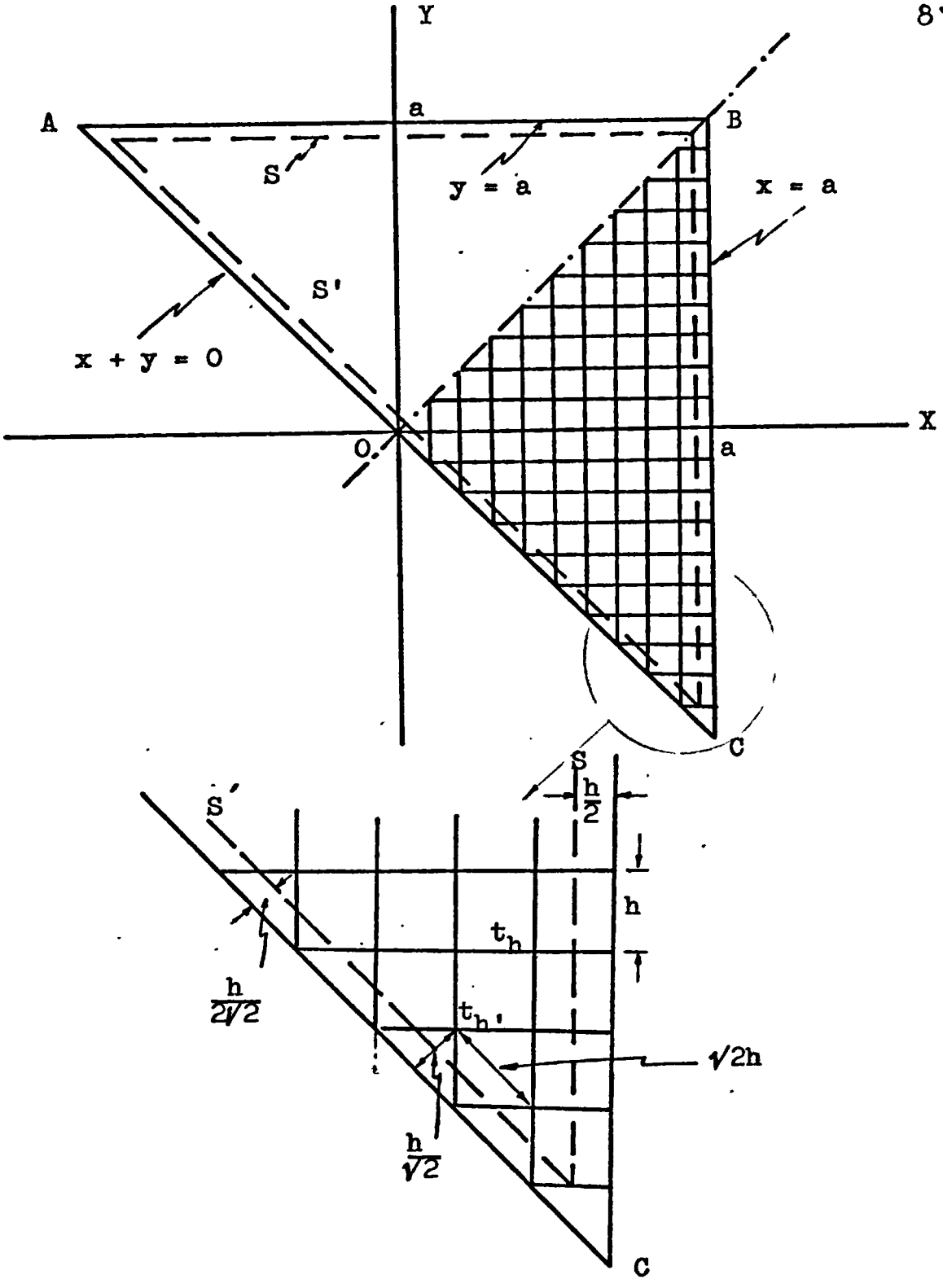

Fig.30 Network for the Right-Angled Isosceles Triangular Duct.

network can be determined by calculating the dimensionless velocities from equation(19) and then computing the average dimensionless velocity, w_b^+, by means of the extended Simpson's rule in two dimensions, equation(4).

Numerical solutions of heat transfer for the hydraulic boundary conditions of uniform velocity profile, fully developed velocity profile and simultaneously developing profiles in the right angled isosceles triangular ducts were obtained by the same procedure as those for the rectangular ducts in sections (3.4), (3.5) and (3.6), with the thermal boundary condition of constant wall temperature. Results obtained from the Atlas computer are shown in fig.31& 32 and Appendix(7.9).

For constant heat input per unit length of the duct, determination of the wall temperature presents some difficulties. From fig.30, p.87, it can be seen that nodal points adjacent the sides AB and BC are at a finite step, h from the duct wall, hence the analysis in section (3.6) is applicable, but the nodal points adjacent to AC are at a distance $h/\sqrt{2} \equiv h'$ from the wall, thus a modified analysis is required.

Consider a surface S at a constant distance h/2 from the sides AB and BC. By a similar reasoning as in section (3.6), heat transfer by conduction through S is

$$\sum^{n} k\,(t_w - t_h)\,dz$$

where n = number of nodal points on AB and BC.

Rate of change of enthalpy through the area between S and the duct wall is

$$\sum^{n} \frac{h^2 \rho\, w_h\, C_p}{8} \frac{dt_h}{dz}\, dz$$

Now consider a surface S' at a distance $h/2\sqrt{2}$ from the duct wall AC.

Temperature gradient at any nodal point on S'

$$= (t_w - t_{h'})/(h/\sqrt{2})$$

Rate of heat transfer by conduction through S'

$$= \sum^{n'} k\sqrt{2}h\, dz\, (t_w - t_{h'})/(h/\sqrt{2})$$

$$= \sum^{n'} 2k\,(t_w - t_{h'})\,dz$$

where n' = number of nodal points on AC.

Rate of change of enthalpy through n' elementary areas, each being $(\sqrt{2}h.h/2\sqrt{2})$, between S' and the duct wall

$$= \sum^{n'} \frac{h^2 \rho}{2} \frac{w_{h'}}{4} C_p \frac{dt_{h'}}{dz}\, dz$$

From the first law of thermodynamics, rate of heat transfer through S and S' = rate of change of enthalpy inside S and S' in the absence of shaft work.

$$\sum^{n} k\,(t_w - t_h) + \sum^{n'} 2k\,(t_w - t_{h'}) = \rho\, w_b\, A_c\, C_p \frac{dt_b}{dz} - \sum^{n} \frac{h^2}{8} \rho\, w_h\, C_p \frac{dt_h}{dz} - \sum^{n'} \frac{h^2}{8} \rho\, w_{h'}\, C_p \frac{dt_{h'}}{dz}$$

As in section (3.6.2), the wall temperature, t_w is assumed constant around any perimeter. If the cross sectional area, A_c, is substituted by $(n + \sqrt{2n'})h.d_h/4$, and the temperatures, t are replaced by the dimensionless temperatures, β, defined on p.52, the above equation can be written as

$$\beta_w = \frac{e}{4}\left(\frac{n + \sqrt{2n'}}{n + 2n'}\right) + \frac{\sum^{n} \beta_h + 2\sum^{n'} \beta_{h'}}{(n + 2n')} - \frac{e^2}{(n + 2n')} \frac{w_b\, d_h^2}{8\alpha\Delta z} \left\{ \sum^{n} \frac{w_h}{w_b} \Delta\beta_h + \sum^{n'} \frac{w_{h'}}{w_b} \Delta\beta_{h'} \right\} \qquad (20)$$

Solutions for constant heat input can now be found for the hydraulic boundary conditions of uniform velocity profile, fully developed velocity profile and simultaneously developing profiles by the same procedures as those in sections (3.6) and (4.1) and by using equation (20) instead of equation (13) to solve for the wall temperature. Numerical results obtained from the Atlas computer are plotted in fig. 33 & 34, p.93 & 94.

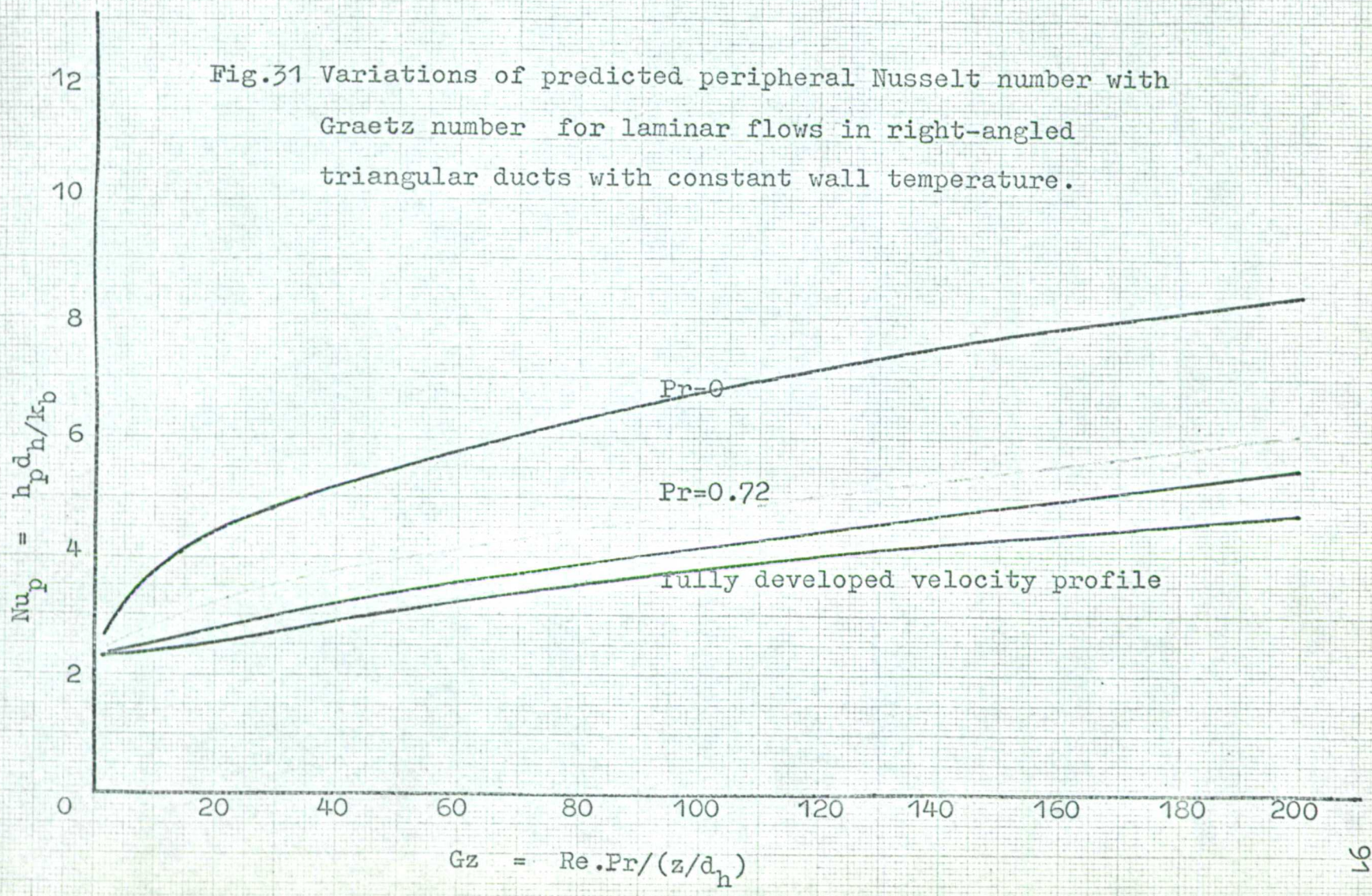

Fig.31 Variations of predicted peripheral Nusselt number with Graetz number for laminar flows in right-angled triangular ducts with constant wall temperature.

Fig.32 Variations of predicted mean Nusselt number with Graetz number for laminar flows in right-angled triangular ducts with constant wall temperature.

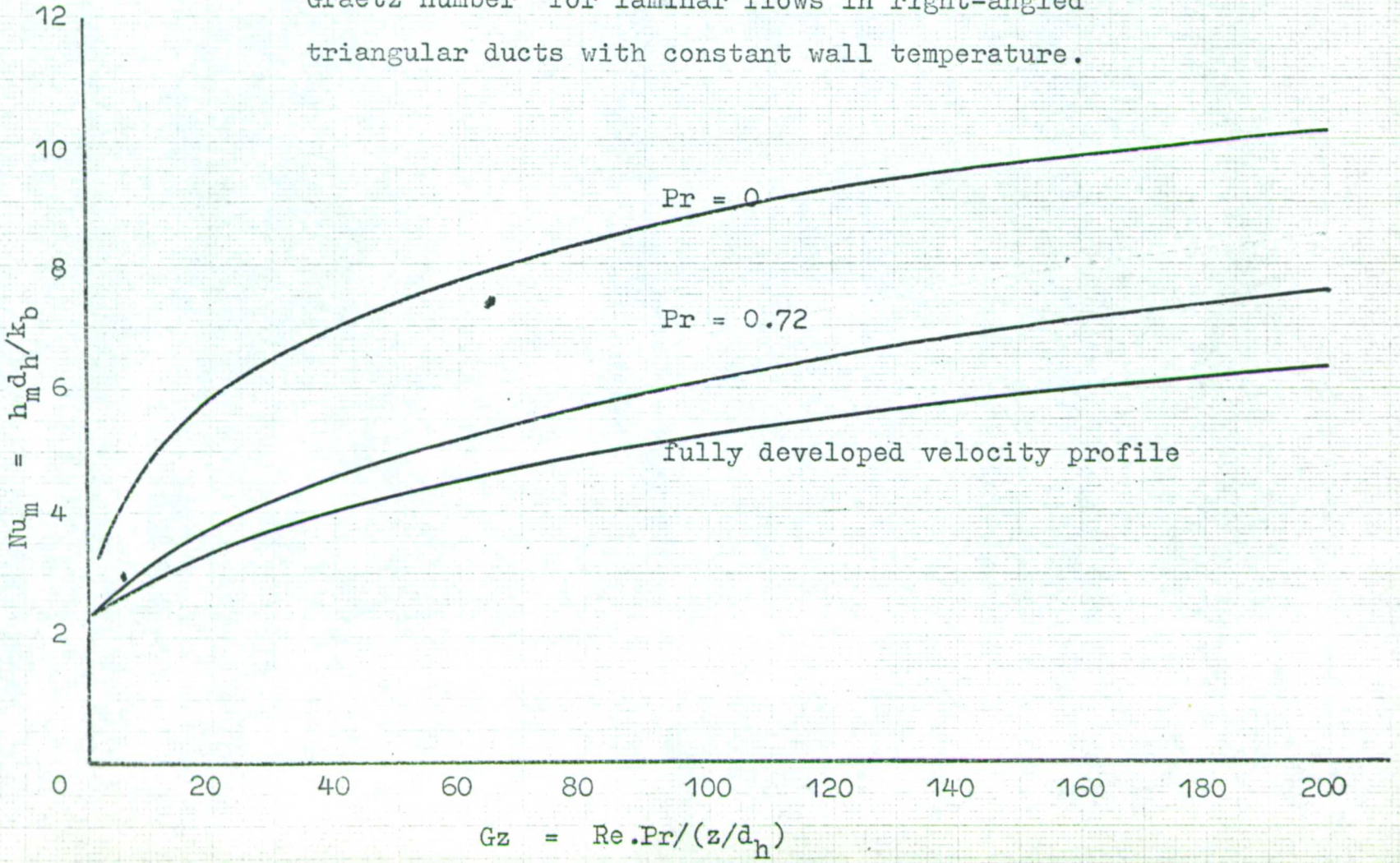

Fig. 33 Predicted peripheral Nusselt number , Nu_p, plotted against Graetz number , Gz, for right-angled isosceles triangular ducts with constant heat input per unit length.

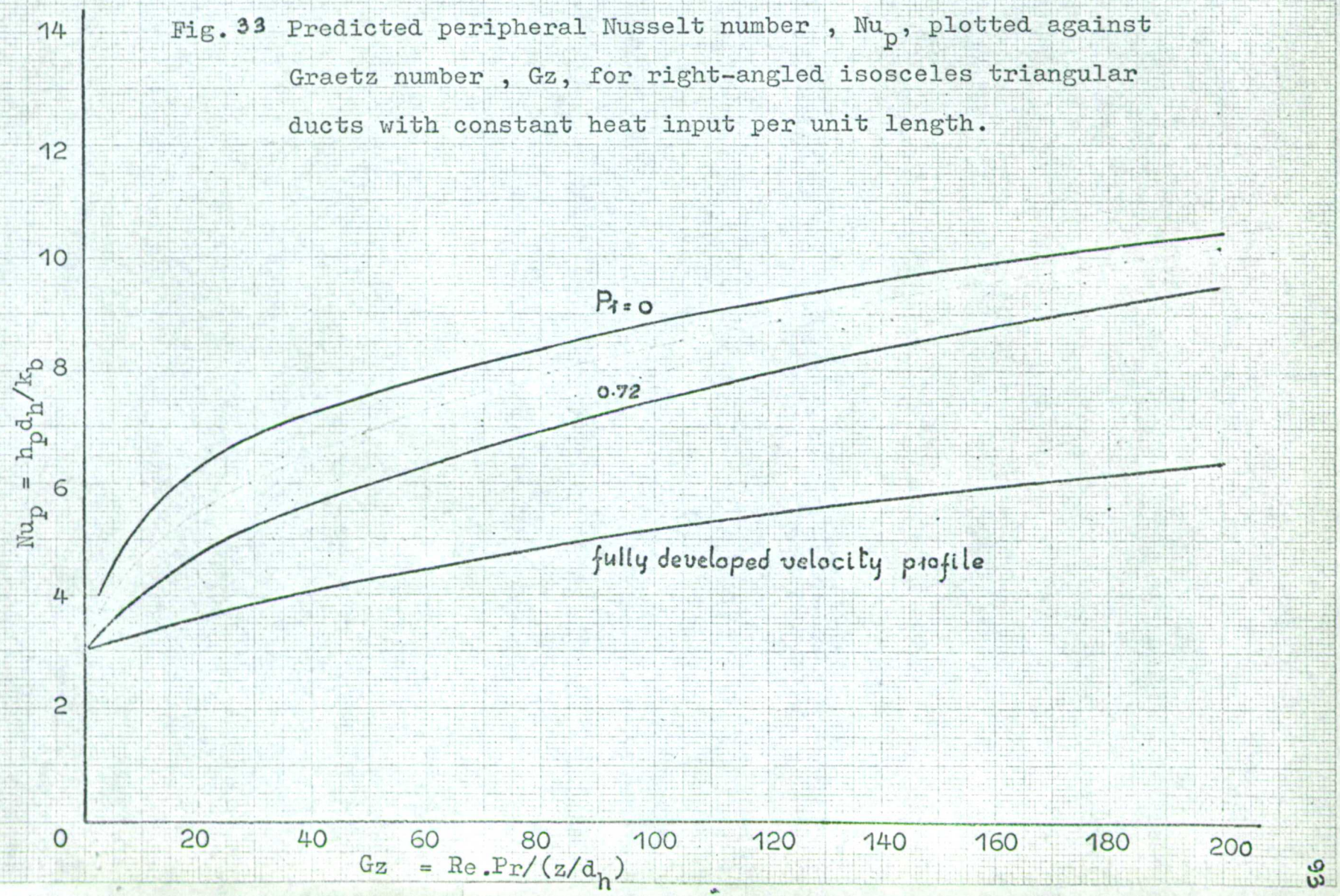

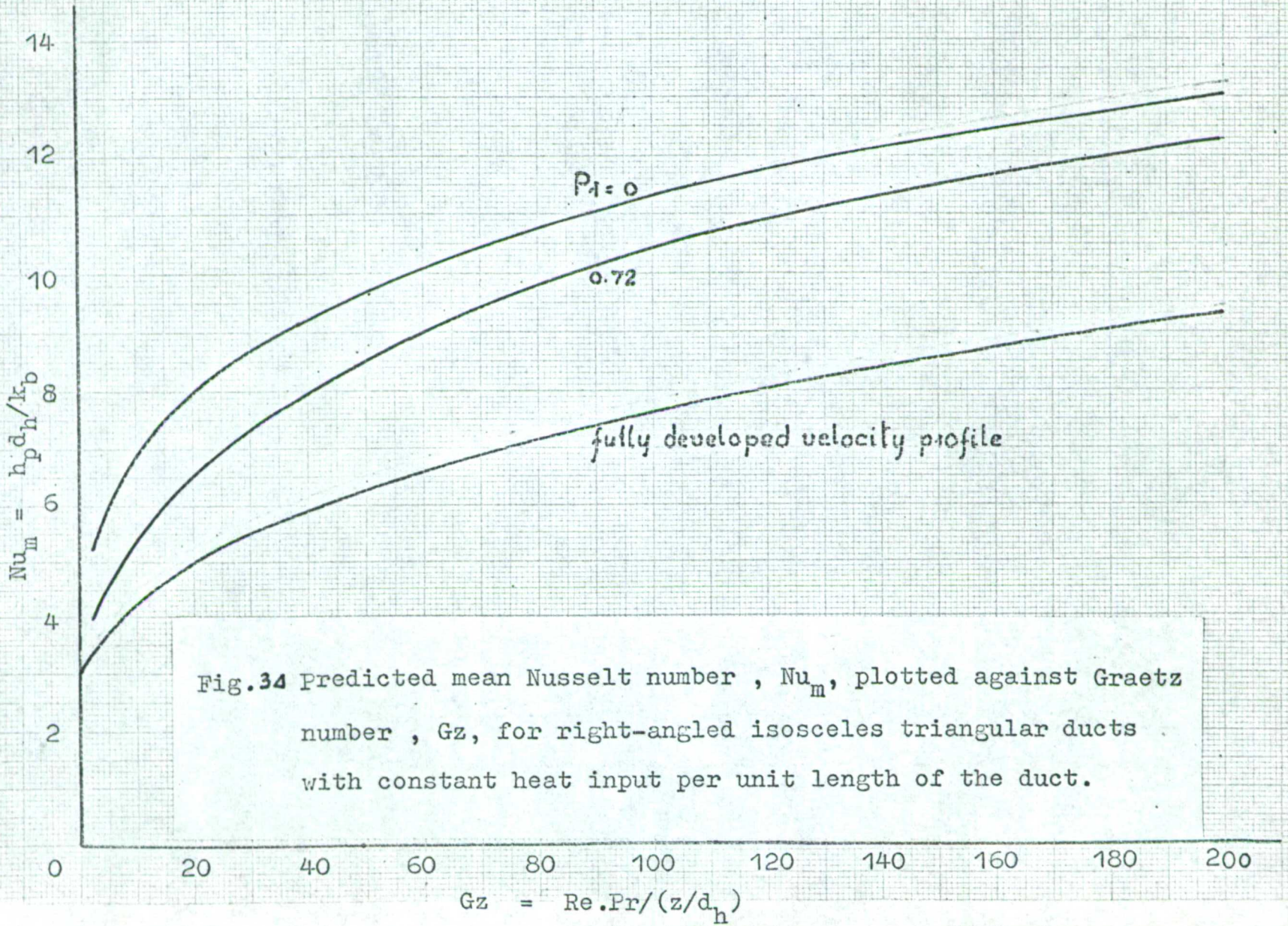

Fig.34 Predicted mean Nusselt number , Nu_m, plotted against Graetz number , Gz, for right-angled isosceles triangular ducts with constant heat input per unit length of the duct.

5.2. EQUILATERAL TRIANGULAR DUCT.

5.2.1 Exact Solution of the Fully Developed Velocity Profile.

The fully developed velocity profile for a laminar flow in an equilateral triangular duct has been determined exactly in ref.18. In fig.35, p.96, if the length of each side of the equilateral triangular duct is 'b' and the origin is at the centre of one of the sides which is on the y axis, the velocity, w, at any point on the cross section is given by

$$w = -\frac{\sqrt{3}}{6}\,b\,\frac{dp}{dz}\,x\,(x + \sqrt{3}y - \frac{\sqrt{3}}{2}b)\,(x - \sqrt{3}y - \frac{\sqrt{3}}{2}b)$$

Define the following parameters :

$$\text{Dimensionless velocity, } w^+ \equiv \frac{-w}{+\frac{\sqrt{3}}{6}\,b^2\,\frac{dp}{dz}}$$

Co-ordinates $x^+ \equiv x/b$ and $y^+ \equiv y/b$.

The above equation becomes

$$w^+ = x^+(x^+ + \sqrt{3}y^+ - \frac{\sqrt{3}}{2})(x^+ - \sqrt{3}y^+ - \frac{\sqrt{3}}{2}) \qquad (21)$$

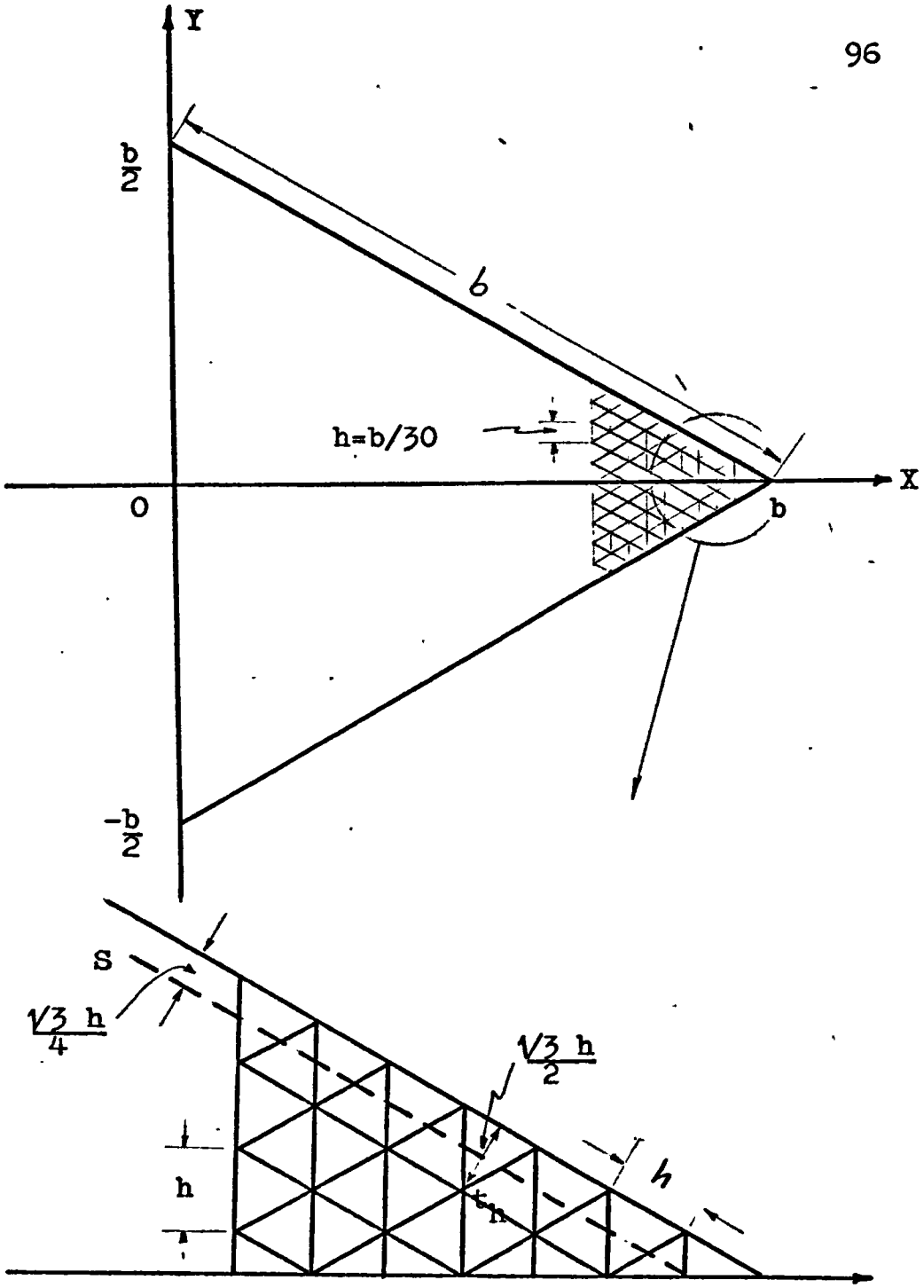

Fig.35 Network for the Equilateral Triangular Duct.

5.2.2 Finite Difference Operator for Equilateral Triangular Network.

To solve the energy equation numerically, for this particular cross section, it is convenient to use a network of equilateral triangles. A new finite difference operator K' is defined as :

$$K'f(x,y) = f_1 + f_2 + f_3 + f_4 + f_5 + f_6 - 6f_0$$

where $f_0, f_1, f_2 \ldots\ldots f_6$ are functions of x and y.

Diagrammatically, K'f(x,y) =

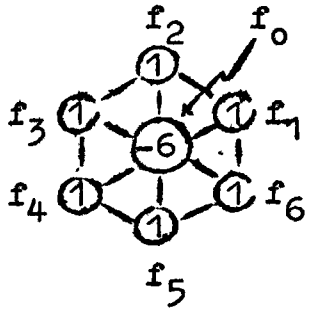

A relationship between the operator K' and $(\partial^2/\partial x^2 + \partial^2/\partial y^2)$, which will be represented by ∇^2, has been obtained on p.23 of Southwell's book (31) as :

$$\frac{1}{6} K'f(x,y) = \frac{h^2}{16}\left\{3\nabla^2 f_0 + \frac{1}{6}(\nabla^2 f_1 + \nabla^2 f_2 + \ldots \nabla^2 f_6)\right\} \qquad (22)$$

From the above equation, it can be seen that a direct evaluation of the term '$\nabla^2 f(x,y)$' at each nodal point requires six neighbouring '$\nabla^2 f$' terms which are also

not known. However, this difficulty can be overcome by the following steps of computations :

(1) For the first approximation, put

$$\nabla^2 f_1 + \nabla^2 f_2 + \ldots\ldots\ldots + \nabla^2 f_6 \simeq 6\nabla^2 f_o$$

Equation (22) becomes

$$h^2 \nabla^2 f(x,y) \simeq \frac{2}{3} K' f(x,y)$$

The above equation is used to compute approximate values of '$\nabla^2 f$' terms over the whole cross sectional area.

(2) Use the values of $\nabla^2 f$ obtained in (1) in equation (22) and recompute a new distribution of $\nabla^2 f$.

(3) Repeat the computation of the distribution of $\nabla^2 f$ by using equation (22) and the values of $\nabla^2 f$ obtained previously until steady values are obtained.

5.2.3 Numerical Solution of the Energy Equation.

The energy equation (2a) in the finite difference form is

$$\nabla^2 t(x,y,z) = \frac{w}{\alpha} \frac{\Delta t}{\Delta z}$$

Replace $\nabla^2 t$ in the above equation by equation (22).

$$\begin{aligned} \Delta t &= t(x,y,z+\Delta z) - t(x,y,z) \\ &= \frac{8}{9} \frac{w_b}{w} \frac{\alpha \Delta z}{w_b d_h^2} \frac{d_h^2}{h^2} \left\{ K' t(x,y,z) - \frac{h^2}{16} (\nabla^2 t_1 + \nabla^2 t_2 \right. \\ &\qquad \left. + \nabla^2 t_3 + \ldots + \nabla^2 t_6) \right\} \quad (23) \end{aligned}$$

Values of $\nabla^2 t_1$, $\nabla^2 t_2$, ... and $\nabla^2 t_6$ are computed by the method described in the preceding section, values of other terms, i.e. w_b/w, $(\alpha\Delta z/w_b d_h^2)$ and $(d_h/h)^2$, are determined by the same procedures as those in section (3.4).

Example

For the triangular network shown in fig.35, p.96,

the finite step, $h = b/30$

Hydraulic diameter, $d_h = 4A_c/P = b/\sqrt{3}$

$e \equiv h/d_h = \frac{b}{30}\cdot\frac{\sqrt{3}}{b} = 1/10\sqrt{3}$

It $(\alpha\Delta z)/(w_b d_h^2)$ is chosen to be 15000, equation (23) is reduced to

$$t(x,y,z+\Delta z) = \frac{8}{9}\cdot\frac{1}{50}\left\{ K't(x,y,z) - \frac{h^2}{16}\left(\nabla^2 t_1 + \nabla^2 t_2 + ... \nabla^2 t_6 \right)\right\} + t(x,y,z) \qquad (24)$$

Initial and wall values of temperatures are required to solve the above equation numerically and they can be determined by using the same dimensionless temperatures as those in sections (3.5) & (3.6).

Hence for constant wall temperature, the dimensionless temperature $\theta \equiv (t_w - t)/(t_w - t_o)$, and the boundary values are :

$$\theta_{w,o} = \theta_w = 0 \quad \text{and} \quad \theta_{b,o} = 1.$$

Numerical solutions for the hydraulic conditions of uniform velocity profile, fully developed velocity profile and simultaneously developing profiles were obtained by means of the Atlas computer and results are plotted on p.102 and 103, and tabulated in Appendix (7.11).

The thermal condition of constant heat input per unit length of the duct requires a slight modification for the determination of the wall temperature, but the basic approach remains the same as that of the rectangular ducts.

Since the nodal points adjacent to the duct wall are at a distance $\sqrt{3}h/2$ from the latter, see fig.35, p.96, a surface S at a distance $\sqrt{3}h/4$ from the duct wall has to be considered instead of h/2 for the rectangular ducts.

By using the first law of thermodynamics and the same approach as that in section (3.6.2), it can be shown that

$$\frac{2}{\sqrt{3}} k n t_w - \frac{2}{\sqrt{3}} k \sum_{1}^{n} t_h = \rho C_p w_b A_c \frac{dt_b}{dz} - \frac{\sqrt{3}}{16} \rho C_p h^2 \sum w_h \frac{dt_h}{dz}$$

The above equation can be written in terms of dimensionless temperature, β, defined on p.52 and rearranged into

$$\beta_w = \frac{\sqrt{3}}{8} e + \frac{1}{n} \sum_{1}^{n} \beta_h - \frac{3}{32} \frac{e^2}{n} \frac{w_b d_h^2}{\alpha \Delta z} \sum_{1}^{n} \frac{w_h}{w_b} \Delta \beta_h \qquad (25)$$

Numerical solutions were obtained for uniform velocity profile, fully developed velocity profile and simulta-

neously developing profiles by the same computing methods as those in sections (3.6) and (4.1) and by using equation (25) to determine the wall temperature. Variations of the Nusselt number with the Graetz number obtained from the computer are plotted in fig.38 & 39, p.104 & 105 and tabulated in Appendix (7.12).

5.2.4 Experimental Results.

Details of the equilateral triangular test section for constant heat input per unit length of the duct have already been described in section (2.6), p.32. Tests were carried out for the boundary conditions of fully developed velocity profile, i.e. with the unheated inlet section, and of simultaneously developing profiles. Results were computed by the same method as those of the rectangular duct in section (3.7.1) and they are presented in fig. 40 and 41, p. 106 and 107.

Fig.36 Predicted peripheral Nusselt number, Nu_p, plotted against Graetz number, Gz, for equialteral triangular ducts with constant wall temperature. fully developed velocity profile

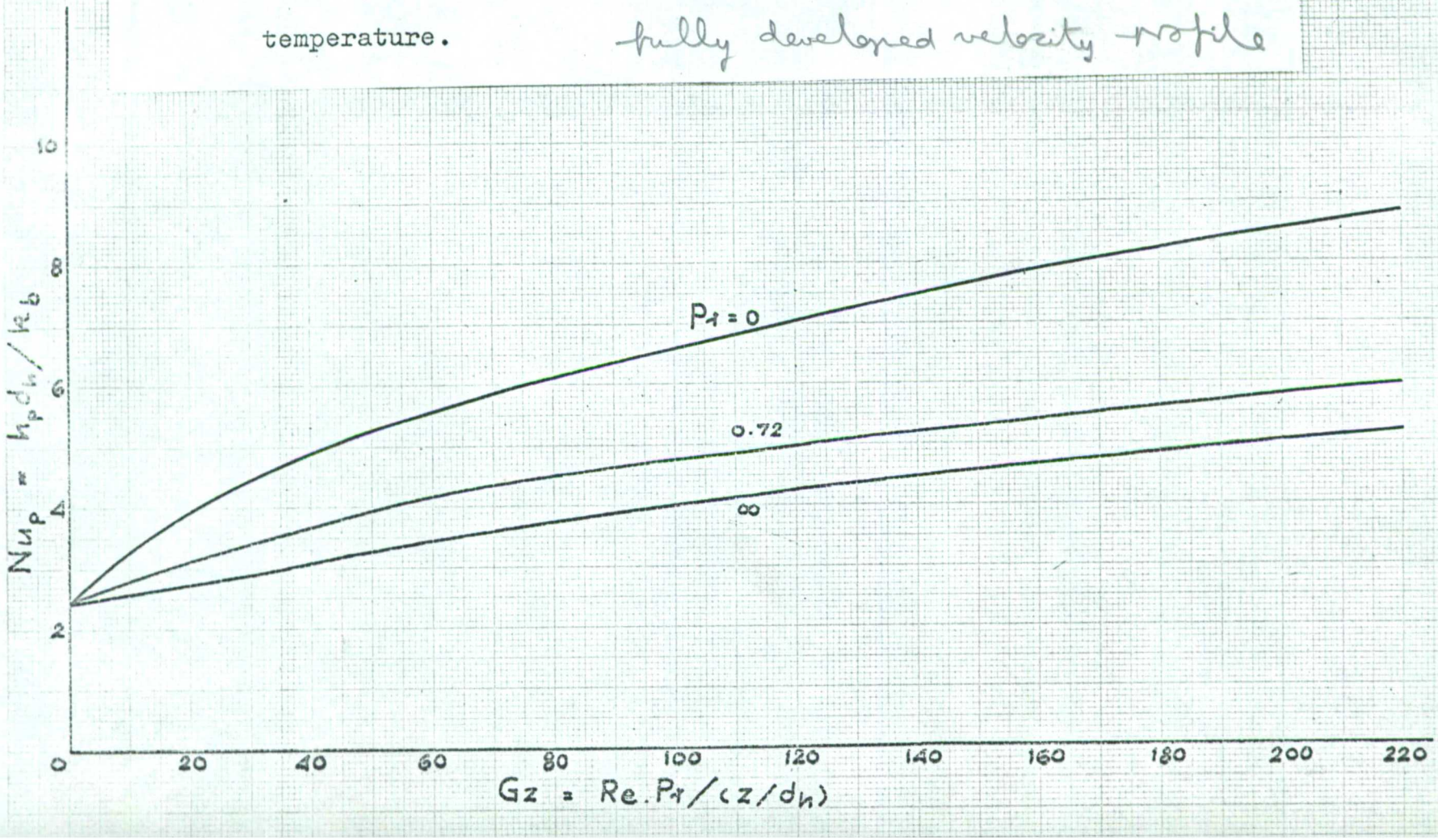

Fig. 37 Predicted mean Nusselt number , Nu_m, plotted against Graetz number , Gz, for equilateral triangular ducts with constant wall temperature.

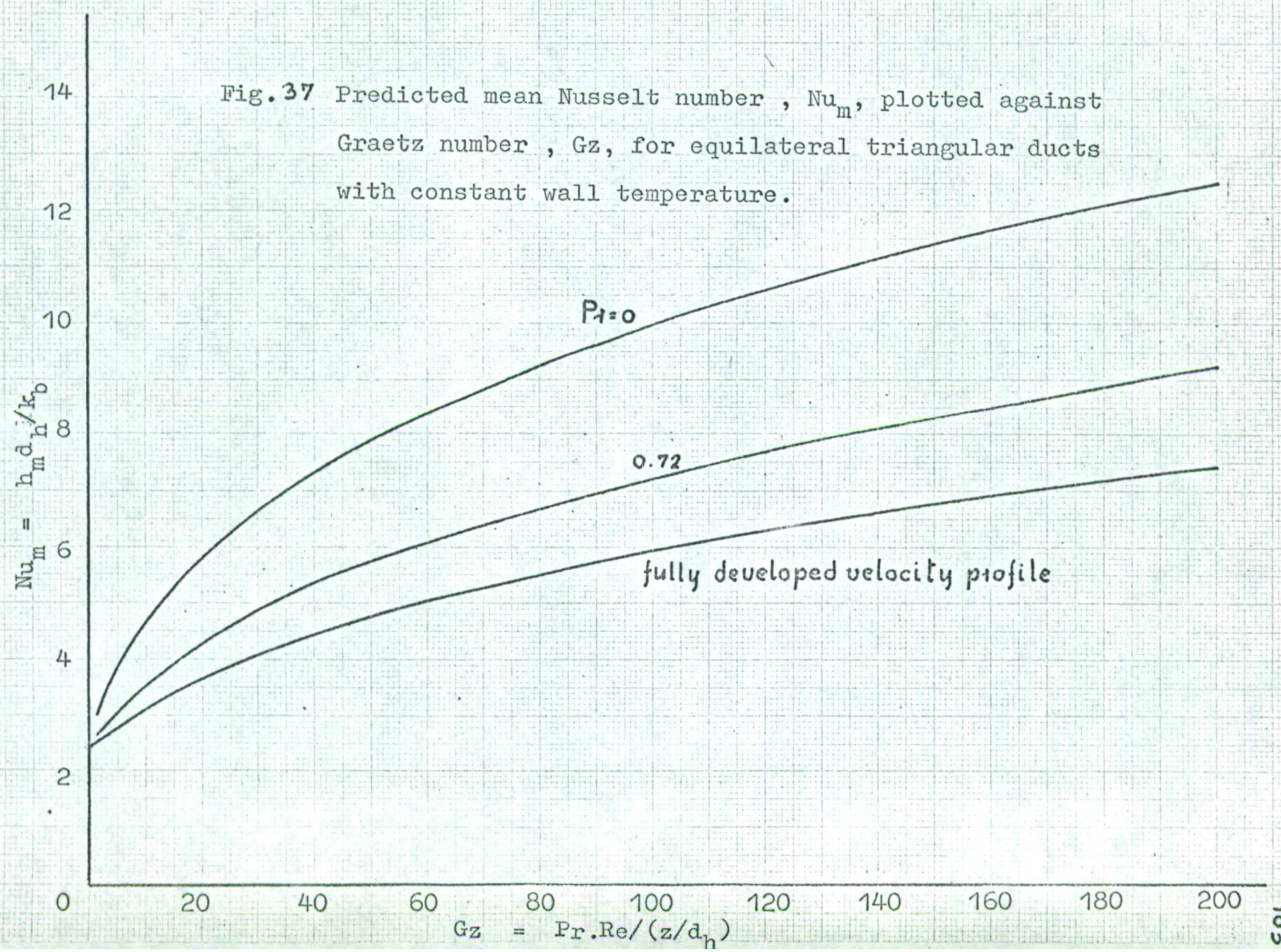

Fig. 38 Predicted peripheral Nusselt number, Nu_p, plotted against Graetz number, Gz, for equilateral triangular ducts with constant heat input per unit length of the duct.

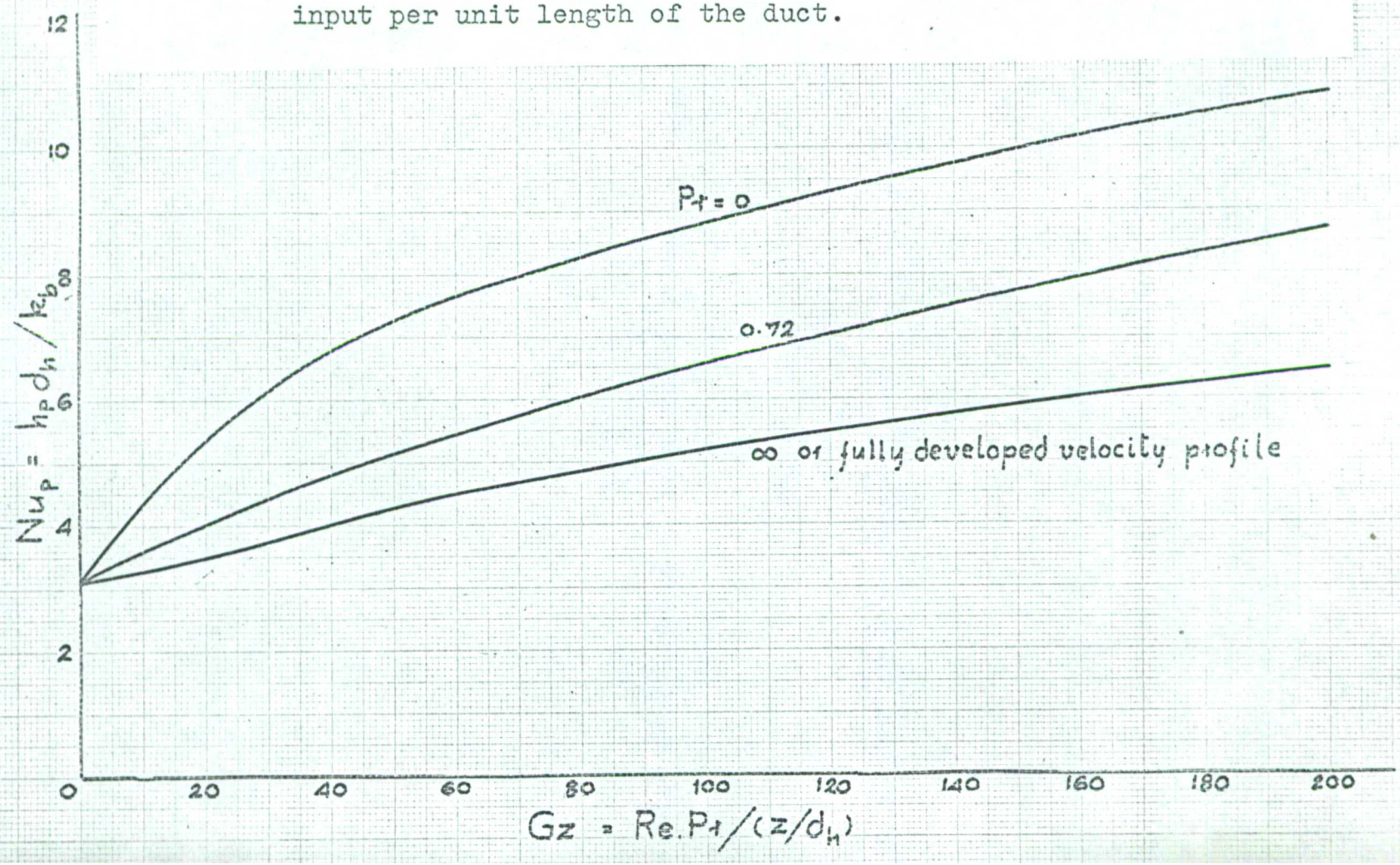

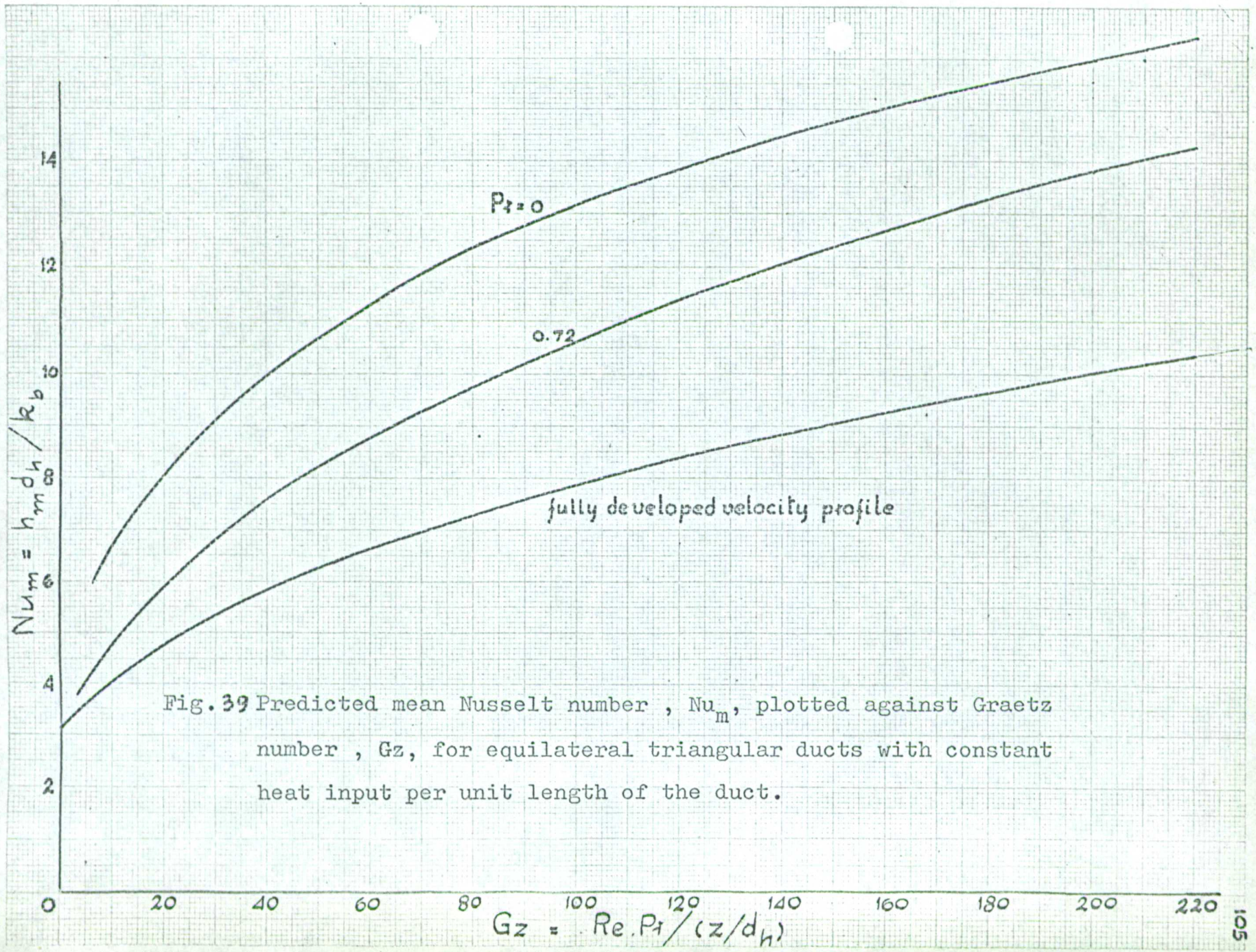

Fig. 39 Predicted mean Nusselt number , Nu_m, plotted against Graetz number , Gz, for equilateral triangular ducts with constant heat input per unit length of the duct.

Fig. 40 Measured logarithmic mean Nusselt numbers plotted against Graetz numbers for fully developed velocity profile in an equilateral triangular duct with constant heat input per unit length of the duct.

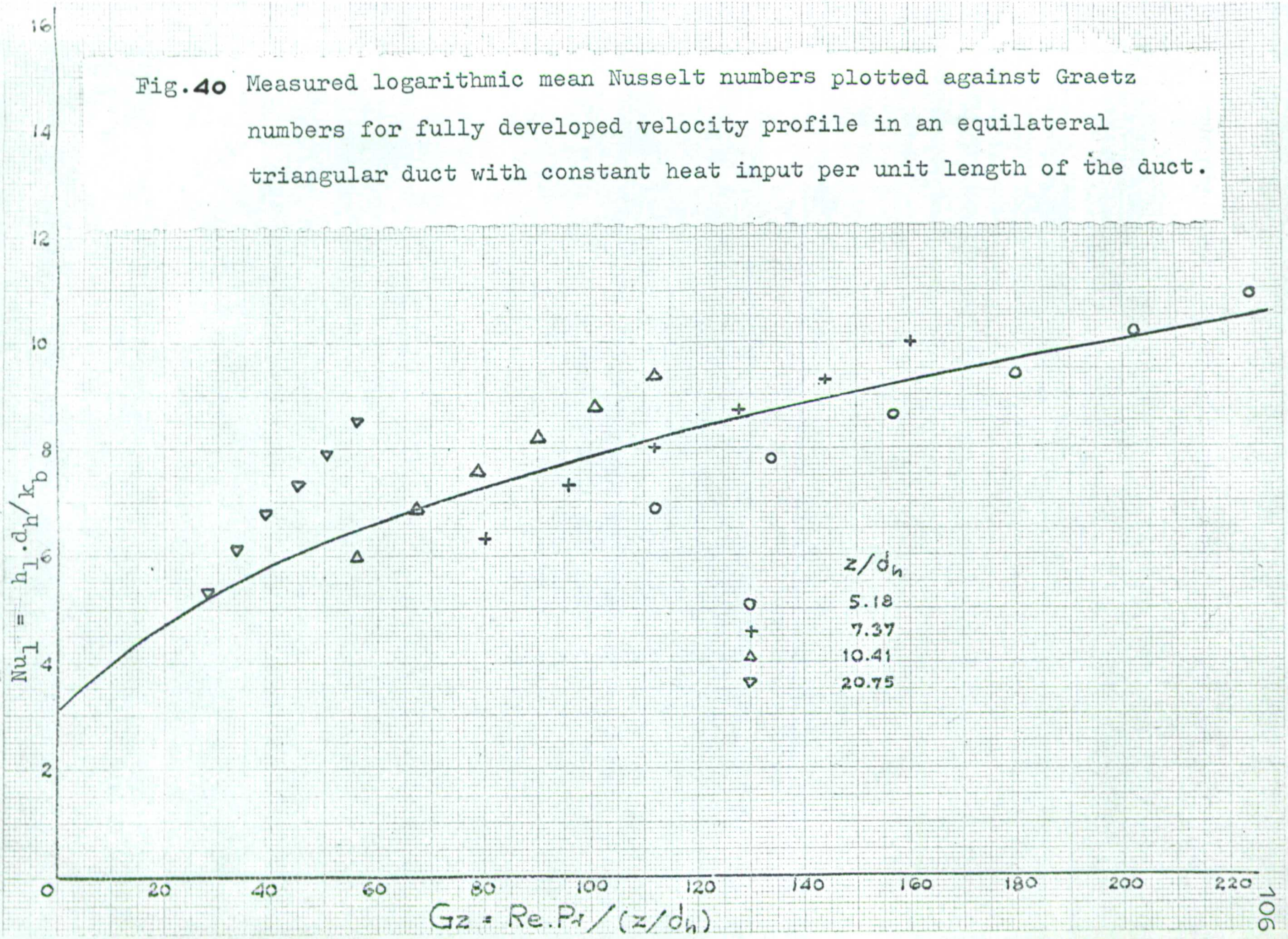

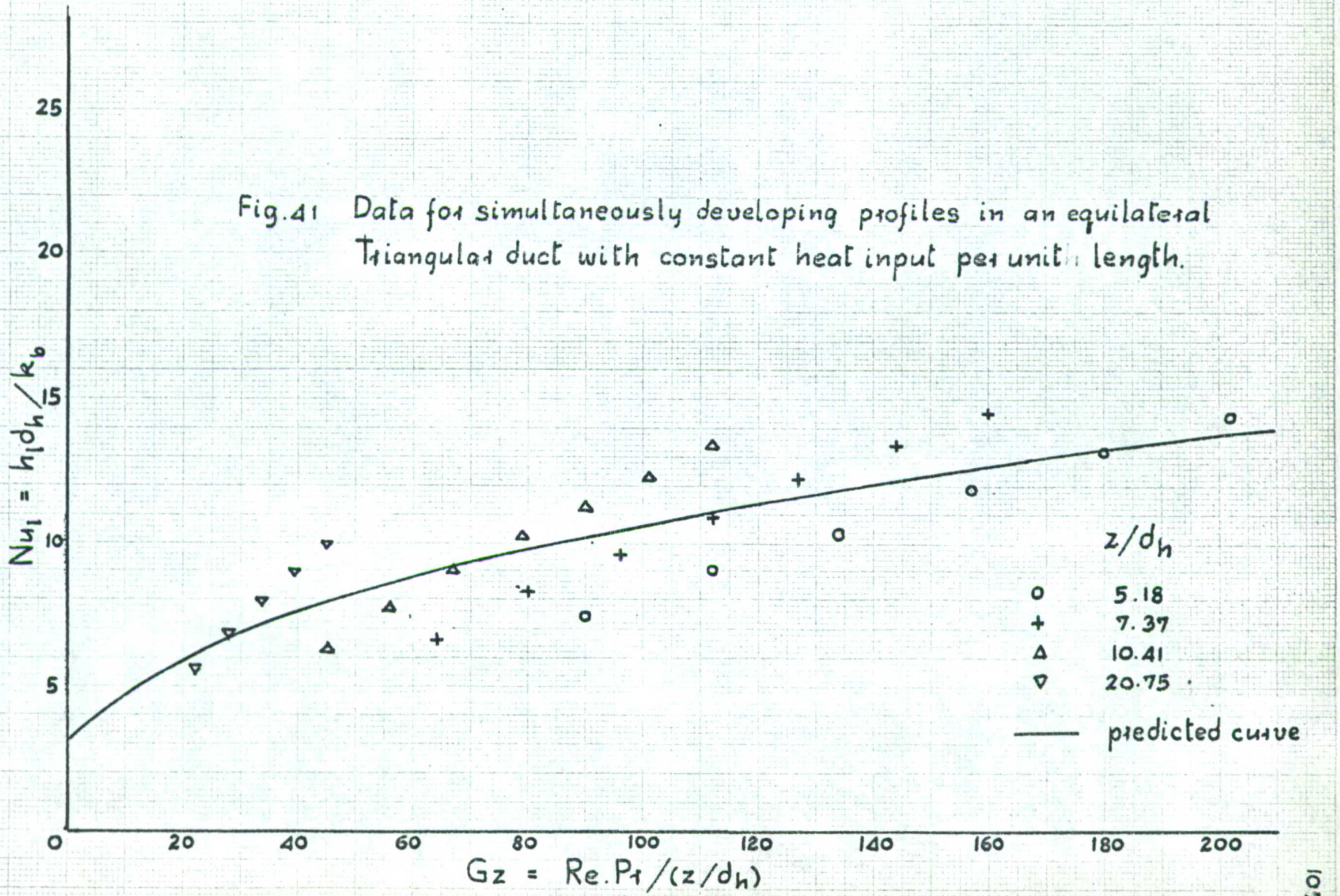

Fig. 41 Data for simultaneously developing profiles in an equilateral Triangular duct with constant heat input per unit length.

CHAPTER 6

DISCUSSION AND CONCLUSION

6.1 PREDICTED NUMERICAL SOLUTIONS.

In the same manner as the exact solutions for the circular ducts (26,28) and parallel plates (27,29), the numerical solutions obtained in sections (3.5,3.6) for fully developed velocity profiles in rectangular ducts with different aspect ratios show that for a given aspect ratio, the Nusselt number has a maximum value at the entry plane of the duct and decreases as the Graetz number decreases. As the Graetz number approaches zero, i.e. at large distances from the entry plane or very small flow rates, the Nusselt number approaches a limiting value which represents fully developed velocity and temperature profiles. The Nusselt number increases with increasing aspect ratio and has its greatest and least values for parallel plates and square ducts respectively.

The results also show a strong effect of the thermal boundary conditions. The comparison of different conditions in fig.17, p.63, shows that for the same aspect ratio, constant heat input per unit length gives higher Nusselt numbers than those of constant wall temperature, a

result similar to that obtained for circular ducts.

Accuracy of the numerical method depends upon the sizes of the squares in the computing network and the finite step along the duct. In computation, it has been found that when comparing the numerical solution of the velocity profile to its exact solution found from equation (5), an accuracy within one per cent can be obtained if the size of squares in the network is less than one tenth of the hydraulic diameter of the duct. The same size of squares has been used for predicting fluid temperatures, hence the same order of accuracy may be expected. For the steps along the axis of the duct, the dimensionless group, $(w_b/w)(\alpha\Delta z/d_h^2 w_b)(d_h/h)^2$ in equation (6) must be less than 1/2, otherwise the solution becomes unsteady. On the other hand, if the sizes of the network and the finite steps are too small, too much time will be required for computation.

Predicted Nusselt numbers for simultaneously developing velocity and temperature profiles in rectangular ducts in fig . 22-25, p.78-81, exhibit variations with the Graetz numbers similar to the solutions for fully developed velocity profiles in fig. 11-17. Theoretical curves for circular ducts (2,3) and parallel plates (8,11) are also shown as a comparison and they show the same trends as the predicted results obtained in this work. At a high Graetz

number, the Nusselt number for the former is greater than that of the latter and their difference decreases as the Graetz number decreases until at the Graetz number of zero, both solutions are asymptotic to the limiting Nusselt number, fig.26, p.82.

As already mentioned on p.76-77, the Prandtl number has a strong effect on the Nusselt number for laminar flow with simultaneously developing profiles. Fig.27 & 28, p.83 & 84, show that at the same Graetz number, a small Prandtl number gives a higher Nusselt number than a larger one. This can be deduced from equation (18) that the velocity profile of a fluid with a small Prandtl number develops more slowly than that of a fluid with a larger Prandtl number. Hence, the solution for the uniform velocity profile, or $Pr = 0$, represents the upper limit and the solution for the fully developed velocity profile, or $Pr = \infty$, corresponds to the lower limit.

Predicted Nusselt numbers for the right-angled isosceles triangular and equilateral triangular ducts in fig.31-34 & 36-39 vary with Graetz numbers in the same manner as those for rectangular ducts.

It may be noticed that all numerical solutions in the present work are presented within a useful range of the Graetz numbers from 0 to 200. For a Graetz number over 200,

the duct is too short for any practical use, or else the flow is too large for the laminar regime, for example, with a flow of atmospheric air at Reynolds number of 1600 and Graetz number of 200, the dimensionless length of the duct (z/d_h), is only 5.76.

6.2 COMPARISON WITH EXPERIMENTAL RESULTS.

Experimental data for fully developed velocity profiles in circular ducts with constant wall temperature (26) shows that at high Graetz numbers, the measured Nusselt numbers are greater than those predicted by Graetz. Experimental results have been obtained for a rectangular duct with the same boundary condition and they showed a similar deviation, fig.21, p.71. For a Graetz number under 70, experimental and predicted results agreed quite well, at Graetz numbers of 100 and 150, the deviations were about 28 and 51 % respectively. The discrepancy was partly due to an effect of the variation of fluid thermal conductivity with temperature. At a high Graetz number, i.e. a short distance from the entry plane, the wall temperature and fluid temperatures close to the wall were much higher than the bulk temperature, and as a result, thermal conductivities of the formers were much larger than that of the latter. From equation (6), p.39, it can be deduced that the fluid temperatures near the wall

increased more rapidly than the predicted values obtained by assuming constant properties at the bulk temperature. Though the opposite effect occurred at the central part of the cross section where fluid temperatures were lower than the bulk temperature, their deviations were less than those of the temperatures near the wall, and hence the overall effect resulted in a higher measured value of the bulk temperature than predicted value . At a low Graetz number, i.e. a large distance from the entry plane, the temperature difference between the wall and the fluid bulk was much less than that at a high Graetz number, the effect of varying thermal conductivity was therefore very small and a good agreement between the measured and predicted results was obtained.

For the thermal condition of constant heat input per unit length of the duct, experimental data was obtained for the rectangular and equilateral triangular ducts with fully developed velocity profiles and simultaneously developing profiles. Results in fig.19, 29, 40 and 41, p.69, 85, 106 and 107, show closer agreements over wider ranges of the Graetz number than those for constant wall temperature. At a low Reynolds number, the measured Nusselt number is slightly lower than the theoretical value. This appears to be due to the opposing free convection effects which were present in all the shown experimental results and became more apparent at a low flow rate. By inverting the test section used in

section (3.7.1), a few tests with additive free convection were performed and it was found that at Reynolds numbers of 1060, 1400 and 1800, the mean Nusselt numbers increased by about 17, 10 and 3 % respectively.

The effect of varying thermal conductivity, which caused a deviation of the measured Nusselt number from its predicted value, was apparent at a low Graetz number, i.e. a long distance from the entry plane, where the temperature difference between the wall and fluid bulk was much larger than that at a short distance, (c.f. constant wall temperature). The same result was also obtained in ref.(33) for Graetz numbers up to 14.

In a test with constant heat input per unit length, it was assumed that the presence of a thin film of Hermetal between the duct wall and thermocouple junction introduced a negligible error in the measurement of wall temperature, section (2.5), p.30. This was confirmed by an experiment in which a thermocouple was directly attached on to the outside surface of a metal can containing boiling water while a thin film of Hermetal was present between another thermocouple and the surface of the can. Readings of both thermocouples were taken with a circuit the accuracy of which was $\pm$ 0.2 deg.F. and no difference was observed betweer the two readings which were subjected to a higher temperature gradient than those of the ducts in the experiments.

6.3 CONCLUSION.

In the present work, numerical solutions have been obtained for laminar flow heat transfer with fully developed velocity profiles and simultaneously developing velocity and temperature profiles in rectangular ducts of various aspect ratios and in right-angled isosceles and equilateral triangular ducts for the thermal boundary conditions of constant wall temperature and constant heat input per unit length of the duct. The solutions give the limiting Nusselt numbers which approach those calculated by other methods,(1) and section (7.1), and moreover, their trends are compatible with those of the corresponding theoretical solutions obtained by various authors for circular ducts (26, 28, 2 and 3) and parallel plates (27, 29, 8 and 11). This indicates that the numerical method employed here is reasonably accurate for both square and triangular networks. Since the method is straight forward and effective, it may be extended to heat transfer in other cross sections such as circular sectors, various triangular and elliptical cross sections. Though suitable computing networks such as rectangular ones for rectangular ducts with very large aspect ratios have to be used and some modifications of the finite difference operators and of the expression for the wall temperature will be required, solutions can still be obtained

without too much difficulties with a help of a fast digital computer.

It can be finally concluded that

(1) for the same Graetz number and thermal boundary condition, a rectangular duct with aspect ratio greater than 2 gives a higher Nusselt number than a circular one, but all triangular ducts give lower Nusselt numbers than circular and rectangular ones;

(2) for the same Graetz number and thermal boundary condition, a flow with simultaneously developing profiles gives higher Nusselt number than that with fully developed velocity profile;

(3) since most experimental values of the Nusselt number are higher than the predicted ones, the latter can be used as a lower limit in design.

(4) a more compact heat exchanger can be designed by using a large number of short tubes rather than a few long tubes.

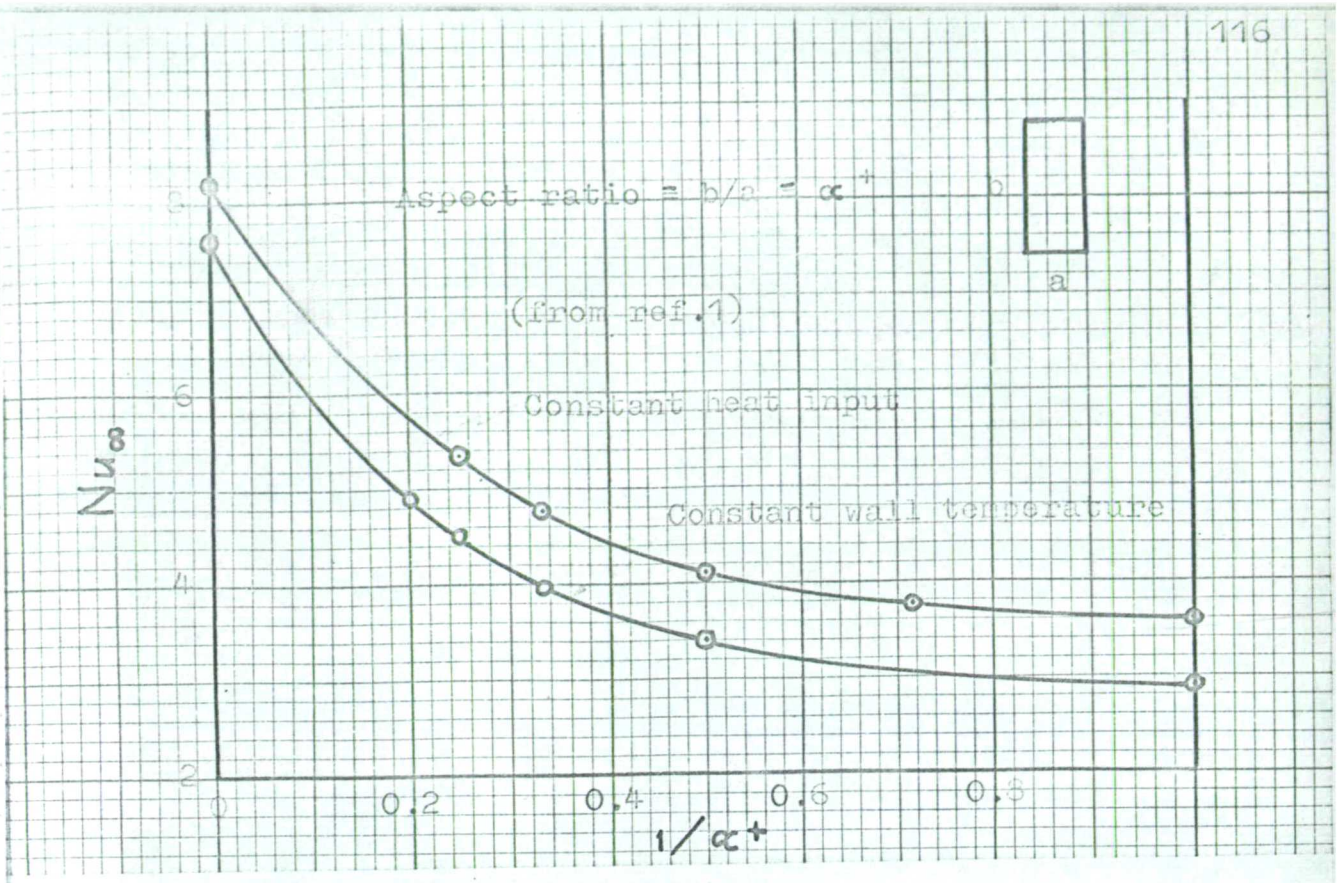

APPENDIX 7.1 Limiting Nusselt numbers, Nu_∞ , for fully developed laminar flow in ducts of various non-circular cross sections.

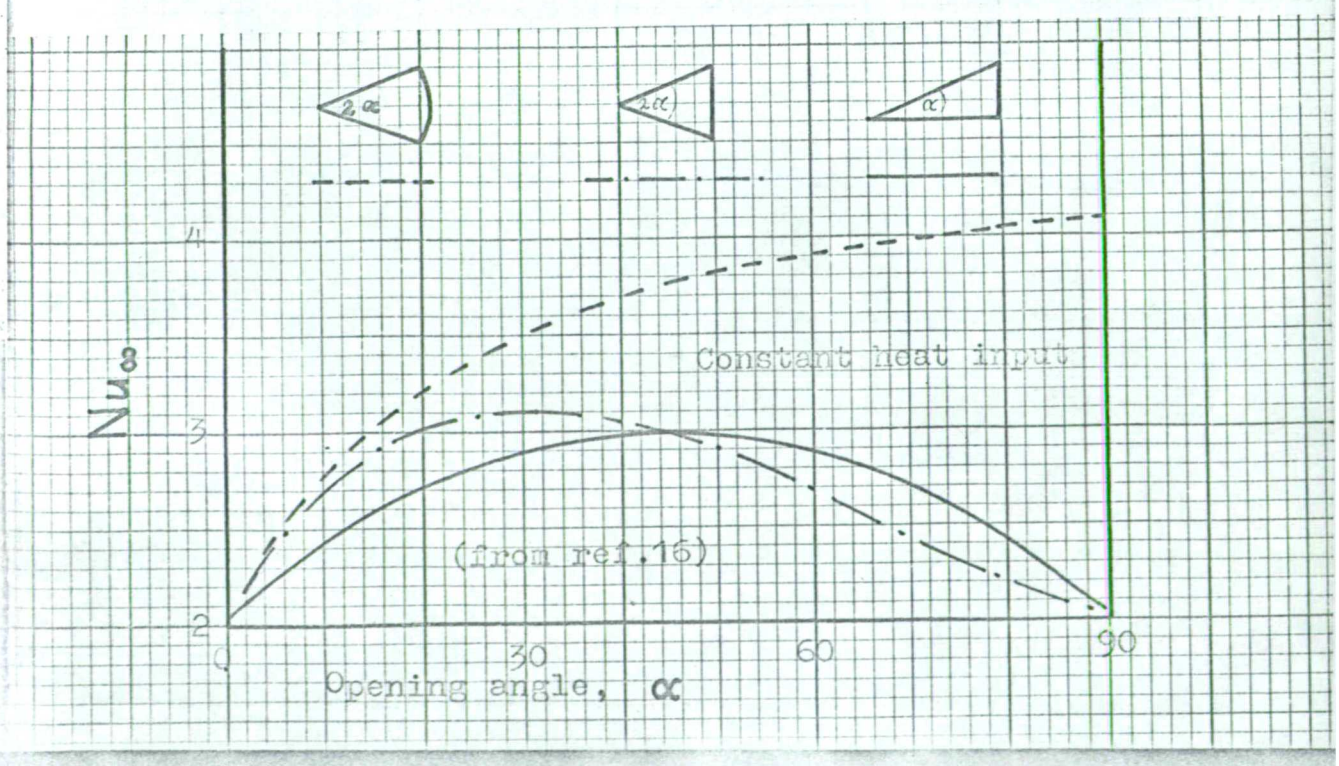

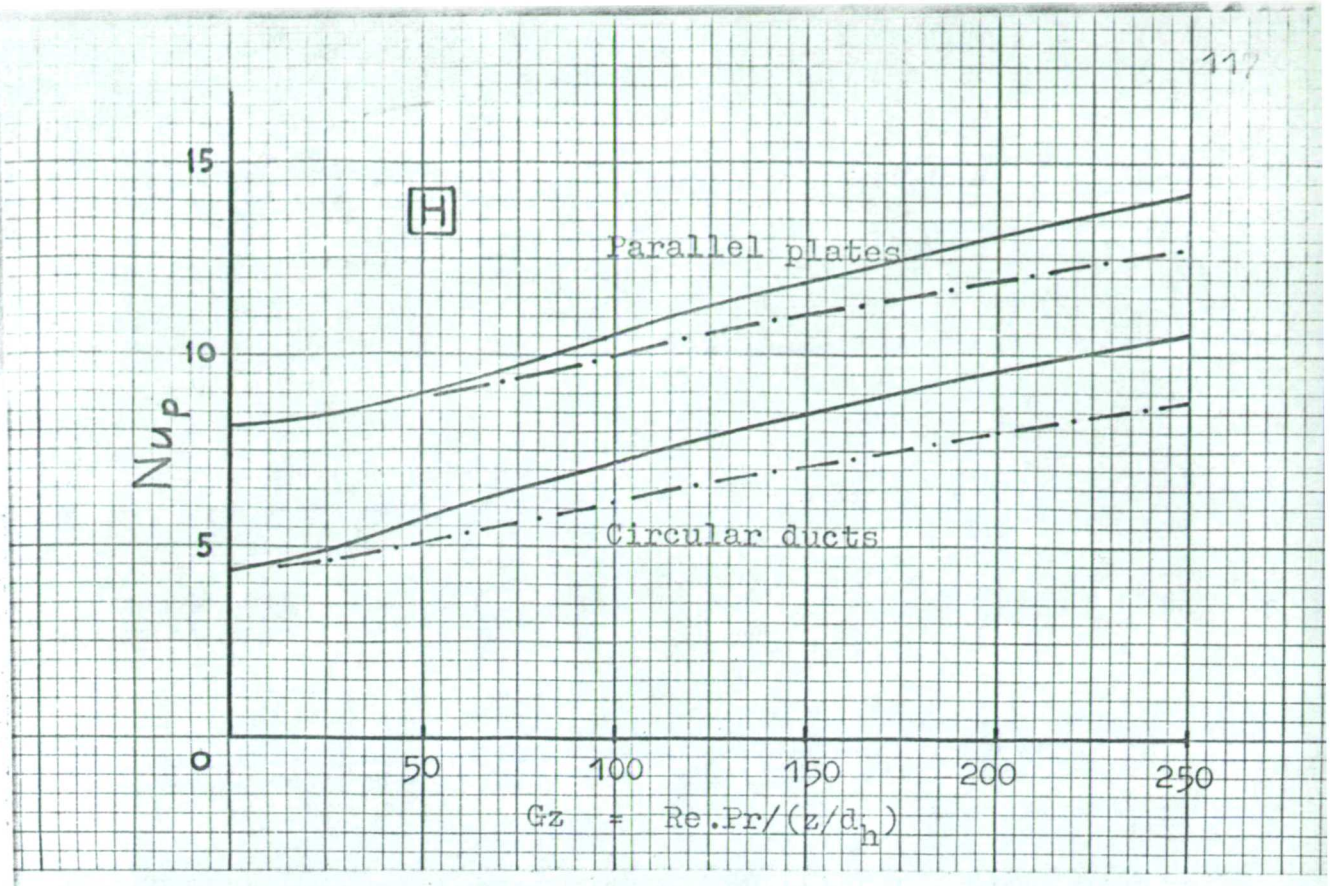

Variations of predicted Nusselt numbers, Nu , with Graetz number for circular ducts and parallel plates; · ——· ——· fully developed velocity profile, ——— simultaneously developing profiles.

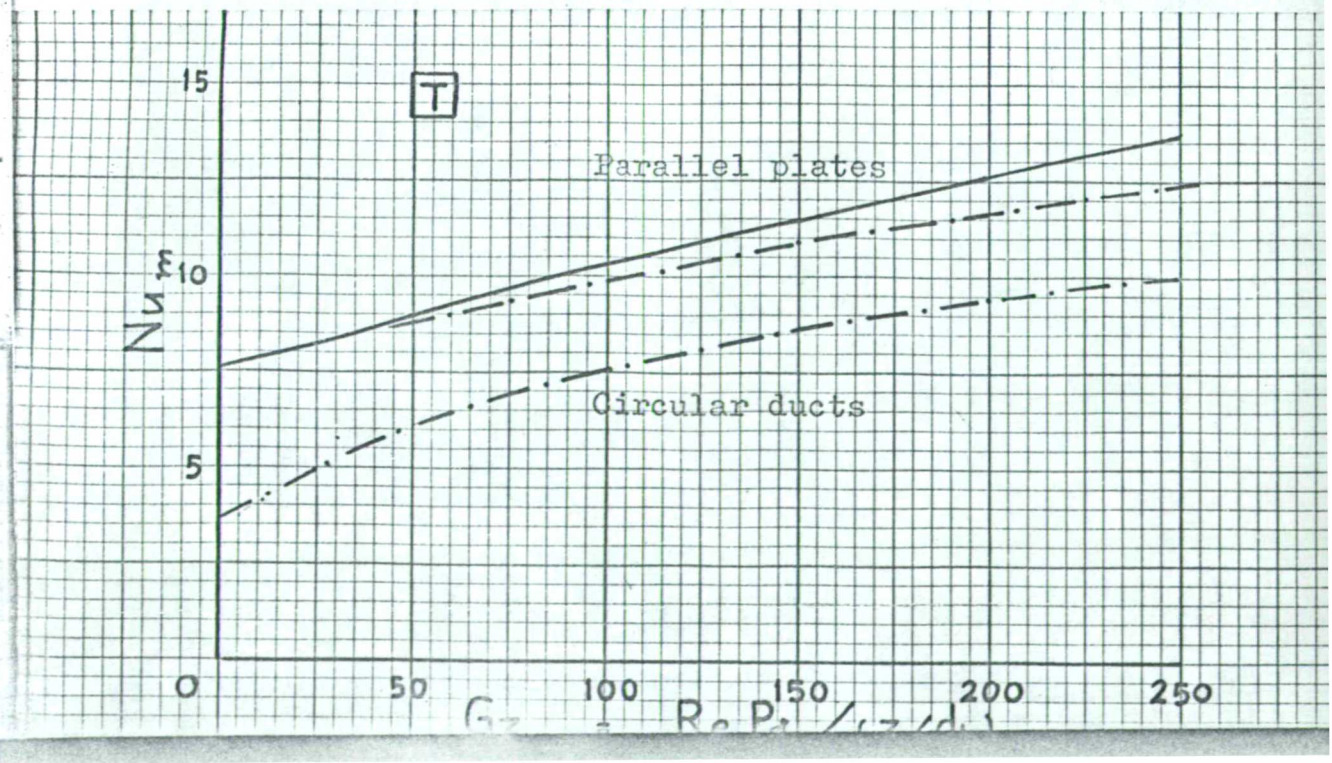

7.3 Predicted Nusselt numbers for fully developed velocity profiles with constant wall temperature.

Peripheral Nusselt numbers, Nu_p

Gz	Aspect Ratio 1.0	2.0	3.0	4.0	5.0	6.0
0	2.65	3.39	3.96	4.51	4.92	5.22
10	2.66	3.43	4.02	4.53	4.94	5.24
20	3.08	3.54	4.17	4.65	5.04	5.34
30	3.24	3.70	4.29	4.76	5.31	5.41
40	3.43	3.85	4.42	4.87	5.22	5.43
60	3.78	4.16	4.67	5.08	5.40	5.64
80	4.10	4.46	4.94	5.32	5.62	5.86
100	4.35	4.72	5.17	5.55	5.83	6.07
120	4.62	4.93	5.42	5.77	6.06	6.27
140	4.85	5.15	5.62	5.98	6.26	6.47
160	5.03	5.34	5.80	6.18	6.45	6.66
180	5.24	5.54	5.99	6.37	6.63	6.86
200	5.41	5.72	6.18	6.57	6.80	7.02

Mean Nusselt numbers, Nu_m

Gz	Aspect Ratio 1.0	2.0	3.0	4.0	5.0	6.0
0	2.65	3.39	3.96	4.51	4.92	5.22
10	3.50	3.95	4.54	5.00	5.36	5.66
20	4.03	4.46	5.00	5.44	5.77	6.04
30	4.47	4.86	5.39	5.81	6.13	6.37
40	4.85	5.24	5.74	6.16	6.45	6.70
60	5.50	5.85	6.35	6.73	7.03	7.26
80	6.03	6.37	6.89	7.24	7.53	7.77
100	6.46	6.84	7.33	7.71	7.99	8.17
120	6.86	7.24	7.74	8.13	8.39	8.63
140	7.22	7.62	8.11	8.50	8.77	9.00
160	7.56	7.97	8.45	8.86	9.14	9.35
180	7.87	8.29	8.77	9.17	9.46	9.67
200	8.15	8.58	9.07	9.47	9.79	10.01

7.4 Predicted Nusselt numbers for fully developed velocity profiles with constant heat input per unit length.

Periperal Nusselt numbers, Nu_p.

Gz	Aspect Ratio 1.0	2.0	3.0	4.0
0	3.60	4.11	4.77	5.35
10	3.71	4.22	4.85	5.45
20	3.91	4.38	5.00	5.62
30	4.18	4.61	5.17	5.77
40	4.45	4.84	5.39	5.87
60	4.91	5.28	5.82	6.26
80	5.33	5.70	6.21	6.63
100	5.69	6.05	6.57	7.00
120	6.02	6.37	6.92	7.32
140	6.32	6.68	7.22	7.63
160	6.60	6.96	7.50	7.92
180	6.86	7.23	7.76	8.18
200	7.10	7.46	8.02	8.44

Mean Nusselt numbers, Nu_m

Gz	Aspect Ratio. 1.0	2.0	3.0	4.0
0	3.60	4.11	4.77	5.35
10	4.48	4.94	5.45	6.03
20	5.19	5.60	6.06	6.57
30	5.76	6.16	6.60	7.07
40	6.24	6.64	7.09	7.51
60	7.02	7.45	7.85	8.25
80	7.66	8.10	8.48	8.87
100	8.22	8.66	9.02	9.39
120	8.69	9.13	9.52	9.83
140	9.09	9.57	9.93	10.24
160	9.50	9.96	10.31	10.61
180	9.85	10.31	10.67	10.92
200	10.18	10.64	10.97	11.23

7.5 Experimental results for heat transfer with fully developed velocity profile in a rectangular duct of aspect ratio of 2.0 with constant heat input per unit length of the duct.

Re	Gz	$t_{w,o}$ deg.F.	t_o deg.F.	t_f deg.F.	t_w deg.F.	t_b deg.F.	Nu_l
735	94	81.0	71.0	97.0	110.5	77.7	8.1
	59				121.0	81.5	7.0
	30				135.5	91.6	6.6
813	104	81.0	70.0	96.0	111.0	76.7	8.4
	65				121.6	80.5	7.4
	33				134.0	90.6	7.0
897	115	80.0	70.0	94.0	109.8	76.3	8.9
	72				119.4	79.7	7.9
	37				131.7	89.1	7.4
980	125	80.5	69.8	93.5	110.0	76.7	9.3
	78.5				120.0	79.3	8.2
	40				131.5	88.3	7.8
1060	136	81.6	70.5	94.0	110.5	76.5	9.6
	85				121.5	80.1	8.5
	43				132.5	89.2	8.1

Re	Gz	$t_{w,o}$ deg.F.	t_o deg.F.	t_f deg.F.	t_w deg.F.	t_b deg.F.	Nu_l
1140	146	78.5	68.5	90.5	109.0	73.7	10.1
	91				119.0	77.0	8.8
	46.5				130.0	85.2	8.4
1220	156	82.5	70.7	93.5	111.5	76.7	10.5
	97.5				122.5	80.0	9.3
	50				133.4	88.8	8.8
1300	166	77.5	67.5	87.7	107.1	72.5	10.8
	104				117.0	75.6	9.5
	53				126.5	83.5	9.1
1390	177	84.0	71.6	94.0	114.5	76.6	11.2
	111				125.5	80.0	9.8
	56.5				137.2	89.3	9.3
1470	188	84.0	71.6	94.0	115.3	77.6	11.6
	117				126.0	80.6	10.4
	60				137.5	89.5	9.8
1560	199	83.5	71.0	93.0	114.0	76.6	12.1
	125				125.0	80.0	10.8
	63.5				136.5	88.5	10.2
1650	211	83.5	70.5	93.0	115.0	76.2	12.8
	132				125.5	79.5	11.5
	67				137.5	88.5	10.8
1720	220	83.7	70.5	93.5	113.5	76.5	13.7
	138				124.0	80.0	12.3
	70.5				138.0	89.0	11.3

7.6 Experimental data for fully developed velocity profile in a rectangular duct of aspect ratio of 2.0 with constant wall temperature.

Z/d_h	Re	Gz	t_o deg.F.	t_f deg.F.	t_w deg.F.	Nu_1
18.02	655	26	70.0	107.5	143.3	4.5
	735	29	70.5	107.5	145.5	4.7
	820	32.5	69.8	106.0	145.8	4.9
	900	36	69.0	104.5	145.8	5.1
	980	39	69.0	103.5	148.0	5.25
	1060	42	69.0	102.5	149.2	5.4
	1140	45	68.0	101.5	150.5	5.55
	1220	48	69.0	100.5	149.8	5.7
	1300	51.5	69.5	100.0	150.8	5.9
	1390	55	69.0	100.0	151.3	6.2
	1470	58	69.0	99.5	151.0	6.5
	1555	62	69.5	100.0	148.0	6.8
9.76	655	48	70.5	102.5	155.0	5.3
	735	54	70.5	100.1	151.5	5.6
	820	59	71.0	99.1	152.5	5.9
	900	65	71.0	98.5	153.0	6.3
	980	71	71.0	97.8	153.0	6.7
	1060	77	72.0	101.0	160.0	7.2

z/d_h	Re	Gz	t_o deg.F.	t_f deg.F.	t_w deg.F.	Nu_1
9.76	1140	82.5	72.0	101.0	160.0	7.7
		88	71.0	99.0	159.0	8.1
		94	70.0	98.5	159.0	8.6
		100	69.5	97.5	158.5	9.0
	1560	106	69.0	97.5	158.5	9.7
5.63	655	84	66.0	93.5	150.5	7.9
		95	66.0	93.0	150.7	8.5
		105	66.5	92.8	150.5	9.3
	900	116	67.0	93.0	151.5	10.1
		128	66.5	92.5	151.5	10.8
	1070	137	66.0	91.0	151.5	11,4
		148	66.0	91.0	151.0	12.0
		159	66.0	90.5	153.0	12.5
	1320	169	65.5	89.5	153.0	13.0

7.7 COMPUTER PROGRAM

```
JOB
LSM44EC1, WIBULSWAS   RUN 40   APRIL 66
COMPUTING 20000 INSTRUCTIONS
OUTPUT
0 LINE PRINTER 500 LINES
STORE 32 BLOCKS
COMPILER EXCHLF

TITLE
SIMULTANEOUSLY DEVELOPING FLOW IN RECTANGULAR DUCT
TITLE
CONSTANT HEAT INPUT  ASPECT RATIO = 2.0


ROUTINE 1

BI=UCF'/AI+D'A152/AI+AI   >>the Navier-Stokes equation in
RETURN                    >>fimite difference form
CLOSE R

ROUTINE 2

>>method to compute velocities

C'=-20A152+8A135+8A151+4A134   >>K W(x,y,z)  at the central axis
D'=B152-A152    >>  W  at the central axis

J=18(17)120
K=J+14
I=J(1)K
C=-20AI+4A(I-1)+4A(I+1)+4A(I-17)+A(I-16)+A(I-18)  >> K W(x,y,z)
C=4A(I+17)+A(I+16)+A(I+18)+C-C'
JUMPDOWN(R1)
REPEAT
REPEAT

>>velocities at central lines
I=33(17)135
C=-20AI+4A(I-17)+4A(I+17)+8A(I-1)+2A(I-18)+2A(I+16)-C'
JUMPDOWN (R1)
REPEAT

I=137(1)151
C=-20AI+4A(I-1)+4A(I+1)+8A(I-17)+2A(I-16)+2A(I-18)-C'
JUMPDOWN (R1)
```

```
REPEAT

>>to evaluate bulk  velocity
W=0
J=18(34)120   >>apply the Simpson's rule in two dimensions
K=J+14
I=J(2)K
W=16BI+4B(I-1)+4B(I+1)+4B(I-17)+4B(I+17)+W
W=B(I-18)+B(I-16)+B(I+16)+B(I+18)+W
REPEAT
REPEAT

W=W/1152   >> bulk velocity
RETURN
CLOSE R


ROUTINE 3

DI=F'C/BI+CI  >> Fourier-Poisson energy equation in
RETURN        >> finite difference form
CLOSE R

ROUTINE 4

NEWLINE 3
CAPTION
  STEP N       GZ       BULK TEMP.     WALL TEMP.   NUP          NUM
NEWLINE 2
RETURN
CLOSE R

ROUTINE 5

>>to evaluate bulk temperature, V
V=0
J=18(34)120   >>the  Simpson's rule in two dimensions
K=J+14
I=J(2)K
V=16BIDI+4B(I-1)D(I-1)+4B(I+1)D(I+1)+4B(I-17)D(I-17)+4B(I+17)D(I+17)+V
V=B(I-18)D(I-18)+B(I-16)D(I-16)+B(I+16)D(I+16)+B(I+18)D(I+18)+V
REPEAT
REPEAT

V=V/1152      >> predicted  bulk temperature

RETURN
CLOSE R
```

```
ROUTINE 6

>>printout instructions

NEWLINE 3
CAPTION
DIMENSIONLESS VELOCITIES
NEWLINE 2
J=0(1)16
K=J+136
NEWLINE
I=J(17)K
PRINT(AI)0,2    >> velocity distribution
REPEAT
REPEAT

NEWLINE 3
CAPTION
DIMENSIONLESS TEMPERATURES
NEWLINE 2
J=0(1)16
K=J+136
NEWLINE
I=J(17)K
PRINT(CI)0,2     >> temperature distribution
REPEAT
REPEAT

JUMPDOWN(R4), N≠P

RETURN
CLOSE R


CHAPTER 0
A►300
B►300
C►300
D►300

READ(E)          >> 3d_h/h
READ(F)          >> (w_b d_h d_h)/(α Δz)
READ(P)          >> number of steps required
READ(A)          >>                accuracy
READ(U)          >> Prandtl number

E=3/E            >> e = h/d_h
E'=ØDIVIDE(F,EE)
```

```
F'=6F
F'=1/F'        >> (α Δz)/(6ee w_b d_h d_h)

>>wall initial  temperatures and velocities
I=0(1)16
AI=0
BI=0
CI=E/4
REPEAT

I=0(17)136
AI=0
BI=0
CI=E/4
REPEAT

>>initial velocities and temperatures
J=18(17)137
K=J+15
I=J(1)K
AI=1
CI=0
REPEAT
REPEAT

R=1
H=4/E          >> NU_F,3

JUMPDOWN(R4)
B152=1
M=0
N=1

>>to compute velocities

1)JUMPDOWN(R2)
2)M=M+1
C=1-W     >>error in bulk velocity

D=1+A
JUMP 3, W>D

D=9MOD(C)
JUMP 4, A>D
JUMP 3, M>25
B152=B152+1.001C    >> correction of the central axis velocity
JUMPDOWN(R2)        >> recompute velocity distribution

JUMP 2
```

```
3)J=18(17)137
K=J+15
I=J(1)K
BI=BI+C
REPEAT
REPEAT

M=0

>>to compute temperatures

4)N=N+1
J=18(17)120
K=J+14
I=J(1)K
C=-20CI+4C(I-1)+4C(I+1)+4C(I-17)+4C(I+17)     >> K t(x,y,z)
C=C(I-18)+C(I-16)+C(I+16)+C(I+18)+C
JUMPDOWN(R3)
REPEAT
REPEAT


>>temperarures at central line
I=33(17)135
C=-20CI+4C(I-17)+4C(I+17)+8C(I-1)+2C(I-18)+2C(I+16)
JUMPDOWN(R3)
REPEAT

I=137(1)151
C=-20CI+4C(I-1)+4C(I+1)+8C(I-17)+2C(I-16)+2C(I-18)
JUMPDOWN(R3)
REPEAT

C=-20C152+8C135+8C151+4C134
D152=F'C/B152+C152

V'=NEE/F      >> actual bulk temperature, equation(12)
A'=0.001V'

5)JUMPDOWN(R5)

C=V'-V
D=ØMOD(C)
JUMP 6, A'>D

J=18(17)137
K=J+15
I=J(1)K
DI=1.001CBI+DI
```

```
REPEAT
REPEAT

JUMP 5

>> computation of wall temperarure

6)C=0
I=18(17)120
C=DI+C
REPEAT

I=18(1)32
C=DI+C
REPEAT

C=0.5D33+0.5D137+C
C=C/23              >>  Σβh/n

D=0
I=18(1)32
D=BIDI-BICI+D
REPEAT

I=35(17)120
D=BIDI-BICI+D
REPEAT

D=0.5B33D33-0.5B33C33+0.5B137D137-0.5B137C137+D    Σ(wh/wb) Δβh
D=DF/8

C=-D/22+C
C=E/4+C             >> wall temperature, equation(13)

I=0(1)16
DI=C
REPEAT

I=17(17)136
DI=C
REPEAT

>>Nusselt numbers, X,Y

X=C-V'
X=0.25/X    >> local NUp

H=H+X
Y=H/N       >> mean NUm
```

```
>>Graetz number
G=E'/N

>>output

JUMP8,N=P
JUMP7,200>N
JUMP10,R≠30
JUMP9
7)JUMP8,100>N
JUMP10,R≠10
JUMP9
8)JUMP9,6>N
JUMP10,R≠5
9)NEWLINE
PRINT(N)0,2
PRINT(G)0,3
PRINT(V)0,3
PRINT(C)0,3
PRINT(X)0,3
PRINT(Y)0,3

R=0
10)R=R+1

JUMPDOWN(R6), N=100
JUMPDOWN(R6), N=P

JUMP11, N=P

I=0(17)136     >> transfer predicted velocities and temperatures
K=I+16         >> to prepare for computations at the next step,
J=I(1)K
AJ=BJ
CJ=DJ
REPEAT
REPEAT

JUMP4, B152>1.95
JUMP 1

11)END
CLOSE

        64  20   995   0.0005   0.72

        ***Z
```

7.8 Heat Transfer for Simultaneously Developing Velocity and Temperature Profiles in Rectangular Ducts.

7.8.1 Predicted mean Nusselt numbers for constant wall temperature and Prandtl number of 0.72.

Gz	Aspect Ratio				
	1.0	2.0	3.0	4.0	6.0
10	3.75	4.20	4.67	5.11	5.72
20	4.39	4.79	5.17	5.56	6.13
30	4.88	5.23	5.60	5.93	6.47
40	5.27	5.61	5.96	6.27	6.78
50	5.63	5.95	6.28	6.61	7.07
60	5.95	6.27	6.60	6.90	7.35
80	6.57	6.88	7.17	7.47	7.90
100	7.10	7.42	7.70	7.98	8.38
120	7.61	7.91	8.18	8.48	8.85
140	8.06	8.37	8.66	8.93	9.28
160	8.50	8.80	9.10	9.36	9.72
180	8.91	9.20	9.50	9.77	10.12
200	9.30	9.60	9.91	10.18	10.51
220	9.70	10.00	10.30	10.58	10.90

7.8.2 Predicted Nusselt numbers for the thermal condition of constant heat input per unit length of the duct and Prandtl number of 0.72.

Peripheral Nusselt number, Nu_p.

Gz	Aspect Ratio 1.0	2.0	3.0	4.0
10	4.18	4.60	5.18	5.66
20	4.66	5.01	5.50	5.92
30	5.07	5.40	5.82	6.17
40	5.47	5.75	6.13	6.43
50	5.83	6.09	6.44	6.70
60	6.14	6.42	6.74	7.00
80	6.80	7.02	7.32	7.55
100	7.38	7.59	7.86	8.08
120	7.90	8.11	8.37	8.58
140	8.38	8.61	8.84	9.05
160	8.84	9.05	9,38	9.59
180	9.28	9.47	9,70	9.87
200	9.69	9.88	10.06	10.24

Predicted mean Nusselt number , Nu_m.

Gz	Aspect Ratio			
	1.0	2.0	3.0	4.0
5	4.60	5.00	5.57	6.06
10	5.43	5.77	6.27	6.65
20	6.60	6.94	7.31	7.58
30	7.52	7.83	8.13	8.37
40	8.25	8.54	8.85	9.07
50	8.90	9.17	9.48	9.70
60	9.49	9.77	10.07	10.32
80	10.53	10.83	11.13	11.35
100	11.43	11.70	12.0	12.23
120	12.19	12.48	12.78	13.03
140	12.87	13.15	13.47	13.73
160	13.50	13.79	14.10	14.48
180	14.05	14.35	14.70	14.95
200	14.55	14.88	15.21	15.49
220	1t.03	15.36	15.83	16.02

7.8.3 Effect of Prandtl numbers on predicted mean Nusselt numbers, Nu_m, for simultaneously developing profiles in a rectangular duct of aspect ratio of 2.0 with constant heat input per unit length of the duct.

Gz	Prandtl Number, Pr.				
	∞	10	0.72	0.1	0
25	5.60	6.15	6.94	7.90	8.65
40	6.64	7.50	8.54	9.75	10.40
60	7.45	8.40	9.77	11.10	11.65
80	8.10	9.20	10.83	12.15	12.65
100	8.66	9.90	11.70	13.05	13.50
140	9.57	11.05	13.15	14.50	14.95
180	10.31	11.95	14.35	15.65	16.15
220	10.95	12.75	15.35	16.70	17.20
260	11.50	13.45	16.25	17.60	18.10
300	12.00	14.05	17.00	18.30	18.90
350	12.55	14.75	17.75	19.10	19.80
400	13.00	15.40	18.50	19.90	20.65

7.8.4 Experimental data for simultaneously developing velocity and temperature profiles in a rectangular duct of aspect ratio of 2.0 with constant heat input per unit length of the duct.

Re	Gz	$t_{w,o}$ deg.F.	t_o deg.F.	t_f deg.F.	t_w deg.F.	t_b deg.F.	Nu_l
735	94	76.5	70.3	100.3	110.6	78.2	11.2
	59				122.0	82.6	9.8
	30				136.6	94.5	9.2
820	104	77.2	71.0	97.8	108.7	78.1	11.6
	65				118.8	82.0	10.4
	33				132.8	92.[illegible]	9.5
900	115	72.7	65.7	94.6	107.8	73.0	12.1
	72				119.5	77.5	10.6
	37				133.5	88.8	[illegible].0
980	125	73.3	66.3	94.0	106.5	73.3	13.[illegible]
	78.5				117.7	77.6	11.4
	40				132.0	88.3	10.7
1060	136	74.5	67.5	95.0	108.6	74.5	13.7
	85				120.1	78.7	11.9
	43				135.1	89.4	11.0
1140	146	77.5	71.4	95.6	109.0	77.8	14.4
	91				120.0	81.3	12.5
	46.5				134.5	90.6	11.3

Re	Gz	$t_{w,o}$ deg.F.	t_o deg.F.	t_f deg.F.	t_w deg.F.	t_b deg.F.	Nu_1
1220	156	77.2	71.0	94.5	108.5	77.1	14.9
	97.5				119.5	80.5	12.8
	50				134.4	89.9	11.7
1300	166	77.5	70.6	94.9	109.0	77.2	15.5
	104				119.8	80.5	13.5
	53				134.0	90.0	12.3
1390	178	77.5	70.7	94.0	107.5	76.7	16.1
	111				118.5	80.2	14.1
	56.5				132.5	89.3	12.6
1470	188	76.8	70.2	92.7	108.0	76.0	16.8
	117				118.6	79.3	14.4
	60				133.0	88.2	13.0
1560	199	76.3	69.5	92.2	107.5	75.3	17.4
	125				118.6	78.8	15.0
					132.5	87.8	13.7
1650	211	76.1	68.0	91.8	108.0	74.2	17.9
	132				118.6	77.8	15.5
					132.5	87.1	14.2

7.9 Predicted Nusselt numbers for right-angled isosceles triangular ducts with constant wall temperature.

fully developed velocity profile see Figs 31 - 32

	Peripheral Nusselt Number			Mean Nusselt number		
Pr	∞	0.72	0	∞	0.72	0
Gz						
10	2.40	2.52	3.75	2.87	3.12	4.81
20	2.53	2.76	4.41	3.33	3.73	5.85
30	2.70	2.98	4.82	3.70	4.20	6.48
40	2.90	3.18	5.17	4.01	4.58	6.97
50	3.05	3.37	5.48	4.28	4.90	7.38
60	3.20	3.54	5.77	4.52	5.17	7.73
80	3.50	3.85	6.30	4.91	5.69	8.31
100	3.77	4.15	6.75	5.23	6.10	8.80
120	4.01	4.43	7.13	5.52	6.50	9.18
140	4.21	4.70	7.51	5.78	6.82	9.47
160	4.40	4.96	7.84	6.00	7.10	9.70
180	4.57	5.22	8.10	6.17	7.33	9.94
200	4.74	5.49	8.38	6.33	7.57	10.13

7.10 Predicted Nusselt numbers for right-angled isosceles triangular ducts with constant heat input per unit length of the duct.

fully developed velocity profile see Fig 3.3 - 3.4

	Peripheral Nusselt Number			Mean Nusselt Number		
Pr	∞	0.72	0	∞	0.72	0
Gz						
10	3.29	4.00	5.31	4.22	5.36	6.86
20	3.58	4.73	6.27	3.98	6.51	7.97
30	3.84	5.23	6.85	5.50	7.32	8.68
40	4.07	5.63	7.23	5.91	7.95	9.20
50	4.28	5.97	7.55	6.25	8.50	9.67
60	4.47	6.30	7.85	6.57	8.99	10.07
80	4.84	6.92	8.37	7.14	9.80	10.75
100	5.17	7.45	8.85	7.60	10.42	11.32
120	5.46	7.95	9.22	8.03	10.90	11.77
140	5.71	8.39	9.58	8.40	11.31	12.14
160	5.95	8.80	9.90	8.73	11.67	12.47
180	6.16	9.14	10.17	9.04	12.00	12.75
200	6.36	9.50	10.43	9.33	12.29	13.04

7.11 Predicted Nusselt numbers for equilateral triangular ducts with constant wall temperature.

fully developed velocity profile see Figs 36 - 37

		Peripheral Nusselt Number			Mean Nusselt Number		
	Pr	∞	0.72	0	∞	0.72	0
Gz							
10		2.57	2.80	3.27	3.10	3.52	4.65
20		2.73	3.11	3.93	3.66	4.27	5.79
30		2.90	3.40	4.46	4.07	4.88	6.64
40		3.08	3.67	4.89	4.43	5.35	7.32
50		3.26	3.93	5.25	4.75	5.73	7.89
60		3.44	4.15	5.56	5.02	6.08	8.36
80		3.73	4.50	6.10	5.49	6.68	9.23
100		4.00	4.76	6.60	5.93	7.21	9.98
120		4.24	4.98	7.03	6.29	7.68	10.59
140		4.47	5.20	7.47	6.61	8.09	11.14
160		4.67	5.40	7.88	6.92	8.50	11.66
180		4.85	5.60	8.20	7.18	8.88	12.10
200		5.03	5.80	8.54	7.42	9.21	12.50

7.12 Predicted Nusselt numbers for equilateral triangular ducts with constant heat input per unit length of the duct.

fully developed velocity profile — see Figs. 38 & 39

	Peripheral Nusselt Number			Mean Nusselt Number		
Pr	∞	0.72	0	∞	0.72	0
Gz						
10	3.27	3.58	4.34	4.02	4.76	6.67
20	3.48	4.01	5.35	4.76	5.87	8.04
30	3.74	4.41	6.14	5.32	6.80	9.08
40	4.00	4.80	6.77	5.82	7.57	9.06
50	4.26	5.13	7.27	6.25	8.20	10.65
60	4.49	5.43	7.66	6.63	8.75	11.27
80	4.85	6.03	8.26	7.27	9.73	12.35
100	5.20	6.56	8.81	7.87	10.60	13.15
120	5.50	7.04	9.30	8.38	11.38	13.82
140	5.77	7.50	9.74	8.84	12.05	14.46
160	6.01	7.93	10.17	9.25	12.68	15.02
180	6.22	8.33	10.53	9.63	13.27	15.50
200	6.45	8.71	10.87	10.02	13.80	16.00

7.13 Experimental data for heat transfer with fully developed velocity profile in an equilateral triangular duct with constant heat input per unit length of the duct. see Fig 40

Re	Gz	$t_{w,o}$ deg.F.	t_o deg.F.	t_f deg.F.	t_w deg.F.	t_b deg.F.	Nu_l
650	90	79.6	66.3	106.5	138.0	74.0	5.5
	64				149.6	77.3	5.0
	45				156.7	82.0	4.8
	22				183.4	97.5	4.3
810	112	75.2	64.2	101.5	133.1	70.3	6.9
	80				144.3	73.0	6.3
	56				151.7	76.7	6.0
	28				177.5	89.1	5.3
970	134	74.5	62.5	98.8	129.7	69.4	7.8
	96				141.0	72.3	7.3
	67				149.5	76.7	6.9
	33.5				175.2	90.5	6.1
1135	157	78.0	63.7	101.7	135.5	70.8	8.6
	112				147.0	74.0	8.0
	79				155.8	78.4	7.6
	39				182.7	93.1	6.8
1300	180	80.0	66.5	103.0	141.8	73.6	9.4
	128				153.5	76.5	8.7
	90				163.2	80.8	8.2
	45				190.3	95.0	7.3

Re	Gz	$t_{w,o}$ deg.F.	t_o deg.F.	t_f deg.F.	t_w deg.F.	t_b deg.F.	Nu_1
1460	202	79.0	65.2	101.4	143.0	72.1	10.0
	144				155.0	75.0	9.3
	101				165.2	79.2	8.8
	50.5				192.2	93.2	7.9
1620	224	79.4	64.8	100.2	142.5	71.4	10.9
	160				154.0	74.4	10.0
	112				165.0	78.5	9.4
	56				191.0	92.0	8.5

7.14 Experimental data for heat transfer with simultaneously developing velocity and temperature profiles in an equilateral triangular duct with constant heat input per unit length of the duct. see Fig 41

Re	Gz	$t_{w,o}$ deg.F.	t_o deg.F.	t_f deg.F.	t_w deg.F.	t_b deg.F.	Nu_1
650	90	69.6	63.3	97.0	112.0	69.7	7.7
	64				120.5	72.3	7.0
	45				127.7	76.3	6.7
	22				151.0	89.4	5.9
810	112	69.7	62.8	97.5	115.0	69.5	9.2
	80				123.8	72.2	8.4
	56				131.9	76.2	7.9
	28				155.8	89.6	6.9

Re	Gz	$t_{w,o}$ deg.F.	t_o deg.F.	t_f deg.F.	t_w deg.F.	t_b deg.F.	Nu_l
970	134	69.8	62.1	97.2	115.2	68.2	10.5
	96				123.7	71.0	9.7
	67				132.2	75.2	9.0
	33.5				156.2	89.1	8.0
1135	157	75.0	68.0	100.9	120.5	74.3	11.9
	112				129.0	77.0	10.9
	79				137.8	80.8	10.3
	39				162.0	93.5	8.8
1300	180	72.7	65.7	97.5	117.0	71.7	13.2
	128				125.6	74.3	12.2
	90				135.7	78.0	11.2
	45				158.7	90.2	9.9
1460	202	73.0	65.7	97.5	118.5	71.7	14.4
	144				127.0	74.3	13.4
	101				136.7	78.0	12.3
	50.5				160.3	90.2	10.7
1620	224	73.0	64.8	96.6	117.4	70.8	15.6
	160				125.5	73.5	14.5
	112				134.7	77.2	13.4
	56				156.7	89.3	11.8

REFERENCES

1. Montgomery, S.R. and Weiss, H.K. "Forced convection heat transfer in ducts of non-circular cross-sections", N.E.L. Report No.1, June 1961.

2. Ulrichson, D.L. and Schmitz, R.A. "Laminar flow heat transfer in the entrance region of circular ducts", Int. J. Heat & Mass Transfer, 1965, 8, 253-258.

3. Kays, W.M. "Numerical solutions for laminar flow heat transfer in circular tubes", Trans. ASME, 1955, 77, 1265-1274.

4. Hudson J.L. and Bankoff, S.C. "Asymtotic solutions for the unsteady Graetz problem", Int. J. Heat & Mass Transfer, 1964, 7, 1303-

5. Bradley, D. and Entwistle, A.C. "Developed laminar flow heat transfer from air for variable physical properties", Int. J. Heat & Mass Transfer, 1965, 8, 621-638.

6. Koppel, L.B. and Smith, J.M. "Laminar flow heat transfer for variable physical properties", Trans. ASME, J. Heat Transfer, 1962, 84, 157-163.

7. Kays, W.M. and Nicoll, W.B. "Laminar flow heat transfer to a gas with large temperature differences", Trans. ASME, J. Heat Transfer, 1963, 85, 329-338.

8. Stefan, K. "Warmeubergeng und Druckabfall bei nicht ausgebildeter Laminarstromung in Rohren un in ebnen Spalten", Chem. Ing. Tech., 1959, 31, 773-778.

9. Han, L.S. "International Developments in Heat Transfer", International Heat Transfer Conference, Colorado, U.S.A., 1961, 591-597.

10. Langhaar, H.L. "Steady flow in the transition length of a straight tube", J. Appl. Mech., 1942, 9, A55-A58.

11. Hwang, C.L. and Fan, L.T. "Finite difference analysis of forced convection heat transfer in the entrance region of a flat rectangular duct", Appl. sci. Res., 1964, A, 13, 401-

12. Siegel, R. and Sparrow, E.M. "Simultaneous development of velocity and temperature distributions in s flat duct with uniform heating", A.I.Ch.E., J.5, 1959, 73-75.

13. Hatton, A.P. and Turton J.S "Heat transfer in the thermal entry length with laminar flow between parallel walls at unequal temperatures", Int. J. Heat & Mass Transfer, 1962, 5, 673-679.

14. Perlmutter, M. and Siegel, R. "Two-dimensional incompressible laminar duct flow with a step change in wall temperature", Int. J. Heat & Mass Transfer, 1961,3, 94-107.

15. Savino, J.M. and Siegel, R. "Laminar forced convection in rectangular channels with unequal heat addition on adjacent sides", Int. J. Heat & Mass Transfer, 1964, 7, 733-741.

16. Sparrow, E.M. and Haji-Shiekh, A. "Laminar heat transfer and pressure drop in isosceles triangular, right triangular and circular sector ducts", Trans. ASME, J. Heat Transfer, 1965, 87, 426-428.

17. Cobble, M.H. "Nusselt number for flow in a cone", Trans. ASME, J. Heat Transfer, 1962, 84, 264-265.

18. Rouse H. "Advanced Mechanics of Fluids", J. Wiley, New York, 1959.

19. Milne, W.E. "Numerical Solutions of Differential Equations", J. Wiley, New York, 1953, 131-133.

20. Crandall, S.H. "Engineering Analyses", J. Wiley, New York, 1956, 246.

21. Secomak Hi-Velocity Fan No.350. Service Electric Co. Ltd., Secomak Works, Honeypot Lane, Stanmore, Middlesex.

22. Schlichting, H. "Boundary Layer Theory", McGraw-Hill, New York, 1960, 89-91.

23. Ferry Metal - Nickel-copper alloy, 45% Ni, 54% Cu, and 1% other elements. Henry Wiggins & Co. Ltd., Wiggins Street, Birmingham 16.

24. Hermetal - Double bond resin. Keniworth Manufacturing Co. Ltd., West Drayton, Middlesex.

25. Coxon, W.F. "Temperature Measurement and Control", Heywood & Co. Ltd., London, 1960.

26. McAdams, W.H. "Heat Transmission", McGraw-Hill, New York, 1954, Kogakusha Co. Ltd., Tokyo, 229-233.

27. Norris, R.H. and Streid, D.D. "Laminar flow heat transfer coefficients for ducts", Trans.ASME, 1940, 36, 525-533.

28. Sellars, J.R., Tribus, M., & Klien, J.S. " Heat transfer to laminar flow in a round tube or flat conduit-the Graetz problem extended". Trans.ASME, 78, 1956, 441-.

29. Cess, R.D. & Shaffer, E.C. "Heat transfer to laminar flow between parallel plates with a prescribed wall heat flux", Appl. sci. Res., Hague, A, 1959, 339-344.

30. Dryden, H.L., Muraghan, F.D., Bateman, H. "Hydrodynamics", National Research Council, Washington, D.C., 1932, 197-.

31. Southwell, R.V. "Relaxation Methods in Theoretical Physics", The Clarendon Press, Oxford, 1946, p.22-23.

32. Scarborough, J.B. "Numerical Mathematical Analysis", Johns Hopkins Press, Bultimore, 1955.

33. Clark, S.H. and Kay, W.M. "Laminar-flow forced convection in rectangular tubes", Trans.ASME, 75, 1953, 859-.